Faculty of Aerospace Engineering

A Tracking Task for Quantifying Loss of Motor Skills due to Parkinson's Disease

R.J. de Vries

May 19, 2016

TU Delft Delft University of Technology

Challenge the future

A Tracking Task for Quantifying Loss of Motor Skills due to Parkinson's Disease

Master of Science Thesis

For obtaining the degree of Master of Science in Aerospace Engineering
at Delft University of Technology

R.J. de Vries

May 19, 2016

Faculty of Aerospace Engineering · Delft University of Technology

Delft University of Technology

Delft University Of Technology
Department Of
Control and Simulation

The undersigned hereby certify that they have read and recommend to the Faculty of Aerospace Engineering for acceptance a thesis entitled **"A Tracking Task for Quantifying Loss of Motor Skills due to Parkinson's Disease"** by **R.J. de Vries** in partial fulfillment of the requirements for the degree of **Master of Science**.

Dated: May 19, 2016

Readers:

prof.dr.ir. M. Mulder

dr.ir. M. M. van Paassen

dr.ir. D. M. Pool

dr.ir. J. J. M. Pel (EMC)

dr.ir. H. Vallery (BMech)

"Don't Panic."

Douglas Adams,
The Hitchhiker's Guide to the Galaxy

Acronyms

CF	Crest Factor
DLPFC	Dorsolateral Prefrontal Cortex
EMC	Erasmus MC
FAB	Frontal Assessment Battery
FCM	Fourier Coefficient Method
FEF	Frontal Eye Field
HC	human controller
MLE	Maximum Likelihood Estimation
MSSE	Mini Mental State Examination
PD	Parkinson's Disease
SOP	Successive Organization of Perception
UPDRS	Unified Parkinson's Disease Rating Scale
VAF	Variance Accounted For

Contents

List of Figures

Chapter 1

Introduction

When people get older, the chance of developing an age-related disorder increases. One of the most common age-related neurodegenerative disorders is Parkinson's Disease (PD), only second to Alzheimer's Disease (De Lau & Breteler, 2006). PD affects the motor control area in the brain, which makes a person lose control over several body functions. This loss of control can have a great impact on the personal life (Lees et al., 2009). However, the quality of life of patients can be improved significantly with correct treatment (Lees et al., 2009).

PD is still an incurable progressive disease and is diagnosed by identifying specific motor symptoms (like tremor, hypokinesia, rigidity and an impaired balance) (De Lau & Breteler, 2006; Goetz et al., 2007) and by using questionnaires (Fahn & Elton, 1987; Dubois et al., 2000). The results of the diagnosis are translated into a low resolution scale (Hoehn et al., 1998), which can only distinguish between five stages. A higher resolution is preferred for a more detailed analysis of the degradation of motor control. A higher resolution scale might help in the early detection of PD and show the effectiveness of medication.

Treatment for PD is based on restoring the dopamine balance in the brain (Lees et al., 2009). Especially motor symptoms respond positively to the dopamine treatment. Unfortunately, non-motor symptoms respond poorly or not at all (Kandel et al., 2013). To date, objective clinical outcome measures to evaluate the effects of dopamine treatment are limitedly available. Usually, PD patients start by taking a relatively small dose. If their motor symptoms decrease, the dose is gradually increased until an optimum is achieved. This has to be done carefully since an overdose can lead to undesired side effects such as delusions (Lees et al., 2009). The improvement in motor control of patients is partially checked subjectively by a neurologist. A more quantifiable measure is desirable to verify if there is indeed an improvement in (fine) motor control due to medication. Fine motor control can be assessed by measuring eye-hand coordination.

Recently, at the neuroscience department of the Erasmus University Medical Center (EMC), eye-hand coordination tests have been developed for non-intrusive early detection of neurodegenerative disorders like PD (De Boer et al., 2013; Muilwijk et al., 2013). These tests rely on registration of eye movements, hand movements and inputs on a touch screen. From this

data, an estimation of the time delays for the eye and hand movements can be calculated. Such data can give insight in the severity of fine motor symptoms in PD patients. However, eye-hand coordination is tested during short intervals only.

A different approach to quantify fine motor control in PD patients, over a longer time interval, is by performing a tracking task (Cassell, 1973; Andersen, 1986). In a tracking task, a subject is asked to control a certain system and keep the error between the input signal and a target signal as small as possible. Experiments in which PD patients were asked to perform a tracking task have been conducted previously (Flowers, 1978; Jones & Donaldson, 1989; Hufschmidt & Lücking, 1995; Jones & Donaldson, 1996; Soliveri et al., 1997). Flowers (Flowers, 1978), Hufschmidt et al. (Hufschmidt & Lücking, 1995) and Solverini et al. (Soliveri et al., 1997) used a pursuit display and showed that for PD patients, the average error was larger compared to a control group. Jones et al. (Jones & Donaldson, 1996) used a preview display and concluded that PD patients had more difficulties in performing tasks with preview as compared to non-preview conditions.

A tracking task makes it possible to objectively quantify the human controller's dynamics using system identification techniques (McRuer et al., 1965; van Paassen & Mulder, 1998). Identifying the degradation in fine motor control of PD patients using human operator models has never been done but can give an unique insight. The study of human operator models started with the crossover model of McRuer et al. (McRuer et al., 1965). Extensive research was done on human controller modeling for compensatory and pursuit tasks (McRuer et al., 1965; Wasicko et al., 1967; van Paassen & Mulder, 1998; Zaal, Pool, Chu, Mulder, et al., 2009; Pool et al., 2011). For preview tasks human controller modeling is still in development (van der El et al., 2015).

This research will explore the potential of a tracking task to quantify degradation in eye-hand coordination of PD patients, by using system identification methods.

The research objective is as follows:

To develop a tracking task that may be used as an additional diagnostic tool for the early detection of degraded eye-hand coordination in Parkinsons patients by using system identification methods.

The structure of the report is as follows. In Part I the graduation paper is presented. The paper is titled *'Using Human Operator Modeling for Quantifying Loss of Motor Skills due to Parkinson's Disease'*. In Part II the appendices of the paper are given. The preliminary report is found in Part III. Finally, the appendices of the preliminary report are given in Part IV.

Part I

Scientific Paper

Using Human Operator Modeling for Quantifying Loss of Motor Skills due to Parkinson's Disease

Rick J. de Vries[*], Daan M. Pool[*], Marinus M. van Paassen[*], Max Mulder[*], Johan J. Pel[**], Casper de Boer[**], Maxim E. Keizer[**] and Johannes van der Steen[**]

[*]Control & Simulation Division, Faculty of Aerospace Engineering, Delft University of Technology, Delft, The Netherlands

[**]Erasmus MC department of Neuroscience, Rotterdam, The Netherlands

***Abstract*—This paper investigated if a pursuit tracking task could be used to quantify the loss of motor skills due to Parkinson's disease (PD) by using system identification methods. A human-in-the-loop experiment consisting of PD patients and a healthy age-gender matched control group was conducted at the Erasmus University Medical Center. A pursuit display combined with a quasi-random multisinus target signal and single integrator dynamics was used. Such a tracking task makes it possible to model human controller behavior to estimate human parameters, such as the control gain and time delays. The performance of patients was found to be worse compared to the control group. The control gain was found to be significantly higher for the control group compared to patients. Patients had a significantly higher neuromuscular damping compared to the control group. Therefore, a tracking task could be used as a tool to quantify the loss of motor skill due to PD. This might improve the early detection and the treatment of PD.**

I. Introduction

WHEN people get older, the chance of developing an age-related disorder increases. One of the most common age-related neurodegenerative disorders is Parkinson's disease (PD), only second to Alzheimer's Disease [1]. PD affects the motor control area in the brain, which makes a person lose control over several body functions. This loss of control can have a great impact on the personal life [2]. However, the quality of life of patients can be improved significantly with correct treatment [2].

PD is still an incurable progressive disease and is diagnosed by identifying specific motor symptoms (like tremor, hypokinesia, rigidity and an impaired balance) [1], [3] and by using questionnaires [4], [5]. The results of the diagnosis are translated into a low resolution scale [6], which can only distinguish between five stages. A higher resolution is preferred for a more detailed analysis of the degradation of motor control. A higher resolution scale might help in the early detection of PD and show the effectiveness of medication.

Treatment for PD is based on restoring the dopamine balance in the brain [2]. Especially motor symptoms respond positively to the dopamine treatment. Unfortunately, non-motor symptoms respond poorly or not at all [7]. To date, objective clinical outcome measures to evaluate the effects of dopamine treatment are limitedly available. Usually, PD patients start by taking a relatively small dose. If their motor symptoms decrease, the dose is gradually increased until an optimum is achieved. This has to be done carefully since an overdose can lead to undesired side effects such as delusions [2]. The improvement in motor control of patients is partially checked subjectively by a neurologist. A more quantifiable measure is desirable to verify if there is indeed an improvement in (fine) motor control due to medication. Fine motor control can be assessed by measuring eye-hand coordination.

Recently, at the neuroscience department of the Erasmus University Medical Center (EMC), eye-hand coordination tests have been developed for non-intrusive early detection of neurodegenerative disorders like PD [8], [9]. These tests rely on registration of eye movements, hand movements and inputs on a touch screen. From this data, an estimation of the time delays for the eye and hand movements can be calculated. Such data can give insight in the severity of fine motor symptoms in PD patients. However, eye-hand coordination is tested during short intervals only.

A different approach to quantify fine motor control in PD patients, over a longer time interval, is by performing a tracking task [10], [11]. In a tracking task, a subject is asked to control a certain system and keep the error between the input signal and a target signal as small as possible. Experiments in which PD patients were asked to perform a tracking task have been conducted previously [12], [13], [14], [15], [16]. Flowers [12], Hufschmidt et al. [14] and Solverini et al. [16] used a pursuit display and showed that for PD patients, the average error was larger compared to a control group. Jones et al. [15] used a preview display and concluded that PD patients had more difficulties in performing tasks with preview as compared to non-preview conditions.

A tracking task makes it possible to objectively quantify the human controller's dynamics using system identification techniques [17], [18]. Identifying the degradation in fine motor control of PD patients using human operator models has never been done but can give an unique insight. The study of human operator models started with the crossover model of McRuer et al. [17]. Extensive research was done on human controller modeling for compensatory and pursuit tasks [17], [19], [18], [20], [21]. For preview tasks human controller modeling is still in development [22].

This research will explore the potential of a single-axis

pursuit tracking task to quantify degradation in eye-hand coordination of PD patients, by using system identification methods. The controlled element will have single integrator dynamics. For such a task the human controller will react on the error only [19], [23]. Therefore, single-loop identification methods can be used [18]. An experiment will be conducted to collect tracking data from PD patients (P) and an age-gender matched control group (C).

This paper is structured as follows. In Section II more insight in PD is given. Section III describes the methods used for the experiment. The results of the experiment are given in Section IV. Finally, the discussion is in Section V and the conclusions can be found in Section VI.

II. Parkinson's disease

The brain consists of three main parts; the cerebrum, the cerebellum, and the brain stem. Within the deep layers of the cerebrum the basal ganglia are located. The basal ganglia are involved in primary functions like action selection, action gating, reward based learning, motor preparation and timing [24], but also non-motor functions like control of emotions [7]. However, the most important function for this study is the control of voluntary motor movements [25]. One of the structures composing the basal ganglia is the substantia nigra. The substantia nigra is responsible for the production of the neurotransmitter dopamine, which is used for communication within the brain. In PD, the dopamine producing neurons in the substantia nigra gradually die. The reduction of dopamine causes communication problems within the brain. The motor cortex is highly dependent on dopamine, and therefore its regulation will be reduced. This leads to the traditional Parkinsonian symptoms like tremor, rigidity, bradykinesia and an impaired balance [7].

III. Method

A. Subjects

Four PD patients were recruited from the department of Neurology of the Erasmus MC Rotterdam. Age ranged from 51-67 years (μ = 61.25, σ = 7.14). For the healthy control group (N=6) age ranged from 51-63 years (μ = 57.67, σ = 4.18). All subjects signed a written consent form. The study was approved by the ethical committees of the EMC and the TU Delft.

The inclusion criteria were similar to the experiment conducted by De Boer et al. [26]. The cognitive functioning was assessed using the Mini Mental State Examination (MMSE) questionnaire [27]. Subjects who did not show cognitive decline (MMSE $\geq$ 26) were included. Patients (μ = 28.50, σ = 1.73) scored similar compared to the controls (μ = 29.67, σ = 0.82)($p = 0.18$). Frontal function deficits were tested by completing the Frontal Assessment Battery (FAB) [5]. Only subjects who showed no or limited frontal function deficits were included (FAB $\geq$ 13). No significant difference between the patients (μ = 16.25, σ = 1.50) and the control group (μ = 17.50, σ = 0.84) was found ($p = 0.13$). The general motor function of PD patients was assessed by using part III of the Movement Disorders Society Unified Parkinson's Disease Rating Scale (MDS-UPDRS) [3]. Using the results of the MDS-UPDRS a Hoehn & Yahr stage could be determined [6]. Patients with a Hoehn & Yahr score above 3 were excluded.

Table I: Subject group

control	age	sex	MMSE	FAB	H&Y
(1)	51	f	30	17	-
(2)	55	m	28	18	-
(3)	58	f	30	18	-
(4)	59	m	30	18	-
(5)	60	f	30	16	-
(6)	63	m	30	18	-
patient	**age**	**sex**	**MMSE**	**FAB**	**H&Y**
(1)	67	m	30	15	II
(2)	65	f	29	17	I
(3)	51	m	26	15	II
(4)	62	f	29	18	0-I

B. Procedure

Upon arrival, subjects completed the MMSE [27] and FAB [5] questionnaires. Thereafter they were asked to perform several tapping tasks, similar to previous experiments by Muilwijk et al. [9] and De Boer et al. [8]. Finally, our tracking task was conducted. The time subjects needed to perform the complete experiment was on average sixty minutes.

This paper focuses on the obtained tracking task data. Before the first run a familiarization run was performed. In this run no moving target was present but it could be used to familiarize with the setup and the dynamics of the controlled system. Subjects were asked to perform a total of eight 50 second runs. The last 40.96 seconds of the runs were used as measurement data. This allows for a run-in time of 9.04 seconds in which subjects could adapt to the task. A performance score was shown after each run, to stimulate subjects to perform at their best level. From the eight runs, the last three runs were selected as measurement data. It was found that the last three runs showed stabilized performance. The total time spent tracking was approximately ten minutes. Patient 1 only performed six runs due to time constraints, other subjects completed all eight planned runs. For every run the gaze, g, was recorded as well. However, for two subjects the eye tracking data was not valid. In these cases the eye tracking system failed to register the eyes correctly. Therefore, the gaze data of subjects Control 4 and Patient 1 were declared invalid.

C. Apparatus

The experiment was performed using a setup of the Erasmus Medical Center at Rotterdam, see Fig. 1. The setup is similar to the one used by Muilwijk et al. [28] and De Boer et al. [26]. A HOTAS Warthog joystick (Thrustmaster, Hillsboro, Oregon, USA) was added to the setup to give control inputs. The main spring was removed from the joystick to reduce the breakout force. The original, heavy, fighter handle was replaced by a light custom grip for comfort and to avoid distraction caused by the buttons. The gaze of the eyes was registered using an infrared video eye tracking system (Chronos Vision,

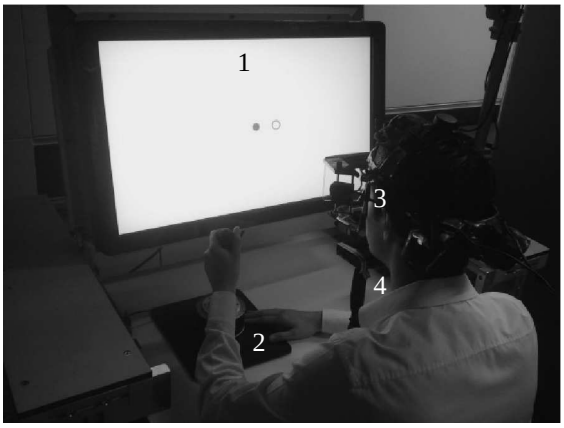

Figure 1: A subject seated in the measurement setup consisting of a screen (1), a modified HOTAS Warthog joystick (2), an infrared eye tracking system (3), and a chin rest (4).

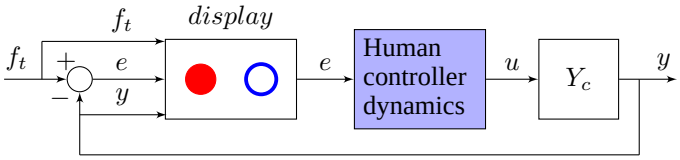

Figure 2: Control scheme studied in this paper.

Berlin, Germany). The subjects were seated in front of a 32-inch screen (ELO touch systems, Leuven, Belgium) on which the pursuit display was presented. Subjects needed to position their head on a chin rest to ensure minimal head movement and to ensure a fixed position for the eye-tracking system.

D. Control task

PD patients and a healthy control group were asked to perform a horizontal-axis target-following pursuit task similar to previous experiments involving PD [12], [14], [16]. A block diagram of this task is shown in Fig. 2. The task of the controller is to keep the error, e, as small as possible by controlling the dynamic system Y_c. Minimizing the error means keeping the system output, y, close to the target signal, f_t, thus: $e = f_t - y$. The error was presented by a pursuit display shown in Fig. 3. In Fig. 3 the red filled circle represents the system output and the blue circle moves according to the target signal. Thus, the task was to manually position the red circle on the moving blue circle.

E. Controlled element dynamics

Subjects had to control a system with single-integrator dynamics: $Y_c = K_c/s$. For single integrator dynamics, a deflection of the joystick gives the controlled element a proportionate velocity. This type of control is often used in daily

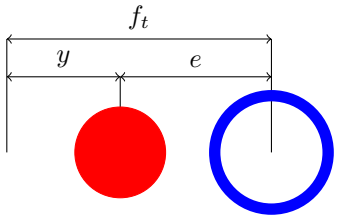

Figure 3: Pursuit display.

life, e.g., automobile heading control by using a steering wheel [17]. The gain constant, K_c, was chosen such that the subjects would never reach the stick deflection limits. A gain of $K_c = 2$ was found to be suitable.

F. Target signal

A quasi-random multisinus target signal, similar to Zaal et al. [29], was designed for the experiment. A multisine signal is preferred for the system identification method [18] and was created as described by Damveld et al. [30]. For this experiment the measurement time, T_m, was equal to 40.96 seconds. The measurement time was shorter compared to earlier identification experiments [29], [21] due to the vulnerable subject group. The signal was generated as a sum of $N_t = 11$ sinusoids, see Eq. (1).

$$f_t(t) = \sum_{k=1}^{N_t} A_t(k) sin[\omega_t(k)t + \phi_t(k)] \tag{1}$$

The frequencies, ω_t, are integer multiples of the base frequency $\omega_m = 2\pi/T_m$. Therefore, $\omega_t = n_t\omega_m$. Eleven frequencies were needed for a more or less equal distributed, on a logarithmic scale, target signal over a wide frequency range from 0.5 to 25 rad/s.

In Eq. (1), A_t represents the amplitude of each sine. The amplitudes were determined by applying a second-order low-pass filter from Zaal et al. [31], see Eq. (2).

$$H_A(j\omega) = \frac{(1 + T_{A_1} j\omega)^2}{(1 + T_{A_2} j\omega)^2} \tag{2}$$

In Eq. (2) $T_{A_1} = 0.1$ and $T_{A_2} = 0.8$. The filter reduces power at the higher frequencies. This results in a signal that is not overly difficult [31]. The amplitudes, combined with the filter, are plotted in Fig. 4.

Phases were selected from a large number of randomly generated sets of phases to achieve an average crest factor [30]. The numerical values of all target signal properties are given in Table II.

G. System identification

The subjects were asked to perform a target-following pursuit task. The combination of the target signal and the

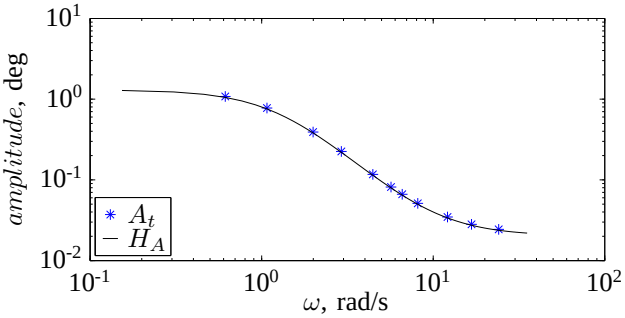

Figure 4: Spectrum of the target signal.

Table II: Target signal components

Target, f_t			
n_t,-	ω_t, rad/s	A_t, deg	ϕ_t, rad
4	0.614	1.079	7.239
7	1.074	0.776	0.506
11	1.994	0.391	7.860
17	2.915	0.225	8.184
23	4.449	0.117	9.012
29	5.676	0.082	6.141
37	6.596	0.066	6.776
53	8.130	0.051	6.265
79	12.118	0.035	4.432
109	16.720	0.028	2.672
157	24.084	0.024	8.009

controlled element reduces the need to use the extra information available (f_t and y) on a pursuit display [19]. Control behavior was based on the error, e, only. Therefore, single-loop identification could be used [23]. A block diagram as in Fig. 5 was adopted. In the diagram f_t is the input signal, e the error, n the remnant, u the control input, y the system output, Y_p the operator dynamics and Y_c the dynamics of the controlled element.

In a tracking task, the operator can be modeled as a quasi-linear controller [32]. The human operator will give a linear response to the error summed with the remnant. The remnant accounts for all the non-linearities in the operators control behavior [17], [33]. The remnant can be dropped if a multisine input signal is used that will give power at certain discrete frequencies [18]. At these frequencies, the signal to noise ratio is very high and the the remnant can be ignored. The frequency response should therefore only be estimated at the frequencies at which the input signal delivers power, ω_t:

$$\hat{Y}_p(j\omega_t) = \frac{U(j\omega_t)}{E(j\omega_t)} \tag{3}$$

It is possible to determine the magnitude and phase of the estimated frequency response. The result is an indication of the model that should be used to describe the operator in an optimal way. A well known model for an operator follows from the original crossover model of McRuer et al. [32] and is called the *extended crossover model*, see Eq. (4). In the model, K_p is the control gain, τ the reaction time delay and in the fraction T_L is the lead time constant and T_I the lag time constant.

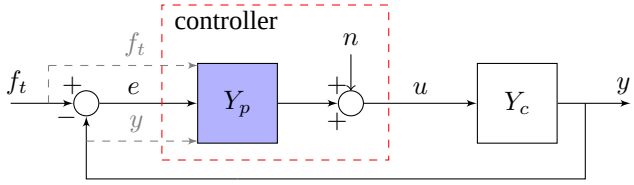

Figure 5: Block diagram of a pursuit target-following task.

Table III: Lower and upper bounds for the initial parameter vector

	K_p -	τ s	ω_{nms} rad/s	ζ_{nms} -
lower bound	0.0	0.0	0.0	0.0
upper bound	10.0	5.0	50.0	5.0

$$Y_p(j\omega) = \underbrace{K_p \frac{T_L j\omega + 1}{T_I j\omega + 1}}_{\text{pilot equalization}} e^{-j\omega\tau} \tag{4}$$

The model will adapt to the controlled element dynamics in such a way that the open-loop system will show single integrator dynamics around the crossover frequency [17]. Depending on the controlled element dynamics, the equalization part of the extended crossover model can be reduced to a pure gain, a pure lead or a pure lag [21]. To make the model valid over a wider frequency range the neuromuscular system dynamics are often included [34]. The neuromuscular system dynamics can be modeled as an second-order system [35], see Eq. (5). The parameters are the natural frequency, ω_{nms}, and the damping, ζ_{nms}.

$$Y_{nms}(j\omega) = \frac{\omega_{nms}^2}{(j\omega)^2 + 2\zeta_{nms}\omega_{nms} j\omega + \omega_{nms}^2} \tag{5}$$

In this experiment the controlled dynamics have single integrator dynamics and thus no lead or lag equalization is expected. This means the human is a proportional controller on e. Therefore, the human control model is reduced to:

$$Y_p(j\omega) = K_p \cdot e^{-j\omega\tau} \cdot Y_{nms}(j\omega) \tag{6}$$

A cost function is used to fit the model on the estimated frequency response function from (3). The cost function, that is to be minimized, used in this paper is:

$$CF(\theta) = \sum_{k=1}^{N_t} \|\hat{Y}_p(j\omega_t(k)) - Y_p(j\omega_t(k);\theta)\|^2 \tag{7}$$

The vector used for the optimization is $\theta = [K_p, \tau, \omega_{nms}, \zeta_{nms}]$. The optimization needed initial parameters. Hundred initial vectors were randomly generated within bounds as presented in Table III, based on Zaal et al. [29].

The model fitting approach was not successful for all collected data sets of patients. As can be seen in Fig. 6a

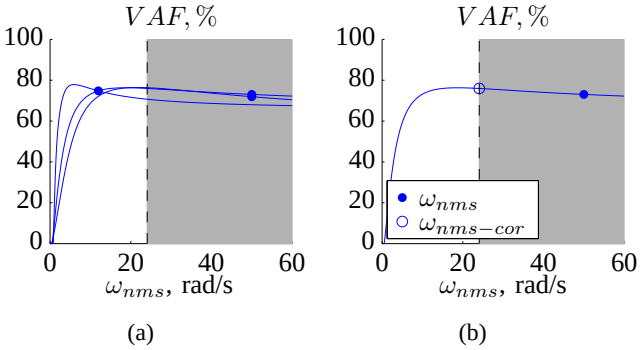

Figure 6: (a) Representative sensitivity parameters of Patient 3. The grey area is the part that lies outside the measurement range. The vertical line is positioned at the highest input frequency. (b) Corrected natural frequency of Patient 3 run 7.

values for ω_{nms} outside the input frequency range (indicated by the grey area) were estimated. The blue markers indicate the obtained result. A sensitivity analysis showed that these parameters were not very sensitive to change. The sensitivity analysis was done using the Variance Accounted for (VAF) [36]:

$$VAF = \left(1 - \frac{\sum_{i=0}^{N} |u(i) - \hat{u}(i)|^2}{\sum_{i=0}^{N} u^2(i)}\right) \times 100\% \quad (8)$$

In Eq. (8) u is the measured and $\hat{u}$ the modeled control signal. A VAF of 100% means that the model is capable of estimating the control signal perfectly. The parameters estimated outside the measurement range were corrected by choosing ω_{nms} at the maximum input frequency as shown in Fig. 6b.

Fig. 7 shows that the effect of the natural frequency correction on the frequency response function is minimal. Furthermore, this correction reduced the cost function only slightly.

H. Power spectrum integrals

To evaluate the collected error time signals in more detail the stepwise integrals of the error signals [37] are calculated. The final value of the integral should correspond with the variance of the signal. At the target signal frequencies steps in the integral are expected [37]. The magnitude of these steps might show in which frequency region patients and the control group have difficulties. To evaluate the integral in more detail an exponential model, Eq. (9) is fitted through the stepwise integrals, at the target signal frequencies, ω_t.

$$f(\omega_t) = K_f \cdot (1 - e^{-\frac{(\omega - \omega_f)}{\lambda_f}}) \quad (9)$$

In Eq. (9) K_f is a measure for the maximum value. ω_f can be used to determine the shift necessary for an optimal fit.

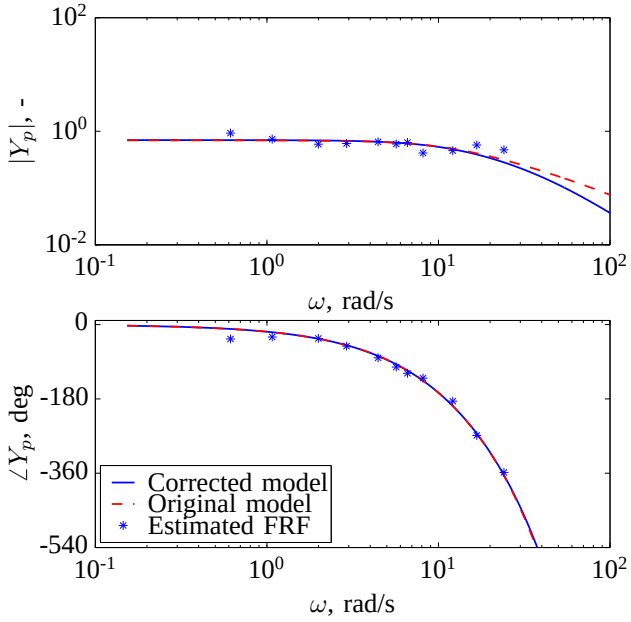

Figure 7: Frequency response function from patient 3, run 7.

λ_f indicates the steepness of the curve. The total difference between the error at the lowest frequency and the highest frequency, Δ, is calculated as in Eq. (10).

$$\Delta = max(f(\omega_t)) - min(f(\omega_t)) \quad (10)$$

I. Relative remnant

The ratio of coherent output to total output can be calculated by the relative remnant [17], as in Eq. (11).

$$\rho_c^2(j\omega_t) = 1 - \frac{\tilde{S}_{cc,n}(j\omega_t)}{S_{cc}(j\omega_t)} \quad (11)$$

In the equation $\tilde{S}_{cc,n}$ is the power of the remnant at an input frequency. The power of the remnant at a certain input frequency was estimated by taking the average power of two data points before and two data points after that input frequency, as indicated by the blue line in Fig. 8. S_{cc} is the power of a selected measured variable, like the gaze, g.

The relative remnant is normally between zero and one, where one indicates a perfect linear response.

J. Dependent measures

During each run of the tracking task several variables were recorded. Time traces of the control signal, u, the error signal, e, the target signal, f_t, the output, y and the gaze, g, were used to calculate dependent variables. The depended variables give insight into the influences of PD on patients while performing a pursuit tracking task.

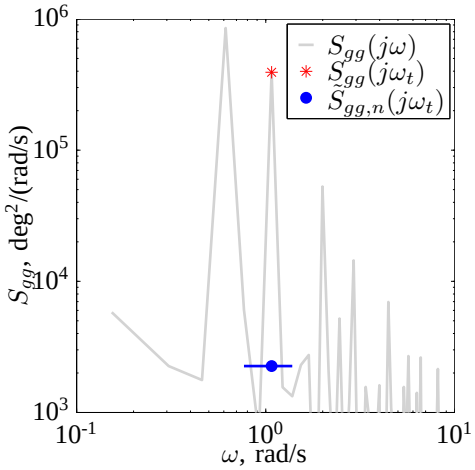

Figure 8: Example data points for relative remnant for a gaze signal of Patient 3, run 7.

1) Tracking performance and control activity: The variance of the error divided by the variance of the target signal is used as a measure for tracking performance, σ_e^2/σ_{ft}^2.

This gives a normalized performance metric. If the metric is below one it means that the controller is reducing the error. If the metric is above one the controller is increasing the error and a better strategy would be not controlling at all (which results in a metric equal to one).

The control activity is calculated as the variance of the control signal divided by the variance of the target signal, σ_u^2/σ_{ft}^2.

When this metric is relatively high it means the controller puts in a lot of effort to control the system while if the score is relatively low the controller is more relaxed.

2) Power spectrum integrals: To evaluate the tracking performance in more detail the the power spectrum integrals of the normalized error are calculated. They are used to determine the contribution of each input frequency to the error [37]. An exponential model with three parameters (K_f, ω_f and λ_f) is fitted to the power spectrum integral at the input frequencies. The stepwise integrals combined with the exponential model might show in which frequency region control problems occur for the patients and the control group.

3) Pilot model parameters: The pilot model parameters (K_p,τ,ω_{nms} and ζ_{nms}) of the measurement runs are estimated using the Fourier coefficient method [18]. Differences in these parameters might indicate difference in behavior between the PD patients and the control group.

4) HC modeling accuracy: To check the quality of the model fits the Variance Accounted for (VAF) is used, as defined in Eq. (8).

5) Relative remnant: The relative remnant of the control signal, Eq. (12), and the gaze, Eq. (13), are calculated.

$$\rho_u^2(j\omega_t) = 1 - \frac{\tilde{S}_{uu,n}(j\omega_t)}{S_{uu}(j\omega_t)} \tag{12}$$

$$\rho_g^2(j\omega_t) = 1 - \frac{\tilde{S}_{gg,n}(j\omega_t)}{S_{gg}(j\omega_t)} \tag{13}$$

The relative remnant of the control signal has a strong correlation with hand movements, while the relative remnant of the gaze correlates with eye movements. Therefore these metrics can be used to quantify the degradation in eye and hand movements due to PD.

K. Hypotheses

Four hypotheses were proposed.

H.I We expect that the score parameter of PD patients will be higher compared to the control group. This was found in previously performed experiments including PD patients [12], [14], [15], [16].

H.II A difference in performance could be explained by a difference in the human control model parameters. A high control gain, K_p, combined with a low delay, τ, normally indicates a good performance [17]. Therefore, it is expected that patients will have a lower control gain [14] and a higher time delay compared to the control group [13].

H.III Due to the eye-hand coordination deficiencies in PD patients it is expected to see a difference in the identified neuromuscular system parameters. It is expected that the ω_{nms} will be lower for PD patients, due to lower muscle tension [38]. The ζ_{nms} is expected to be higher due to bradykinesia (slowness in movement) [14], one of the symptoms of PD.

H.IV The relative remnant of the control signal, ρ_u^2, of PD patients is expected to be lower compared to the control group, especially at the higher frequencies. Hand movements were found earlier to be slower for PD patients [8] which makes it harder to react on the high frequencies. Similar results are expected for the relative remnant of the gaze, ρ_g^2.

IV. Results

A. Tracking performance and control activity

To evaluate the difference between the PD patients and the control group the tracking performance and the control activity are evaluated, see Fig. 9. In this figure the variance bars indicate the 95% confidence intervals.

Fig. 9(a) shows that PD patients performed significantly ($p \leq 0.001$) worse compared to the control group. This is as expected [12], [16]. For the control activity, in Fig. 9(b), no significant difference was found. However, it can be seen that the patients show a larger spread, which could indicate a greater variety within the PD patients group.

The integrals of the error power spectra are plotted in Fig. 10(a). Fig. 10(a) shows patients already perform worse for the lowest input frequency. At higher input frequencies the integral flattens since they contribute little to the error.

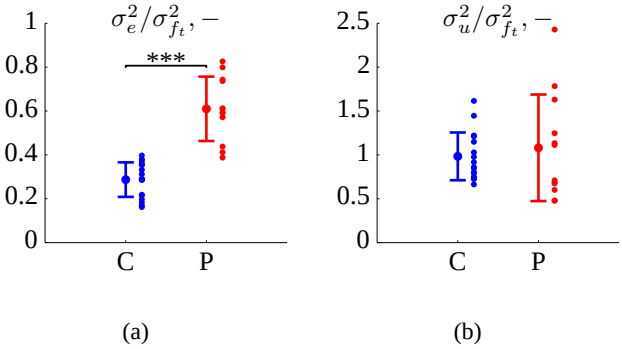

Figure 9: Tracking performance and control activity. (a) Score parameter. (b) Normalized control activity.

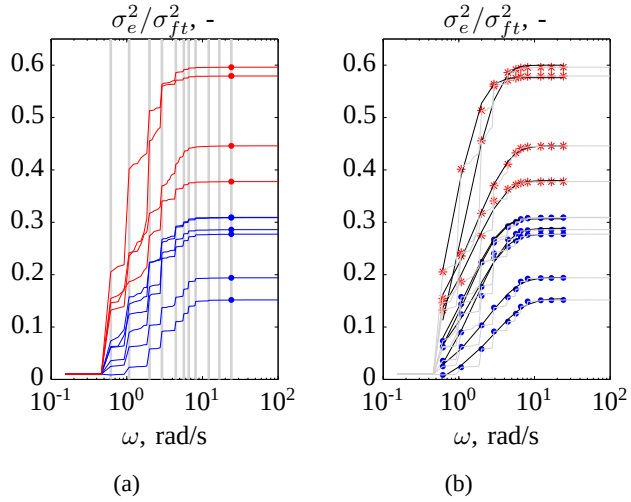

Figure 10: Integral of the power spectrum of the error signal. Red data is from patients and blue from the control group. (a) The dots indicate the variance of the signal. The vertical grey lines indicate the input frequencies. (b) The dots indicate the power of the power spectrum at the input frequencies. The black lines represent the exponential models fitted through the dots.

The difference between the error power spectra was evaluated by fitting an exponential model (Eq. (9)) to the data, see Fig. 10(b). It can be seen that the exponential model is able to capture the general shape of the integral.

The results of the parameter estimation for the exponential model are presented in Fig. 11. Fig. 11a shows that the higher total error for PD patients results in a higher K_f. Fig. 11b shows that ω_f is not significantly different. However, for the patient data points two pairs can be seen, one pair with positive values and one pair with negative values. This is due to the different model steepness of the two pairs, expressed by λ_f. A lower value of λ_f means a steeper curve. For λ_f the difference between the patients and the control group was not significant, but a trend is visible, see Fig. 11c. It seems that the curve of

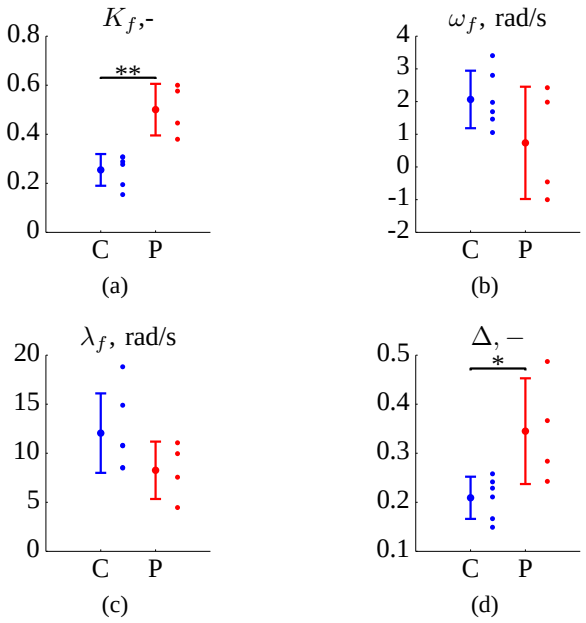

Figure 11: Parameters estimated for the exponential function.

the PD patients tends to be steeper. This is mostly determined by the lower input frequencies and suggest that patients show reduced performance at the low frequencies. Δ is plotted in Fig. 11d and shows that patients not only started with a larger error, but also kept increasing the difference for the consecutive frequencies.

B. Frequency response function

Using the methods described in Section III the frequency response function, $\hat{Y}_p$, of the subjects can be estimated. Representative frequency responses and fitted models, Y_p, of a patient and a control are plotted in Fig. 12. It can be seen that the model correspond good with the estimated frequency responses. The subjects show proportional, gain-like, control dynamics. The gain of the control group is higher and the peak due to the neuromuscular system is more pronounced. For other subjects similar model fits were found. The absence of the neuromuscular peak for the patients made it difficult to estimate the neuromuscular parameters, as explained in Section III-G.

C. Human control model parameters

The human control model has four parameters (K_p, τ, ω_{nms} and ζ_{nms}) to be estimated. The results of the estimation can be found in Fig 13, with their 95% confidence intervals.

The gain and the time delay are the key contributions for performance in our task [17]. In Fig. 13A the gains are plotted. It can be seen that the control group uses a higher gain, K_p, compared to the patients ($p < 0.01$). For the time delay, τ,

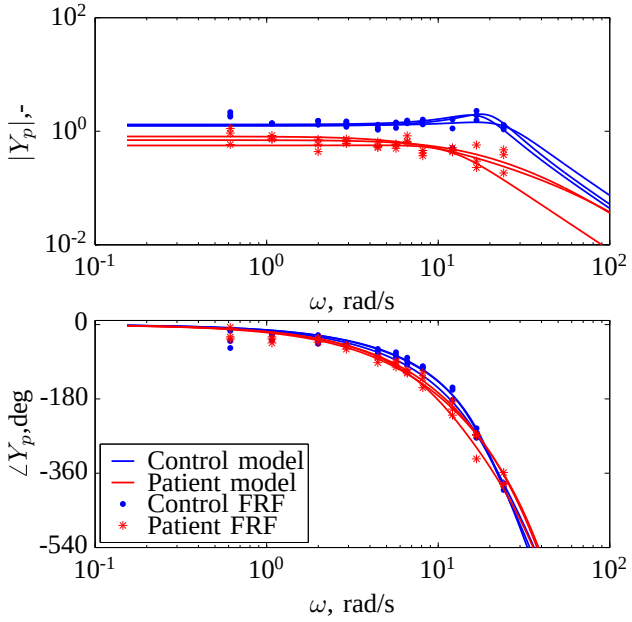

Figure 12: Frequency response functions and fitted models of the measurement runs from Control 1 and Patient 1. The dots indicate the estimated describing functions and the lines the fitted models.

the results are less distinctive, see Fig. 13B. Patients tend to have a similar or marginally higher time delay. Therefore, the difference in performance can mainly be explained by the difference in gain.

The damping parameter, ζ_{nms}, is presented in Fig. 13C. The damping is estimated higher for the patients compared to the control group. The neuromuscular frequency, ω_{nms}, remains approximately constant around 18 rad/s on average, see Fig. 13D.

D. Model fit quality

As defined by Eq. (8) the VAF is a measure to determine the quality of the model fit. A score of 60% means that the model is able to describe 60% of the measured data and 40% can be attributed to the remnant. Previous research showed that scores above the 60% make it possible for the model to describe the measured data in a realistic manner [29], [34], [33]. For the control group the behavior could be modeled correctly on average, as can be seen in Fig. 14. The VAFs of patients are modeled significantly lower compared to the control group ($p < 0.01$). This means that the model is better able to describe data from the control group. Two degraded VAFs stand out in the patient group, both below the 20%. They are both of Patient 1. An explanation might be the jerky, discontinues, control strategy of this subject. The identification method has difficulties in describing this type of behavior.

E. Relative remnant data

The relative remnant was calculated for the control signal and the gaze. Example time traces can be found in Fig. 15.

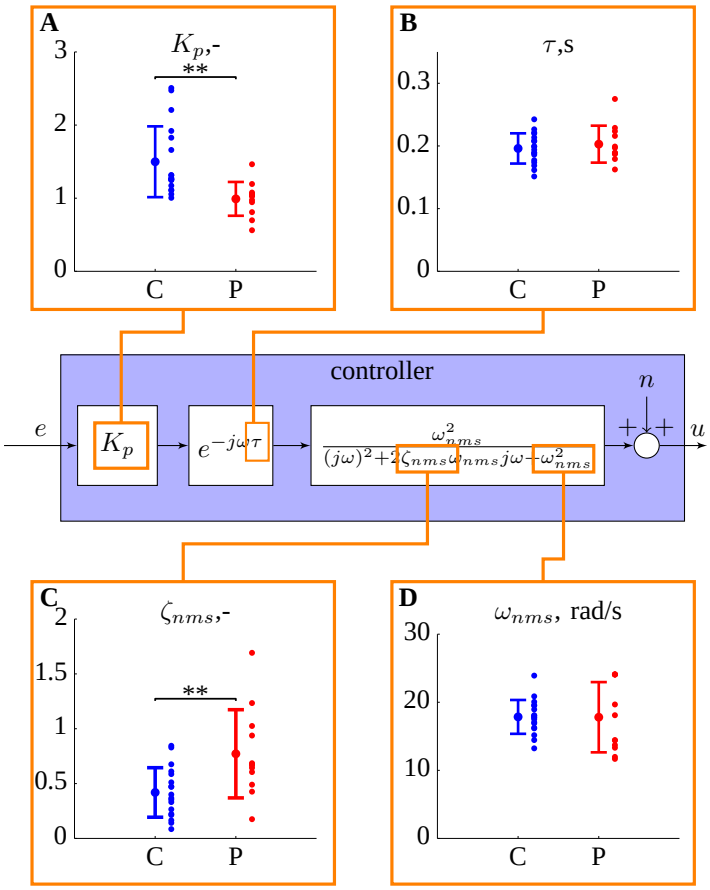

Figure 13: Results of the parameter estimation.

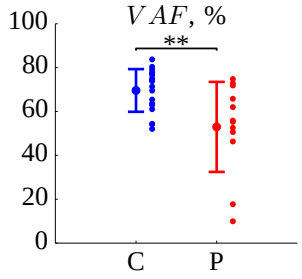

Figure 14: Quality of the model fits, using Eq. (8).

The traces are only shown between ten and thirty seconds for the sake of visibility. It can be seen that the subject's gaze is mostly directed on the target signal. The controlled element is following the target signal, but some delay and overshoot is present.

The relative remnant can be used to study the linearity of the subjects [17]. Normally, values are found between zero and one, but negative values are found when the average noise

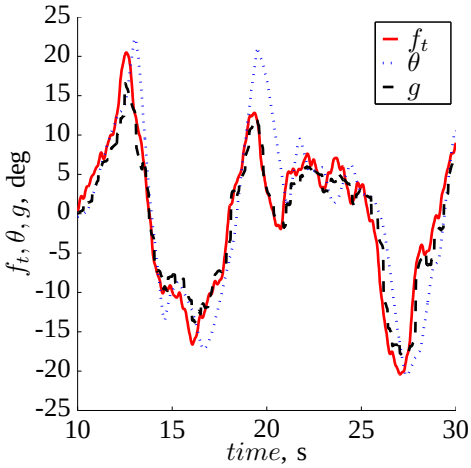

Figure 15: Representative time traces for the target signal from Control 6, run 8.

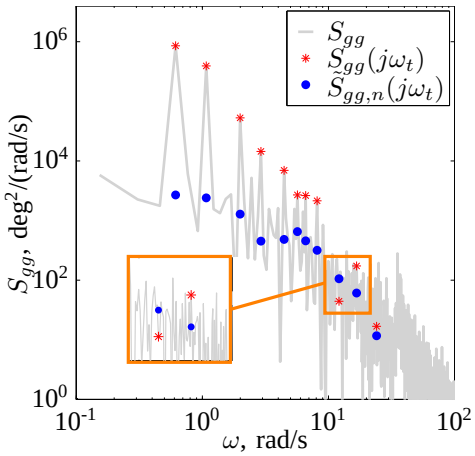

Figure 16: Relative remnant parameters for the gaze from Patient 3, run 7. An example is given in which the contribution of the remnant is higher compared to the power. Which results in a negative relative remnant value.

level is higher at a certain input frequency, as can be seen in Fig. 16.

In the relative remnant plots the data of the patients is shifted slightly to the right for visibility. In Fig. 17 the relative remnant of the control signal is plotted. For the low frequencies both groups are close to one, indication linear control on the low frequencies. For the higher frequencies the spread increases, especially for the patients group. Furthermore, the patients seem to have a lower ρ_u^2.

The relative remnant of the gaze data of the subjects is plotted in Fig. 18. A similar trend as in Fig. 17 is found. However, the difference between the control group and patients is more distinct. The control group was able to provide linear

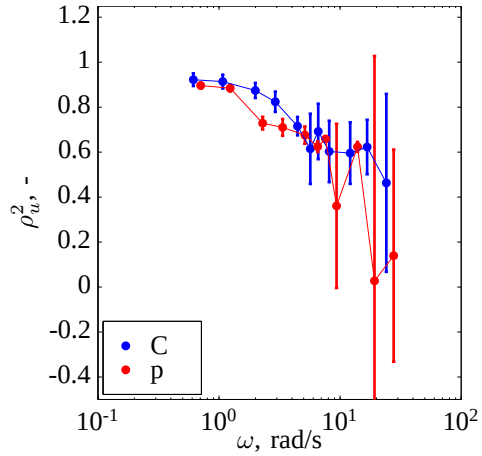

Figure 17: Relative remnant of the control input.

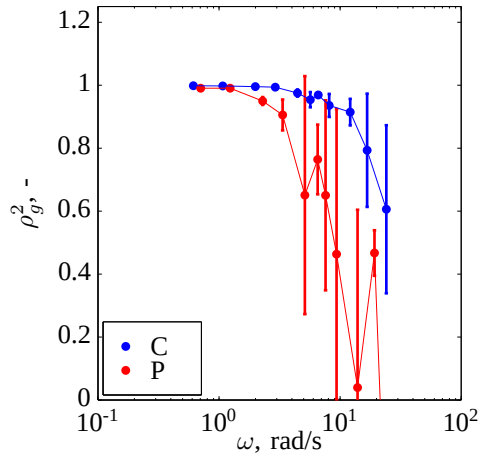

Figure 18: Relative remnant of the gaze.

gaze up to higher frequencies.

The relative remnant data results suggest that for both the eye and hand movements the patients are less able to provide linear control.

V. Discussion

The goal of this paper was to quantify the loss of motor skill due to PD, using human operator modeling. A single-axis pursuit tracking task, with a controlled element with single integrator dynamics, was performed by four patients and six healthy controls. The collected data showed a distinct difference in task performance between patients and the control group. To performance of the control group was on average 112% better compared to patients. This difference was as expected (Hypothesis I) [12], [14], [15], [16]. A more detailed analysis based on the error power spectrum showed that the

difference in tracking accuracy already occurred in the low frequency region.

Hypothesis II expected patients to have a lower control gain and a higher time delay compared to the control group. This hypothesis can be partly confirmed. The control gain of the control group was on average 51% higher compared to patients, similar to [14]. Hufschmidt et al. attributed the lower gain of PD patients to a basic abnormality of motor behavior, such as the lack of motor initiative [14]. The time delay showed no significant difference between patients and the control group, in contrast to earlier studies [13]. The inclusion of only early-stage PD patients might be the reason no significant difference was found. Summarizing, the difference in performance could be almost completely attributed to a difference in control gain.

Hypothesis III expected a lower neuromuscular frequency and a higher damping for patients. This hypothesis could only be partly confirmed. However, the results have to be treated carefully since the neuromuscular dynamics were indeed difficult to identify for some patients. The damping was found to be 84% higher for patients. Specific PD symptoms,like bradykinesia and rigidity, could be an explanation [14]. For the neuromuscular frequency no significant difference was found. The neuromuscular frequency of patients was expected to be lower compared to the control group [38]. A combination of identification difficulties (especially the low sensitivity of the parameter, as explained in Section III-G) and the early stage of the patients might explain why this hypotheses could not be completely confirmed.

Hypothesis IV expected the relative remnant of the control signal and the gaze to be lower for patients compared to the control group. This hypothesis can be confirmed. The lower relative remnant for the control signal can be partly attributed to the slower hand movements [8]. It is related to the lower relative remnant for the gaze. The relative remnant of the gaze shows that patients already have problems with processing the visual input. Therefore it can be expected that their control input will be affected by the impaired visual input. The gaze data could not be obtained for all subjects, therefore this results should be treated carefully as well.

For this study six healthy controls and four PD patients were included. For a better insight more subjects should participate. The quality of the data is affected by the measurement setup [18]. The joystick had a break-out force of 3.6N, which is not favorable in these type of experiments. A break-out force prevents subjects from controlling on the high frequencies. The measurement time of 40.96 seconds in combination with a sampling rate of 50 Hz results in 2048 data points available for identification. This is relatively low compared to similar tracking experiments [39], [33]. This is the reason MLE identification was not used, since it needs more samples [20].

Despite the limitations of the study, a clear distinction was found between the patients and the control group. The questionnaires were not able to differentiate between the control group and the patients, see Table I, while the tracking performance showed a significant difference between the two groups. Therefore, tracking tasks show potential as an additional diagnostic tool. More research should be done on the subject. This paper has not evaluated the behavior of PD patients in a preview task [40], [22]. Since it is known that PD patients depend more on visual information [41], [13] a preview tracking task might reveal further aspects of degraded eye-hand control. Another tracking task might use the touch screen as input device, instead of the joystick. The used neuromuscular model lumps the neuromuscular and input device systems together [35]. Taking the joystick out of the loop might improve the estimation of the neuromuscular parameters. It could also reveal other motor constraints in PD, since larger movements have to be made by the subjects.

VI. Conclusion

This paper investigated if human operator modeling can be used to quantify loss of motor skills due to PD. A human-in-the-loop experiment was performed and using single-loop identification the control behavior of subjects could be modeled. Patients performed worse compared to the control group. Identified parameters from the human operator model were used to quantify the motor skill of subjects. A human operator model of four parameters (K_p,τ,ω_{nms} and ζ_{nms}) was used from which two (K_p and ζ_{nms}) were significantly different between patients and the control group.

It is concluded that the pursuit tracking task was able to quantify and detect the loss of motor skills due to PD. For the modest samples size collected, the tracking task was able to objectively distinguish between early-stage patients and healthy subjects. In the future, a tracking task might be used as an additional diagnostic tool for early detection of PD. Another application could be monitoring the effect of medication on a patient's (fine) motor skills. An accurate and straight forward quantification of motor skills makes it easier to determine an optimal medication dose.

References

[1] L. M. L. De Lau and M. M. B. Breteler, "Epidemiology of Parkinson's disease." *The Lancet. Neurology*, vol. 5, no. June, pp. 525–535, 2006.

[2] A. J. Lees, J. Hardy, and T. Revesz, "Parkinson's disease," *The Lancet*, vol. 373, no. 9680, pp. 2055–2066, 2009.

[3] C. G. Goetz, S. Fahn, P. Martinez-Martin, W. Poewe, C. Sampaio, G. T. Stebbins, M. B. Stern, B. C. Tilley, R. Dodel, B. Dubois, R. Holloway, J. Jankovic, J. Kulisevsky, A. E. Lang, A. Lees, S. Leurgans, P. a. LeWitt, D. Nyenhuis, C. W. Olanow, O. Rascol, A. Schrag, J. a. Teresi, J. J. Van Hilten, and N. LaPelle, "Movement disorder society-sponsored revision of the unified Parkinson's disease rating scale (MDS-UPDRS): Process, format, and clinimetric testing plan," *Movement Disorders*, vol. 22, no. 1, pp. 41–47, 2007.

[4] S. Fahn and R. Elton, "Unified rating scale for parkinson's disease," *Recent developments in Parkinson's disease. Florham Park. New York: Macmillan*, pp. 153–163, 1987.

[5] B. Dubois, A. Slachevsky, I. Litvan, and B. Pillon, "The FAB: A Frontal Assessment Battery at Bedside," *Neurology*, vol. 55, no. 11, pp. 1621–1626, 2000.

[6] M. M. Hoehn, M. D. Yahr *et al.*, "Parkinsonism: onset, progression, and mortality," *Neurology*, vol. 50, no. 2, pp. 318–318, 1998.

[7] E. Kandel, J. H. Schwartz, T. M. Jessell, and S. Mack, *Principles of Neural Science*. New York, Chicago, San Francisco: McGraw-Hill Medical, 2013.

[8] C. De Boer, J. Van Der Steen, R. J. Schol, and J. J. M. Pel, "Repeatability of the timing of eye-hand coordinated movements across different cognitive tasks," *Journal of Neuroscience Methods*, vol. 218, no. 1, pp. 131–138, 2013.

[9] D. Muilwijk, S. Verheij, J. J. M. Pel, A. J. W. Boon, and J. Van Der Steen, "Changes in Timing and kinematics of goal directed eye-hand movements in early-stage Parkinson's disease." *Translational neurodegeneration*, vol. 2, no. 1, p. 1, 2013.

[10] K. J. Cassell, "The usefulness of a temporal correlation technique in the assessment of human motor performance on a tracking device," *Medical and biological engineering*, vol. 11, no. 6, pp. 755–761, 1973.

[11] O. T. Andersen, "A system for quantitative assessment of dyscoordination and tremor," *Acta Neurologica Scandinavica*, vol. 73, no. 3, pp. 291–294, 1986.

[12] K. Flowers, "Some frequency response characteristics of parkinsonism on pursuit tracking," *Brain*, vol. 101, no. 1, pp. 19–34, 1978.

[13] R. D. Jones and I. M. Donaldson, "Tracking tasks and the study of predictive motor planning in Parkinson's disease," *Images of the Twenty-First Century. Proceedings of the Annual International Engineering in Medicine and Biology Society,*, pp. 1055–1056, 1989.

[14] A. Hufschmidt and C.-H. Lücking, "Abnormalities of tracking behavior in parkinson's disease," *Movement disorders*, vol. 10, no. 3, pp. 267–276, 1995.

[15] R. D. Jones and I. M. Donaldson, "Removal of the Visuospatial Component from Tracking Performance and its Application to Parkinson' s Disease," *IEEE Transactions On Biomedical Engineering*, vol. 43, no. 10, pp. 1001–1010, 1996.

[16] P. Soliveri, R. G. Brown, M. Jahanshahi, T. Caraceni, and C. D. Marsden, "Learning manual pursuit tracking skills in patients with Parkinson's disease," *Brain*, vol. 120, no. 8, pp. 1325–1337, 1997.

[17] D. T. McRuer, D. Graham, E. S. Krendel, and W. J. Reisener, "Human Pilot Dynamics in Compensatory Systems, Theory Models and Experiments with Controlled Element and Forcing Function Variations," Air Force Flight Dynamics Laboratory, Wright-Patterson Air Force Base (OH), Wright-Patterson AFB (OH), Technical Report AFFDL-TR-65-15, 1965.

[18] M. M. van Paassen and M. Mulder, "Identification of Human Operator Control Behaviour in Multiple-Loop Tracking Tasks," in *Proceedings of the Seventh IFAC/IFIP/IFORS/IEA Symposium on Analysis, Design and Evaluation of Man-Machine Systems, Kyoto Japan*. Pergamon, 1998, pp. 515–520.

[19] R. J. Wasicko, D. T. McRuer, and R. E. Magdaleno, "Human pilot dynamic response in single-loop systems with compensatory and pusuit displays," *Air Force Flight Dynamics Laboratory*, vol. Tech. Rep. No. AFFDL-TR-66-137, 1967.

[20] P. M. T. Zaal, D. M. Pool, Q. P. Chu, M. Mulder, M. M. Van Paassen, and J. A. Mulder, "Modeling Human Multimodal Perception and Control Using Genetic Maximum Likelihood Estimation," *Journal of Guidance, Control, and Dynamics*, vol. 32, pp. 1089–1099, 2009.

[21] D. M. Pool, P. M. T. Zaal, H. J. Damveld, M. M. Van Paassen, J. C. Van Der Vaart, and M. Mulder, "Modeling Wide-Frequency-Range Pilot Equalization for Control of Aircraft Pitch Dynamics," *Journal of Guidance, Control, and Dynamics*, vol. 34, no. 5, pp. 1529–1542, 2011.

[22] K. van der El, D. M. Pool, H. J. Damveld, M. M. Van Paassen, and M. Mulder, "An Empirical Human Controller Model for Preview Tracking Tasks," *IEEE Transactions on Cybernetics*, 2015.

[23] M. C. Vos, D. M. Pool, H. J. Damveld, M. M. van Paassen, and M. Mulder, "Identification of multimodal control behavior in pursuit tracking tasks," in *Systems, Man and Cybernetics (SMC), 2014 IEEE International Conference on*, Oct 2014, pp. 63–68.

[24] V. S. Chakravarthy, D. Joseph, and R. S. Bapi, "What do the basal ganglia do? A modeling perspective." *Biological Cybernetics*, vol. 103, no. 3, pp. 237–253, 2010.

[25] O. Hikosaka, Y. Takikawa, and R. Kawagoe, "Role of the basal ganglia in the control of purposive saccadic eye movements." *Physiological reviews*, vol. 80, no. 3, pp. 953–978, 2000.

[26] C. de Boer, J. J. Pel, J. J. van den Dorpel, A. J. Boon, and J. van der Steen, "Behavioral Inhibition Errors in Parkinson's Disease Tested Using an Antisaccade and Antitapping Task," *Journal of Parkinson's disease*, vol. 4, no. 4, pp. 599–608, 2014.

[27] M. F. Folstein, S. E. Folstein, and P. R. McHugh, "Mini-mental state: a practical method for grading the cognitive state of patients for the clinician," *Journal of psychiatric research*, vol. 12, no. 3, pp. 189–198, 1975.

[28] D. Muilwijk, S. Verheij, J. J. M. Pel, A. J. W. Boon, and J. Van Der Steen, "Changes in Timing and kinematics of goal directed eye-hand movements in early-stage Parkinson's disease." *Translational neurodegeneration*, vol. 2, no. 1, p. 1, 2013.

[29] P. M. T. Zaal, D. M. Pool, Q. P. Chu, M. M. Van Paassen, M. Mulder, and J. A. Mulder, "Modeling Human Multimodal Perception and Control Using Genetic Maximum Likelihood Estimation," *Journal of Guidance, Control, and Dynamics*, vol. 32, no. 4, pp. 1089–1099, 2009.

[30] H. J. Damveld, G. C. Beerens, M. M. Van Paassen, and M. Mulder, "Design of Forcing Functions for the Identification of Human Control Behavior," *Journal of Guidance, Control, and Dynamics*, vol. 33, no. 4, pp. 1064–1081, Jul. 2010.

[31] P. M. T. Zaal, D. M. Pool, J. De Bruin, M. Mulder, and M. M. Van Paassen, "Use of Pitch and Heave Motion Cues in a Pitch Control Task," *Journal of Guidance, Control, and Dynamics*, vol. 32, no. 2, pp. 366–377, 2009.

[32] D. T. McRuer and H. R. Jex, "A Review of Quasi-Linear Pilot Models," *IEEE Transactions on Human Factors in Electronics*, vol. HFE-8, no. 3, 1967.

[33] D. M. Pool, M. M. Van Paassen, and M. Mulder, "Modeling Human Dynamics in Combined Ramp-Following and Disturbance-Rejection Tasks," *AIAA Modeling and Simulation Technologies Conference*, no. August, 2010.

[34] H. G. H. Zollner, D. M. Pool, H. J. Damveld, M. M. van Paassen, and M. Mulder, "The Effects of Controlled Element Break Frequency on Pilot Dynamics During Compensatory Target-Following," in *Proceedings of the AIAA Guidance, Navigation, and Control Conference 2 - 5 August 2010, Toronto, Ontario Canada*, M. Silvestro, Ed., no. AIAA 2010-8092, American Institute of Aeronautics and Astronautics. American Institute of Aeronautics and Astronautics, Aug. 2010, pp. 1–12.

[35] H. J. Damveld, D. A. Abbink, M. Mulder, M. Mulder, M. M. van Paassen, F. C. T. van der Helm, and R. J. A. W. Hosman, "Measuring the Contribution of the Neuromuscular System During a Pitch Control Task," in *Proceedings of the AIAA Modeling and Simulation Technologies Conference, Chicago (IL)*, no. AIAA-2009-5824, Aug. 2009.

[36] F. M. Nieuwenhuizen, P. M. T. Zaal, M. Mulder, M. M. van Paassen, and J. A. Mulder, "Modeling Human Multichannel Perception and Control Using Linear Time-Invariant Models," *Journal of Guidance, Control, and Dynamics*, vol. 31, no. 4, pp. 999–1013, July-August 2008.

[37] G. C. Beerens, H. J. Damveld, M. Mulder, and M. M. van Paassen, "Design of Forcing Functions for the Identification of Human Control Behavior," in *Proceedings of the AIAA Modeling and Simulation Technologies Conference, Chicago, Illinois, Aug. 10-13, 2009*. American Institute of Aeronautics and Astronautics, Aug. 2009.

[38] D. M. Corcos, C.-M. Chen, N. P. Quinn, J. McAuley, and J. C. Rothwell, "Strength in parkinson's disease: Relationship to rate of force generation and clinical status," *Annals of Neurology*, vol. 39, no. 1, pp. 79–88, 1996.

[39] F. M. Drop, D. M. Pool, H. J. Damveld, M. M. Van Paassen, and M. Mulder, "Identification of the Feedforward Component in Manual Control With Predictable Target Signals," *IEEE Transactions on Cybernetics*, vol. 43, no. 6, pp. 1936–1949, Dec. 2013.

[40] K. Ito and M. Ito, "Tracking Behavior of Human Operators in Preview Control Systems," *Electrical Engineering in Japan (English translation of Denki Gakkai Ronbunshi)*, vol. 95, no. 1, pp. 120–127, 1975.

[41] J. Cooke, J. Brown, and V. Brooks, “Increased dependence on visual information for movement control in patients with parkinson’s disease,” *Canadian Journal of Neurological Science*, vol. 5, no. 4, pp. 413–415, 1978.

Part II

Paper Appendices

Appendix A

FRFs and human operator models

In this chapter the operator describing functions and the fitted human operator models of all subjects and all performed runs are found in Section A-1. For the experiment only the last three runs were used as measurement data. The numerical values of the estimated parameters from the measurement runs are presented in Section A-2. Finally, in Section A-3 the crossover frequencies and the phase margins are plotted.

A-1 FRFs and fitted models

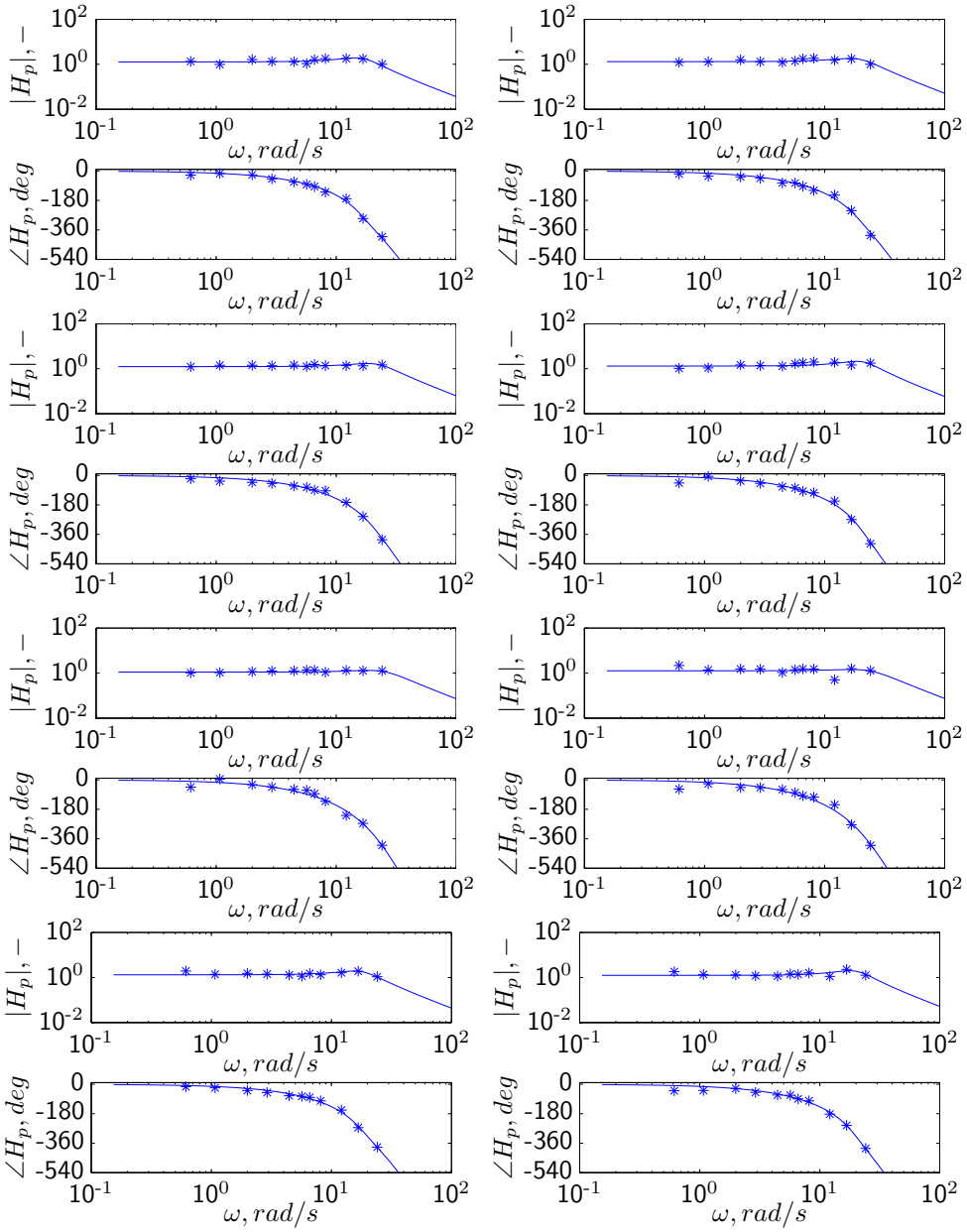

Figure A-1: FRFs and fitted models for all performed runs of Control 1.

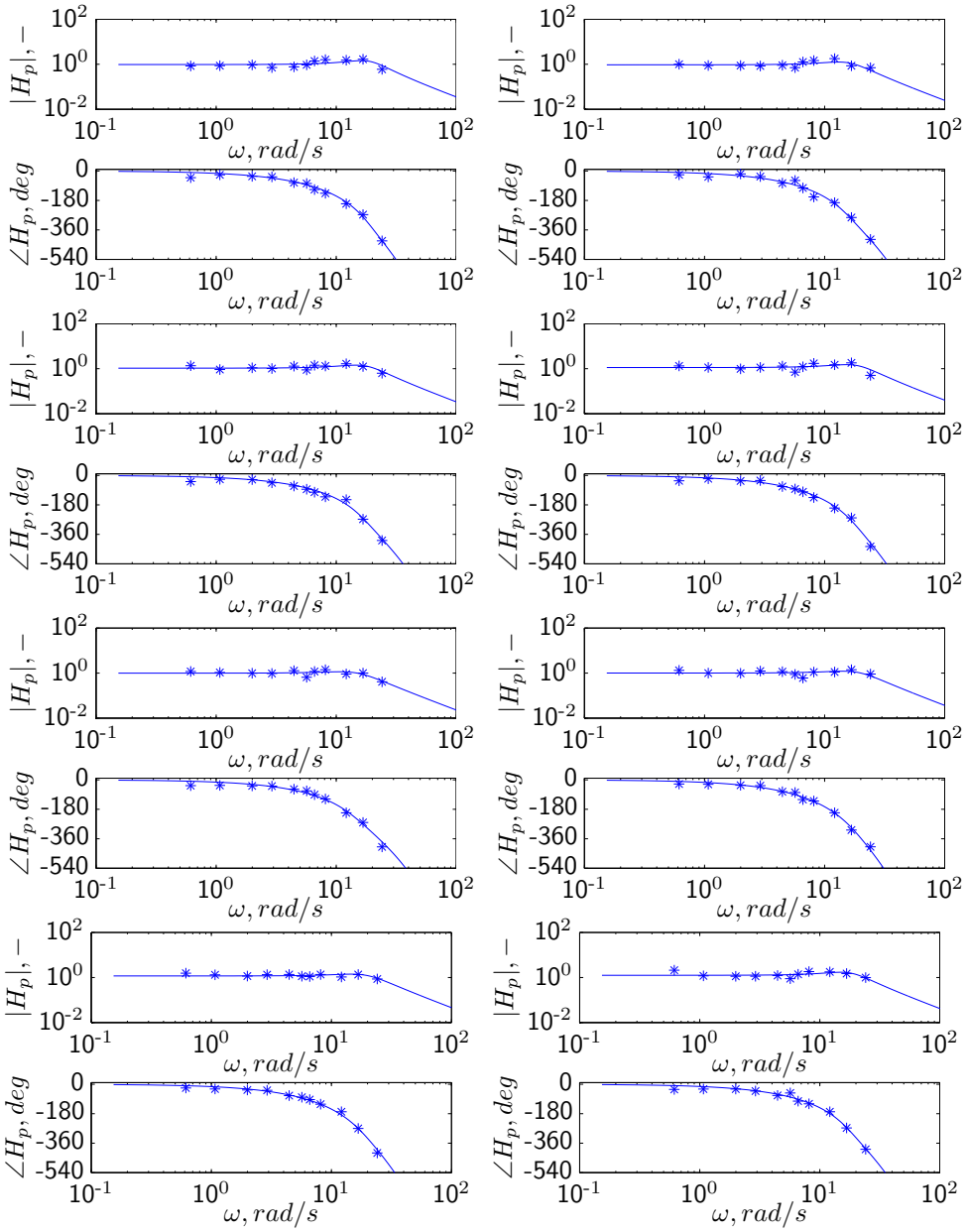

Figure A-2: FRFs and fitted models for all performed runs of Control 2.

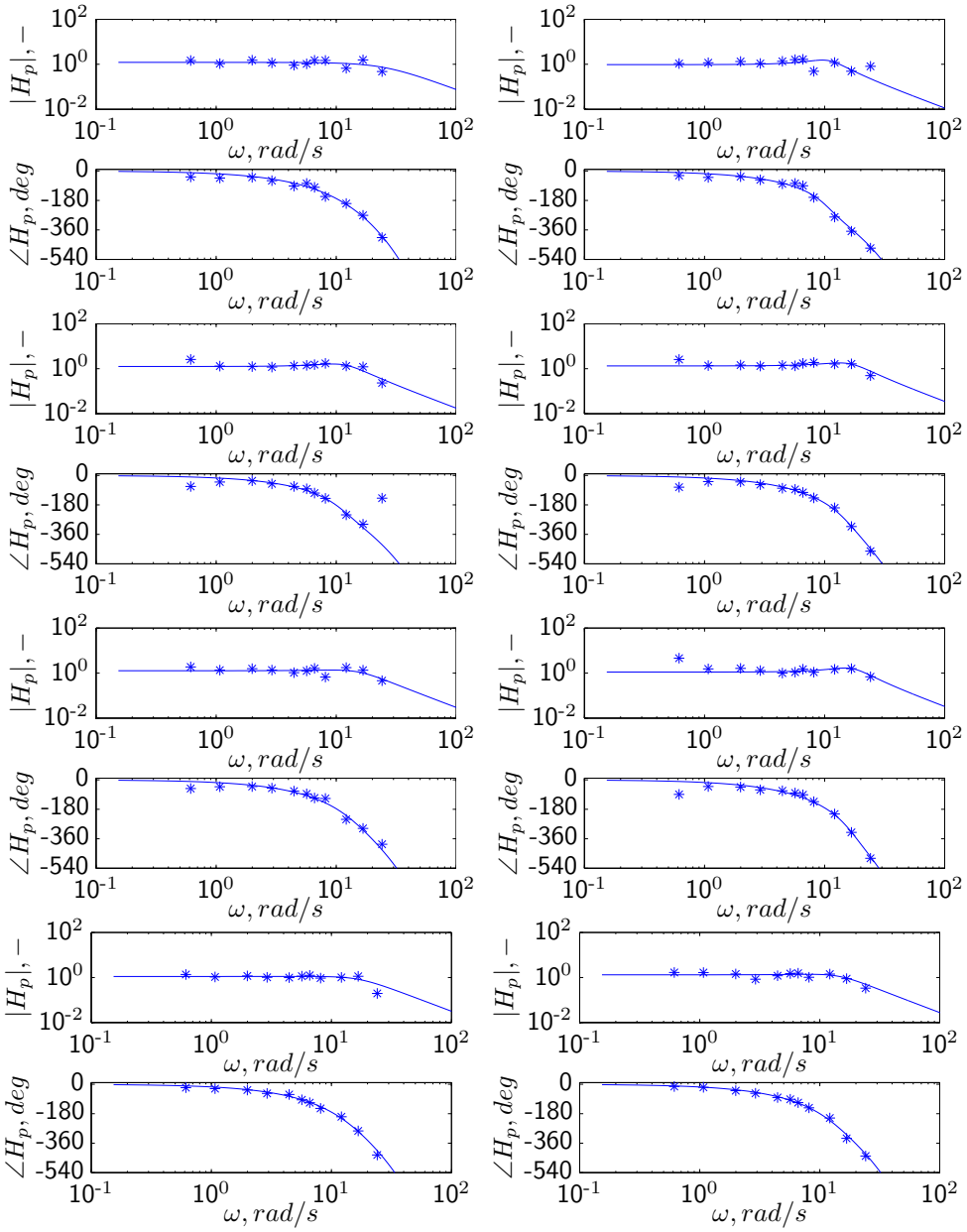

Figure A-3: FRFs and fitted models for all performed runs of Control 3.

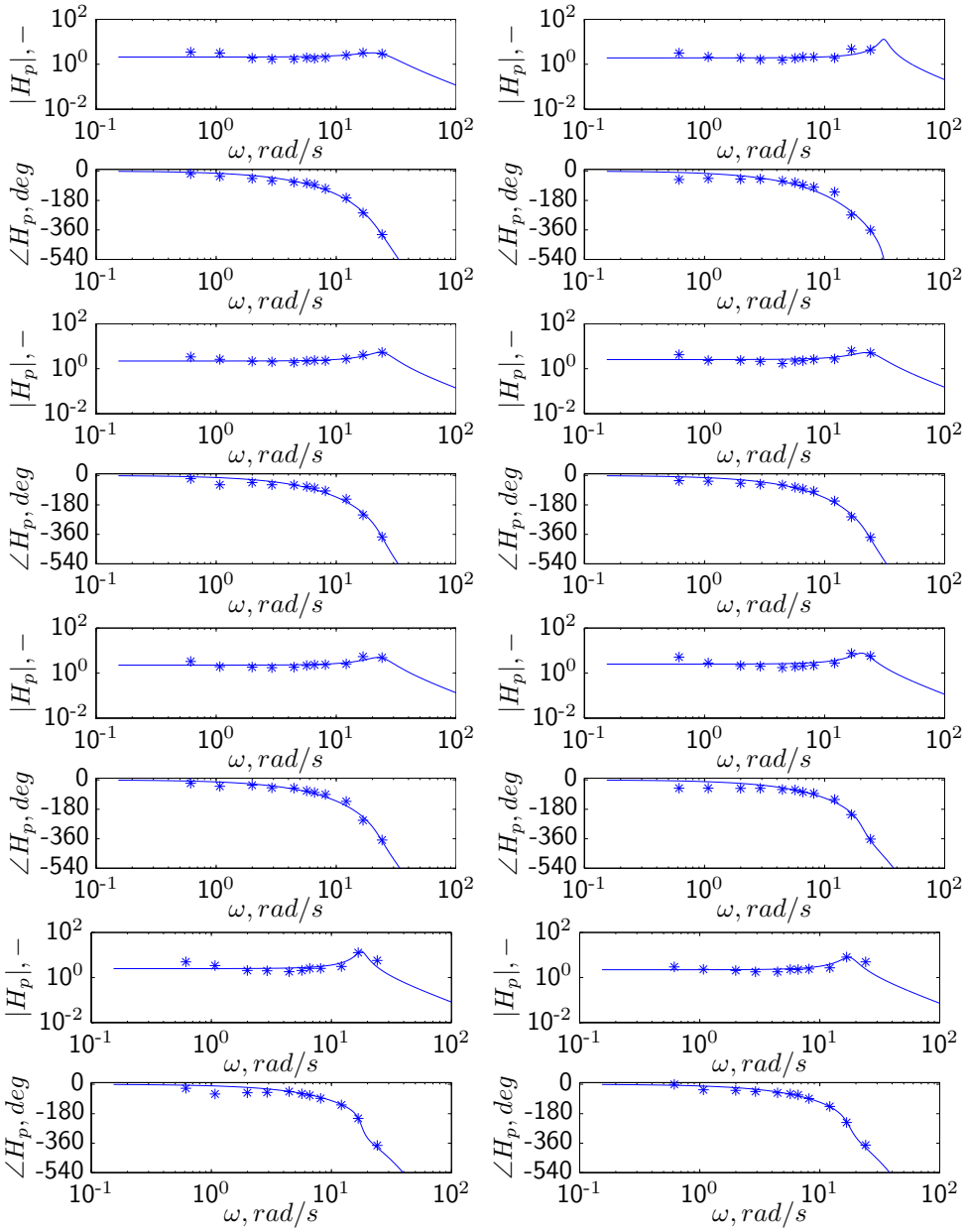

Figure A-4: FRFs and fitted models for all performed runs of Control 4.

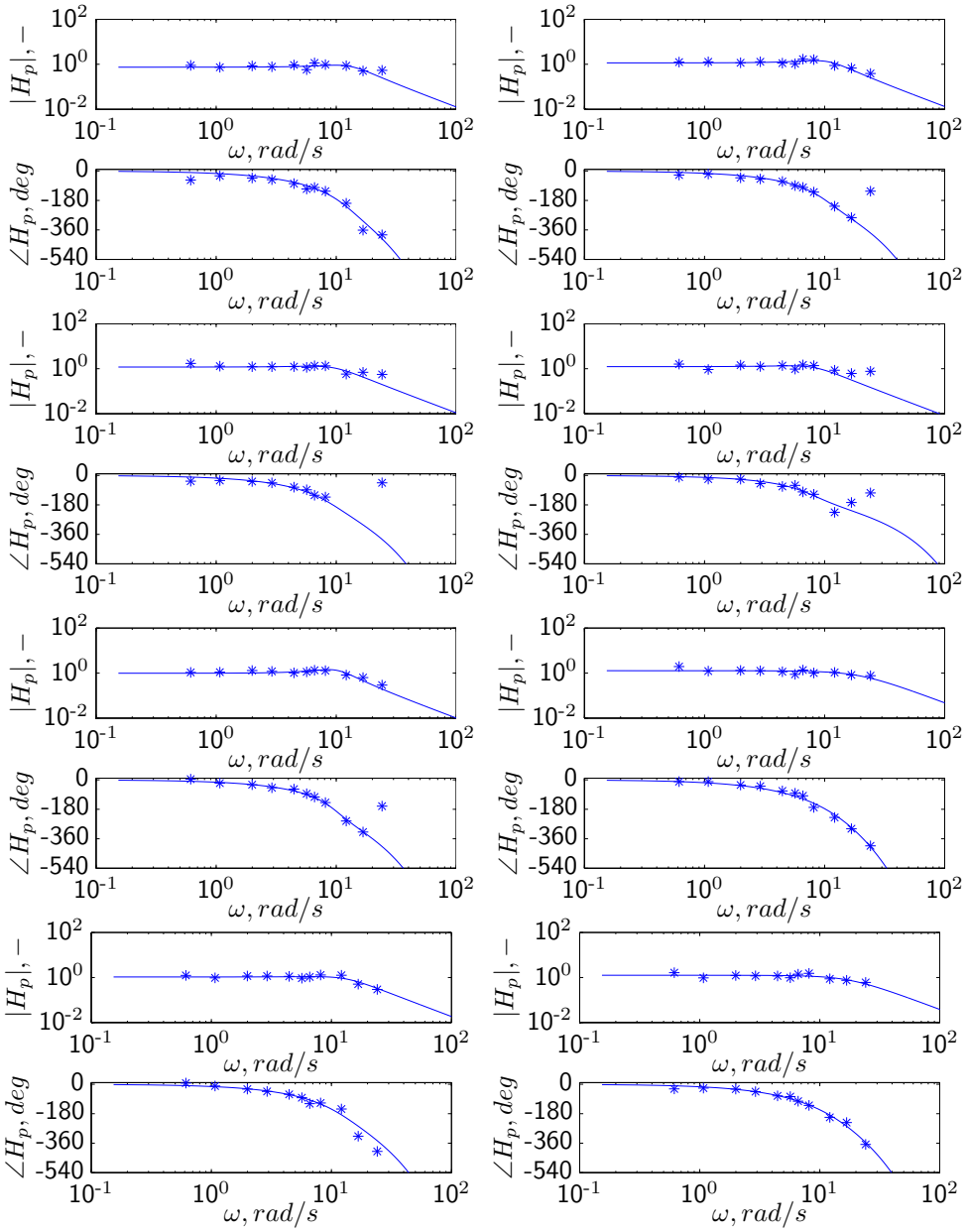

Figure A-5: FRFs and fitted models for all performed runs of Control 5.

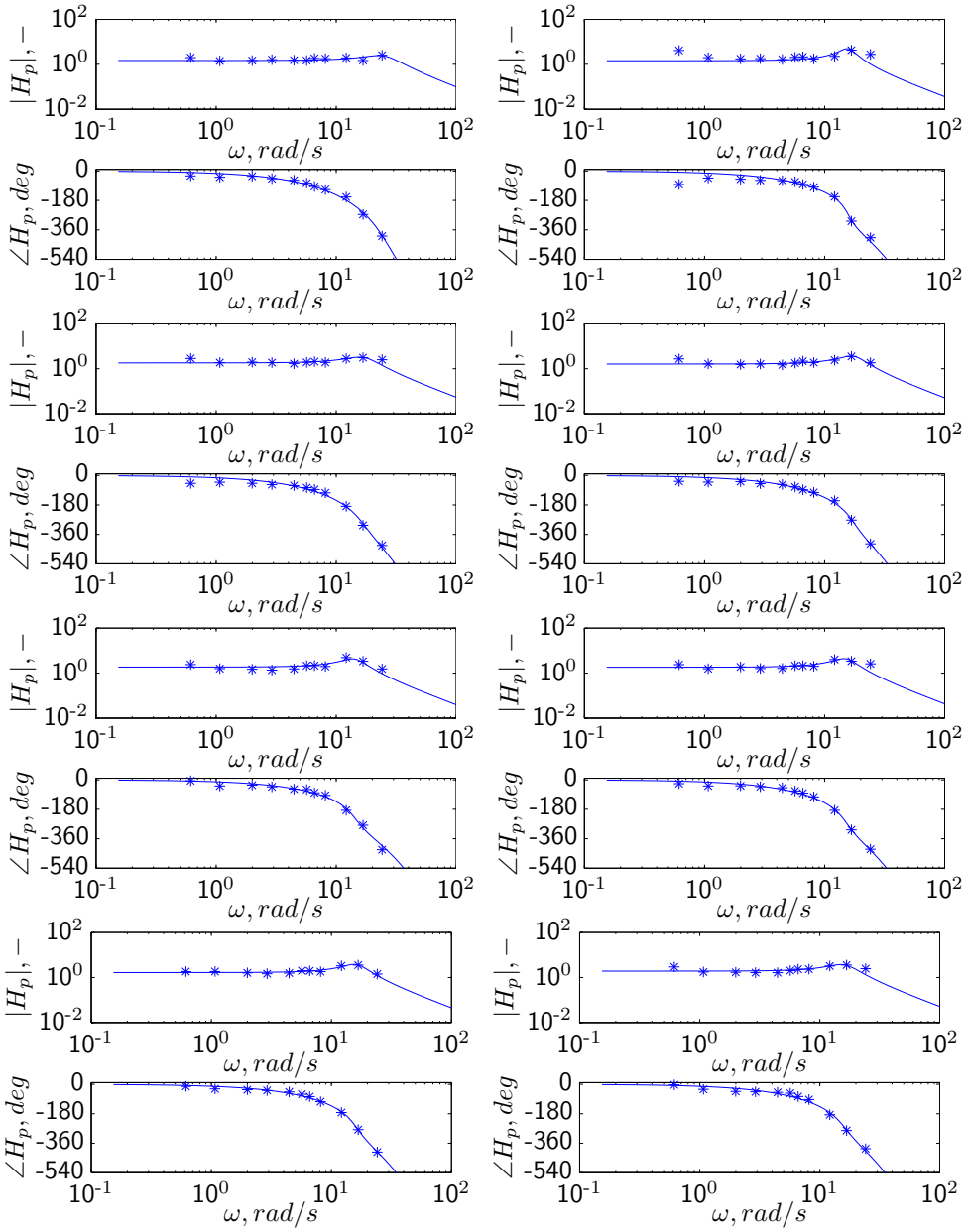

Figure A-6: FRFs and fitted models for all performed runs of Control 6.

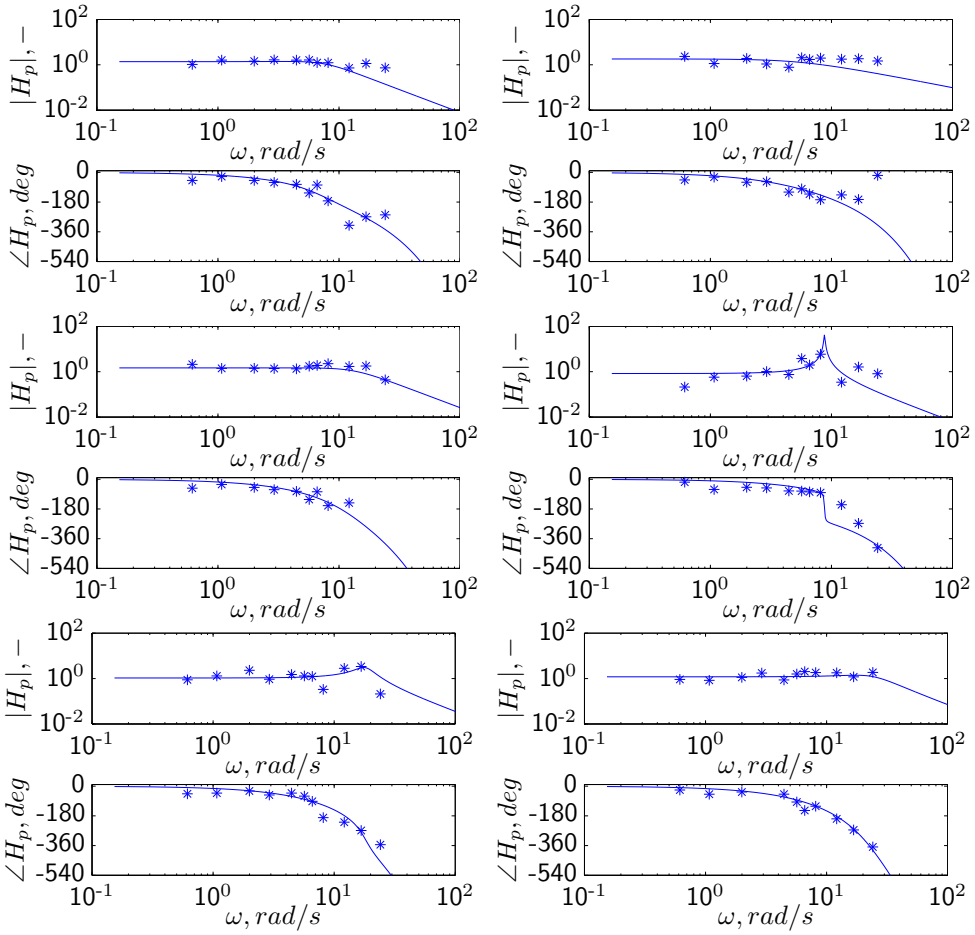

Figure A-7: FRFs and fitted models for all performed runs of Patient 1.

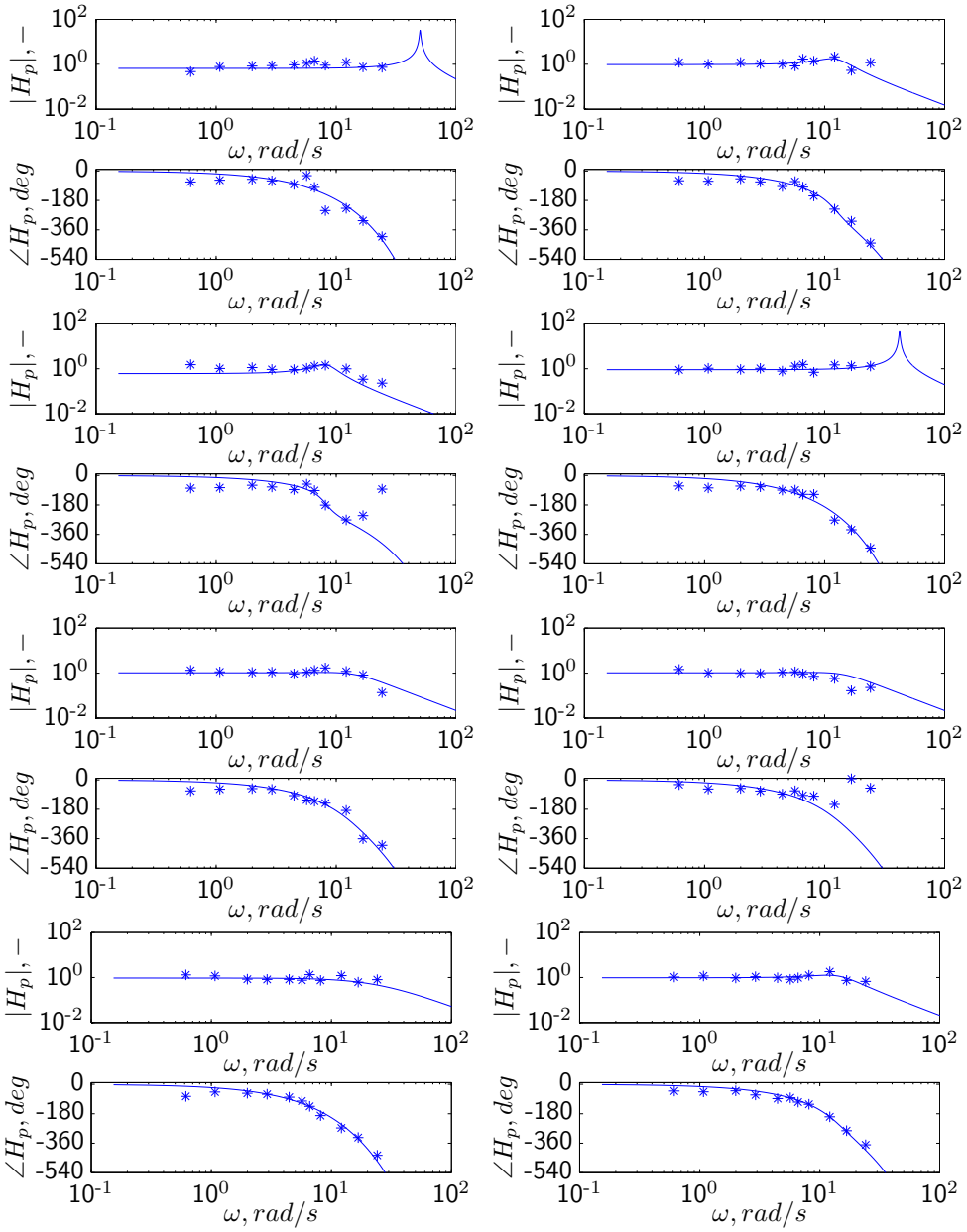

Figure A-8: FRFs and fitted models for all performed runs of Patient 2.

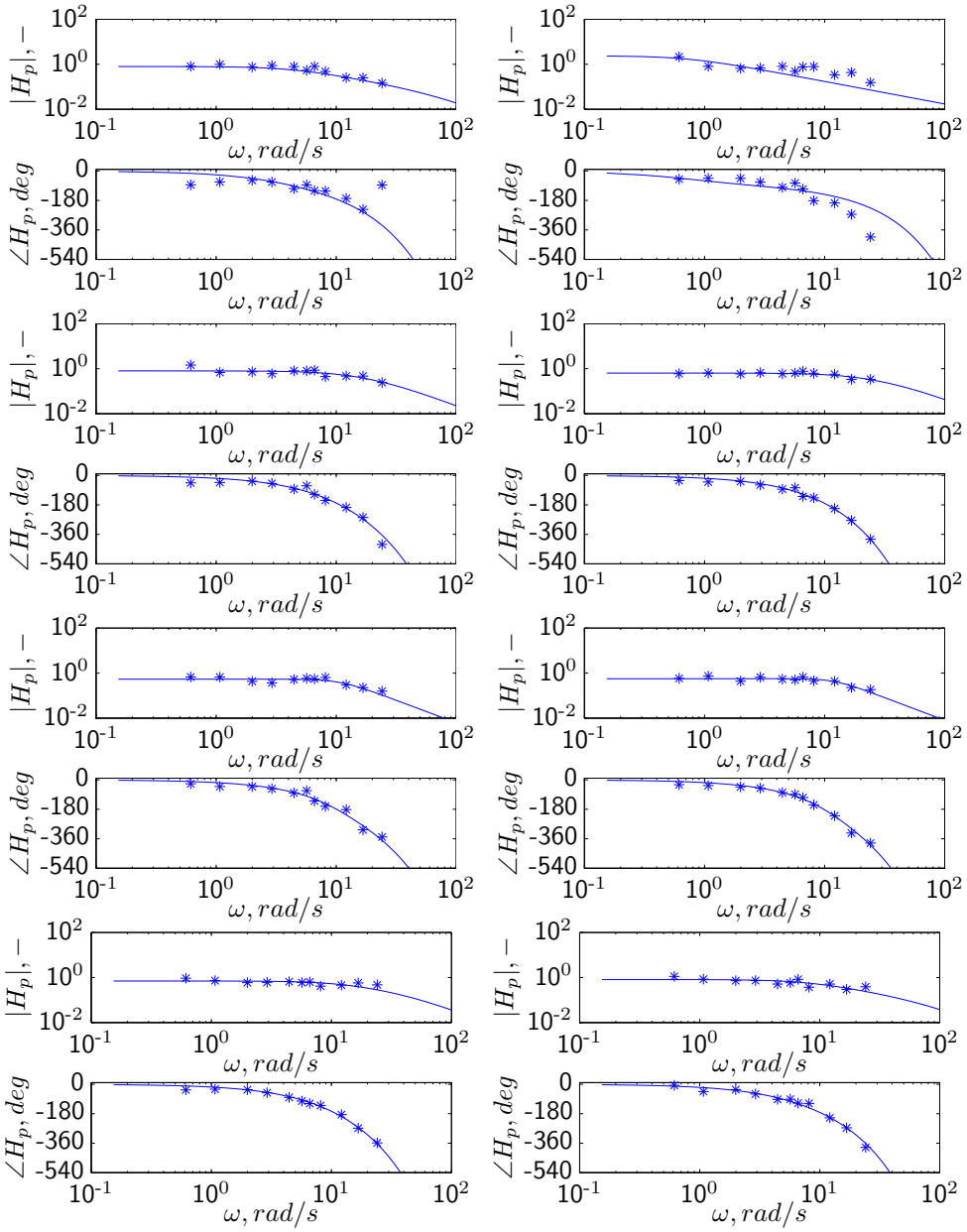

Figure A-9: FRFs and fitted models for all performed runs of Patient 3.

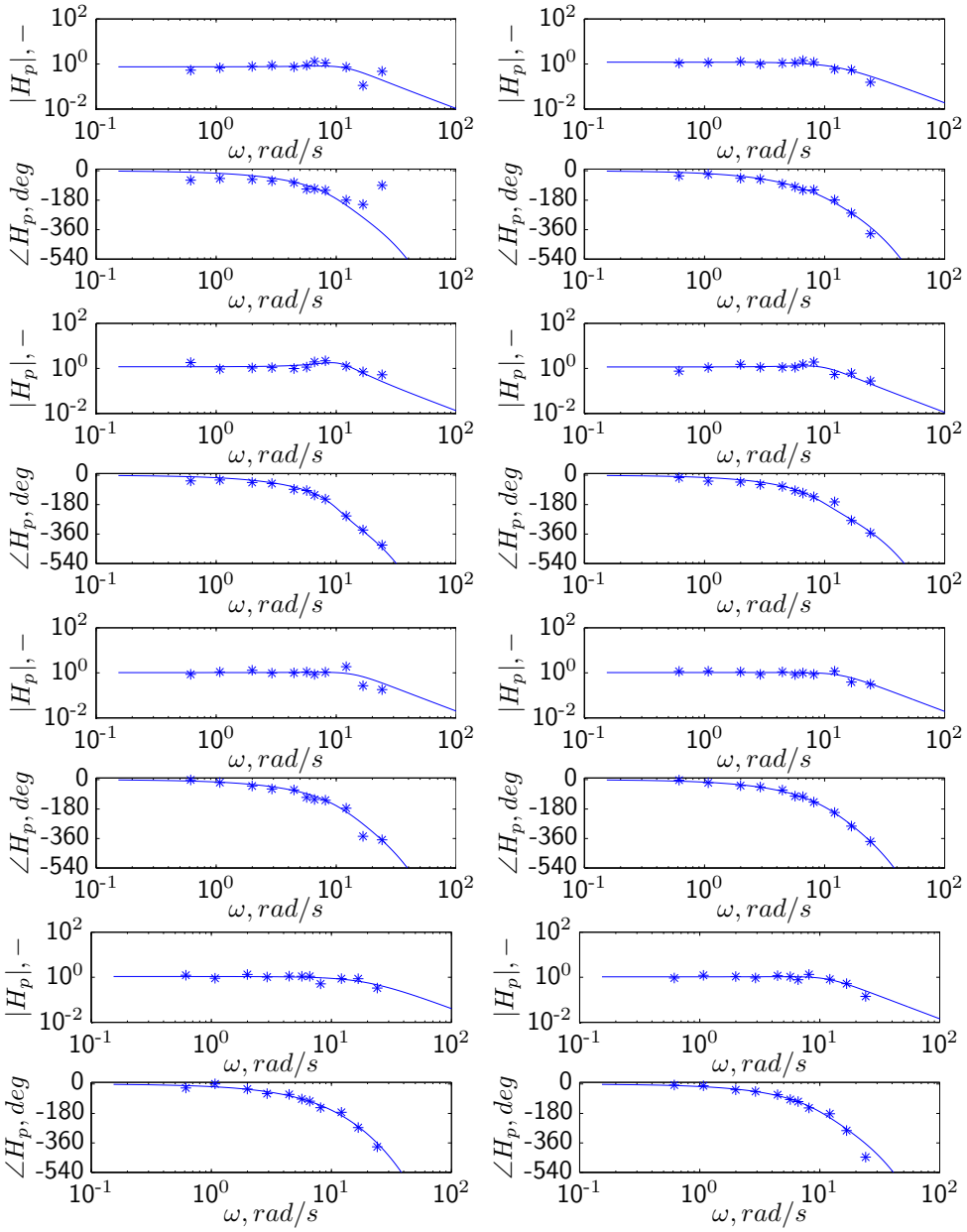

Figure A-10: FRFs and fitted models for all performed runs of Patient 4.

A-2 Numerical values of the estimated parameters

Numerical values of the estimated parameters from measurement runs of the control group are presented in Table A-1. The values for patients are presented in Table A-2

Table A-1: Control group estimated parameters.

	K_p	τ	ω_{nms}	ζ_{nms}
	-	s	rad/s	-
C1 run 6	1.26	0.22	24.91	0.51
C1 run 7	1.32	0.19	18.03	0.37
C1 run 8	1.25	0.20	20.06	0.33
C2 run 6	1.00	0.23	18.94	0.47
C2 run 7	1.17	0.21	19.57	0.47
C2 run 8	1.25	0.19	18.08	0.40
C3 run 6	1.11	0.24	17.06	0.35
C3 run 7	1.11	0.21	16.91	0.68
C3 run 8	1.31	0.21	14.44	0.59
C4 run 6	2.51	0.17	20.87	0.16
C4 run 7	2.47	0.16	17.84	0.08
C4 run 8	2.21	0.17	17.73	0.14
C5 run 6	1.28	0.22	19.50	0.84
C5 run 7	1.05	0.15	13.28	0.61
C5 run 8	1.26	0.18	17.52	0.83
C6 run 6	1.83	0.20	15.16	0.21
C6 run 7	1.66	0.19	16.25	0.22
C6 run 8	1.92	0.19	16.17	0.26

Table A-2: Patient group estimated parameters.

	K_p	τ	ω_{nms}	ζ_{nms}
	-	s	rad/s	-
P1 run 3	1.46	0.19	13.32	0.69
P1 run 5	1.06	0.22	18.09	0.18
P1 run 6	1.19	0.22	24.08	0.49
P2 run 5	1.03	0.23	14.40	0.60
P2 run 7	0.95	0.28	24.08	1.03
P2 run 8	0.98	0.19	14.43	0.43
P3 run 6	0.56	0.19	11.97	0.66
P3 run 7	0.70	0.20	24.08	1.23
P3 run 8	0.81	0.20	24.08	1.69
P4 run 6	1.03	0.18	13.71	0.68
P4 run 7	1.08	0.19	19.67	0.94
P4 run 8	1.04	0.16	11.68	0.64

A-3 Crossover frequencies and phase margins

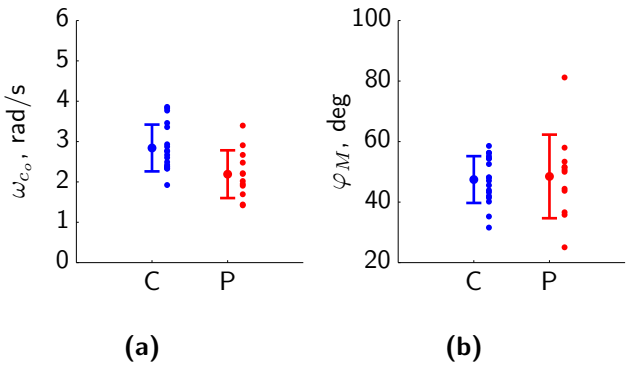

(a) **(b)**

Figure A-11: Crossover frequencies (A-11a) and phase margins (A-11b).

Appendix B

Corrected neuromuscular parameters

As described in the scientific paper, the model fitting approach was not successful for all collected data sets of patients. This chapter presents the data for all runs in which the neuromuscular frequency was corrected.

B-1 Patient 1

For patient 1 run 6 was corrected. Table B-1 presents the original parameters and the corrected parameters. Figure B-1 shows the FRFs, the original model and the corrected model.

Table B-1: Corrected parameters for Patient 1.

	K_p	τ	ω_{nms}	ζ_{nms}
	-	s	rad/s	-
original (run 6)	1.15	0.27	38.59	0.01
corrected (run 6)	1.19	0.22	24.08	0.49

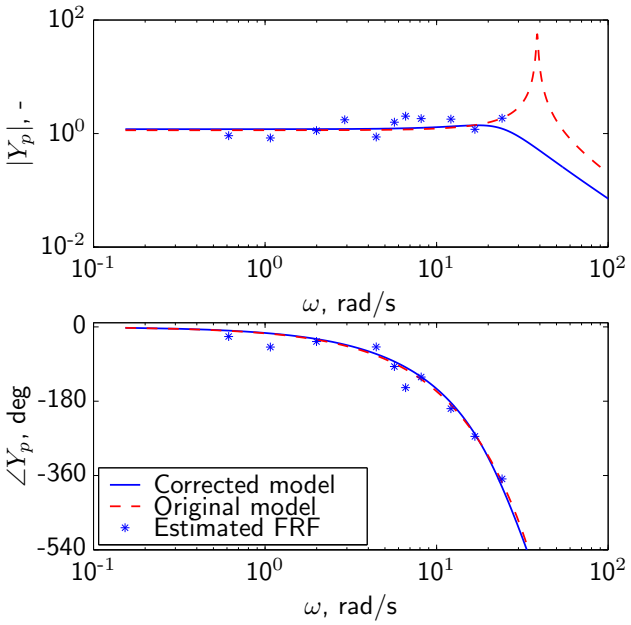

Figure B-1: FRFs and models from Patient 1, run 6.

B-2 Patient 2

For patient 2 run 7 was corrected. Table B-2 presents the original parameters and the corrected parameters. Figure B-2 shows the FRFs, the original model and the corrected model.

Table B-2: Corrected parameters for Patient 2.

	K_p	τ	ω_{nms}	ζ_{nms}
	-	s	rad/s	-
original (run 7)	0.94	0.29	50.00	1.73
corrected (run 7)	0.95	0.28	24.08	1.03

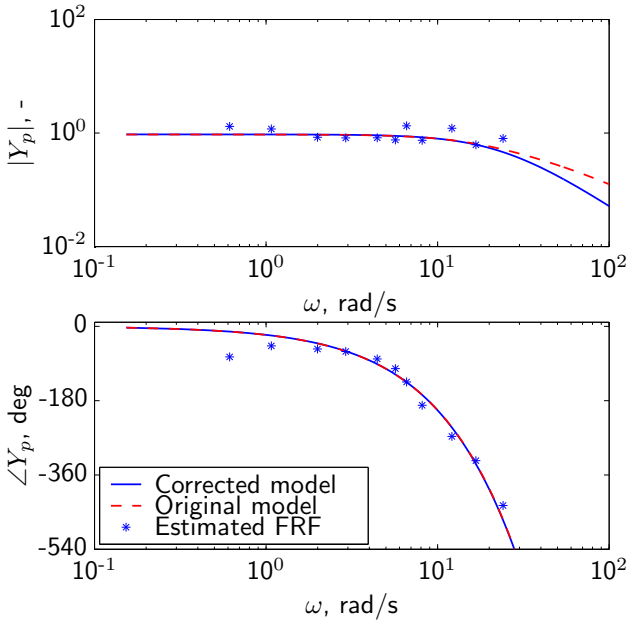

Figure B-2: FRFs and models from Patient 2, run 7.

B-3 Patient 3

For patient 3 run 7 and 8 were corrected. Table B-3 presents the original parameters and the corrected parameters. Figure B-3 shows the FRFs, the original model and the corrected model for run 7. Figure B-4 shows the FRFs, the original model and the corrected model for run 8.

Table B-3: Corrected parameters for Patient 3.

	K_p	τ	ω_{nms}	ζ_{nms}
	-	s	rad/s	-
original (run 7)	0.69	0.22	50.00	2.16
corrected (run 7)	0.70	0.20	24.08	1.23
original (run 8)	0.81	0.21	50.00	3.27
corrected (run 8)	0.81	0.20	24.08	1.69

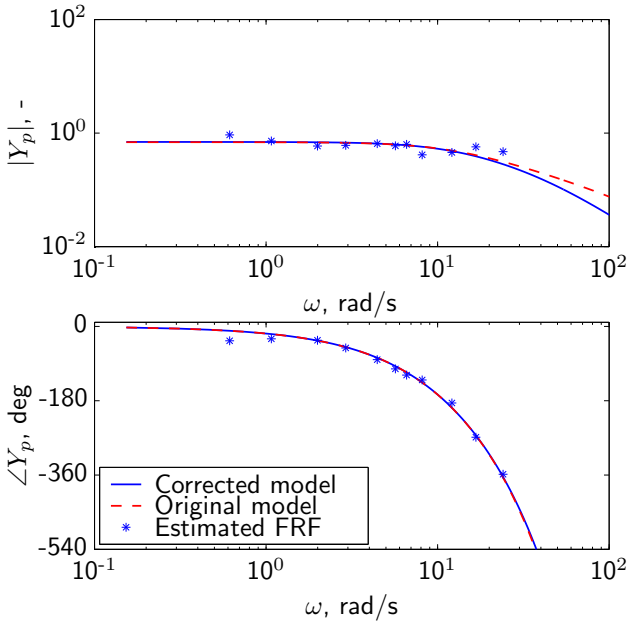

Figure B-3: FRFs and models from Patient 3, run 7.

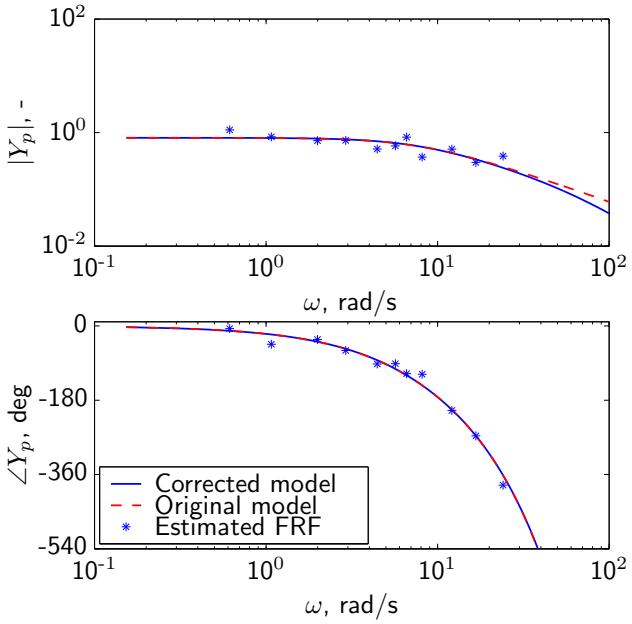

Figure B-4: FRFs and models from Patient 3, run 8.

Appendix C

Verification experiment

This chapter shows the results of the parameter estimation of the verification study. Data was obtained from four subjects (students and staff of the C&S department) with extensive tracking experience (DE). An experiment was conducted using the setup from the main experiment (described in the paper). The performance of the experts was found on average to be 135% better compared to the control group and 400% better compared to the patients, see Figure C-1. Human parameters were estimated using the method presented in the paper and are plotted in Figure C-2. It was found that the control gain of the experts was on average 60% higher compared to the control group and 145% higher compared to the patients. Similar delays were estimated. The damping of the experts was on average 74% lower compared to the control group and 86% lower compared to patients. The neuromuscular frequency was similar. Data obtained by this verification experiment can be used as reference.

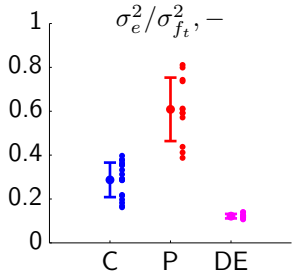

Figure C-1: Tracking performance.

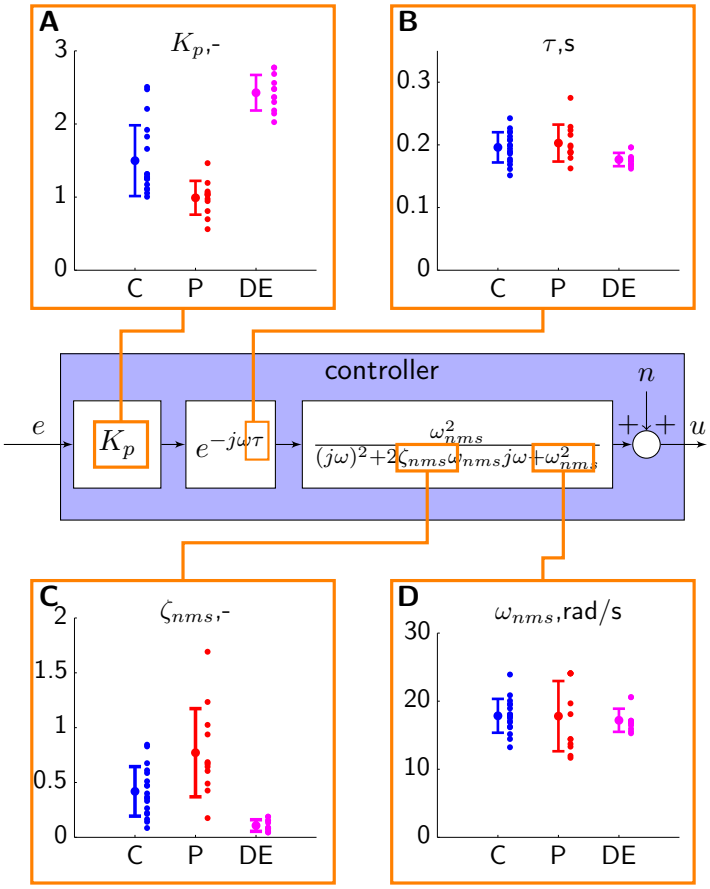

Figure C-2: Results of the parameter estimation.

Part III

Preliminary Report

Chapter 1

Introduction into Parkinson's Disease

In this chapter the main brain areas that are affected by PD are described in Section 1-1. The brain network involved in eye-hand coordination, and the locations that may be affected due to PD are explained in Section 1-2. Currently used questionnaires are described in Section 1-3. Finally, in Section 1-4 an example of the current tools at the EMC for testing eye-hand coordination is presented.

1-1 Brain areas involved in Parkinson's Disease

PD is a degenerative neurological disorder and it occurs mostly in people from middle or older age. The incidence of the disease rises with age. Between 50 and 59 years of age there are 17.4 PD patients per 100,000, while between 70 and 79 years of age this number increases to 93.1 per 100,000 (Lees et al., 2009). The causes of PD are still largely unknown. De Lau & Breteler (2006) state that genetic predisposition is thought to play a role in only 10% of the cases, and thus 90% of the cases are apparently idiopathic. However, in some occupations (farmers, forestry workers, gardeners, teachers and welders) the occurrence of PD is increased (De Lau & Breteler, 2006).

The brain consists of three main parts; the cerebrum, the cerebellum, and the brain stem, see Figure 1-1a. Within the deep layers of the cerebrum the basal ganglia are located. The basal ganglia are involved in primary functions like action selection, action gating, reward based learning, motor preparation and timing (Chakravarthy et al., 2010), but also non-motor functions like control of emotions (Kandel et al., 2013). The most important functions for this study are control of voluntary motor movements (Hikosaka et al., 2000). One of the structures composing the basal ganglia is the substantia nigra, see Figure 1-1b. The substantia nigra are responsible for the production of the neurotransmitter dopamine. Neurotransmitters are used for communication within the brain. In PD the dopamine producing neurons in the substantia nigra die. This reduces the production of dopamine and causes problems with communication within the brain. The motor cortex is highly dependent on dopamine, and

therefore its regulation will be reduced. This leads to the traditional Parkinsonian symptoms like tremor, rigidity, bradykinesia and an impaired balance (Kandel et al., 2013).

PD is still an incurable progressive disease but treatment can improve the quality of life significantly (Lees et al., 2009). Currently, treatment for PD is based on restoring the dopamine balance in the brain. Especially motor symptoms respond positively to the dopamine treatment. Unfortunately, non-motor symptoms respond poorly or not at all (Kandel et al., 2013). To date, objective clinical outcome measures to evaluate the effect of dopamine treatment are limitedly available. Usually PD patients start by taking a relatively small dose and, if the patient improves, this is gradually increased till an optimum dose is achieved. This has to be done carefully since an overdose can lead to unwanted side effects like delusions. The improvement of patients is partially checked subjectively. The patient is asked whether he or she feels better. A more quantifiable measure is desirable to check if there is indeed an improvement in motor control due to medication. This is where the current research can possibly improve current clinical practice.

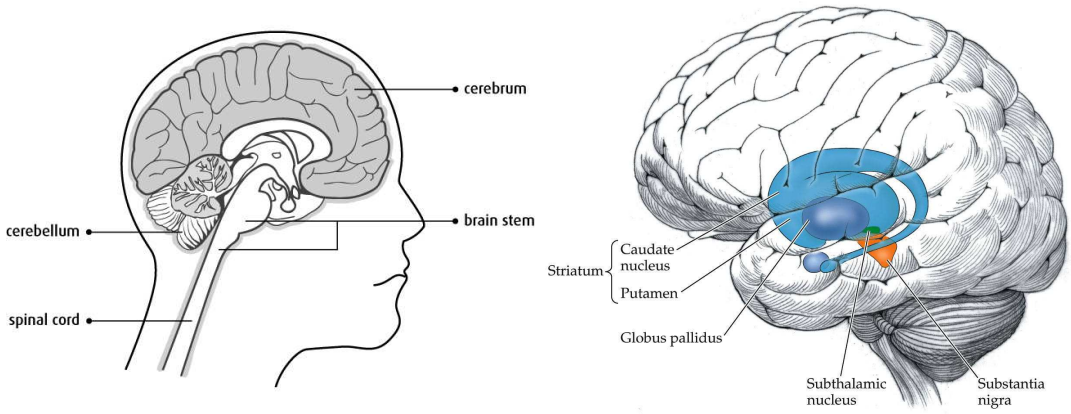

(a) Major parts of the brain, source: http://becuo.com/

(b) Basal ganglia, source: http://www.upright-health.com/

Figure 1-1: An overview of the brain and the basal ganglia.

1-2 Eye and hand movement control

In daily life, during many tasks the hand and eyes have to work together. An example is shaking hands with a person. The eye sees a hand appearing and the brain processes this information and steers the hand toward the other hand to shake it. In this section the brain areas involved in such processes are described in more detail.

The outer layer of the cerebrum, known as the cortex, consists of four lobes. The frontal lobe, the parietal lobe, the occipital lobe and the temporal lobe, see Figure 1-2.

Visual information is received by the eye. It is projected on the retina where the visual information is turned into electrical signals. These signals are transferred by the optical nerve all the way to the occipital lobe in the back of the head. In the occipital lobe, information

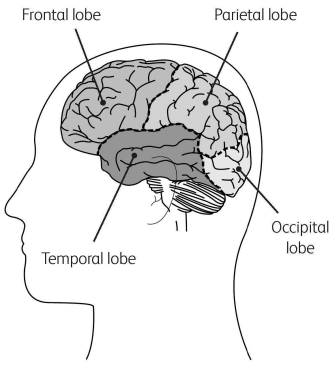

Figure 1-2: Division of the brain into lobes, source: http://www.dementiatoday.com/

is processed about the color, shape and contrast of the visual stimuli. The occipital lobe sends the information to, among others, the parietal lobe. The parietal lobe is involved in transformation of visual information into a 3D map, and thus gives information about the position of the objects received. For a reflexive movement the parietal lobe will trigger the superior colliculus in the midbrain. The superior colliculus provides the amplitude and direction in which the eye muscles have to move. This is the shortest and thus fastest route for generation of reflexive saccades. A saccade is a quick movement of the eyes where it changes from fixation on one point to another.

When memory is involved, e.g. for an intentional saccade (the eyes see the hand appear and you decide to look at it), the information from the parietal lobe will first pass trough the frontal lobe. In the frontal lobe especially the Frontal Eye Field (FEF) and the Dorsolateral Prefrontal Cortex (DLPFC) are important (Pierrot-Deseilligny et al., 2004). The FEF is responsible for the preparing and triggering of intentional saccades while the DLPFC is involved in saccade inhibition, short-term spatial memory and in decisional processes (Pierrot-Deseilligny et al., 2003). The next station is the basal ganglia, which decides whether to execute the saccade. Finally, the superior colliculus is reached again, see Figure 1-3.

The hand coordination for intentional movements follows a similar path. After the basal ganglia the signal goes to the motor cortex in the frontal lobe, instead of the superior colliculus, which is responsible for actuating the muscles needed for the action, see Figure 1-3.

As described in Section 1-1, the basal ganglia dysfunction in PD patients. Because the basal ganglia play an important role in the eye-hand coordination, PD is likely to influence such behavior.

1-3 Standardized clinical ratings

In this study, we aim at including early stage PD patients. To test whether a patient meets our inclusion criteria, we will use several standardized clinical ratings. In this section four scores will be described: the Frontal Assessment Battery (FAB), the Mini Mental State Examination (MSSE), the Unified Parkinson's Disease Rating Scale (UPDRS) and the Hoehn & Yahr stage.

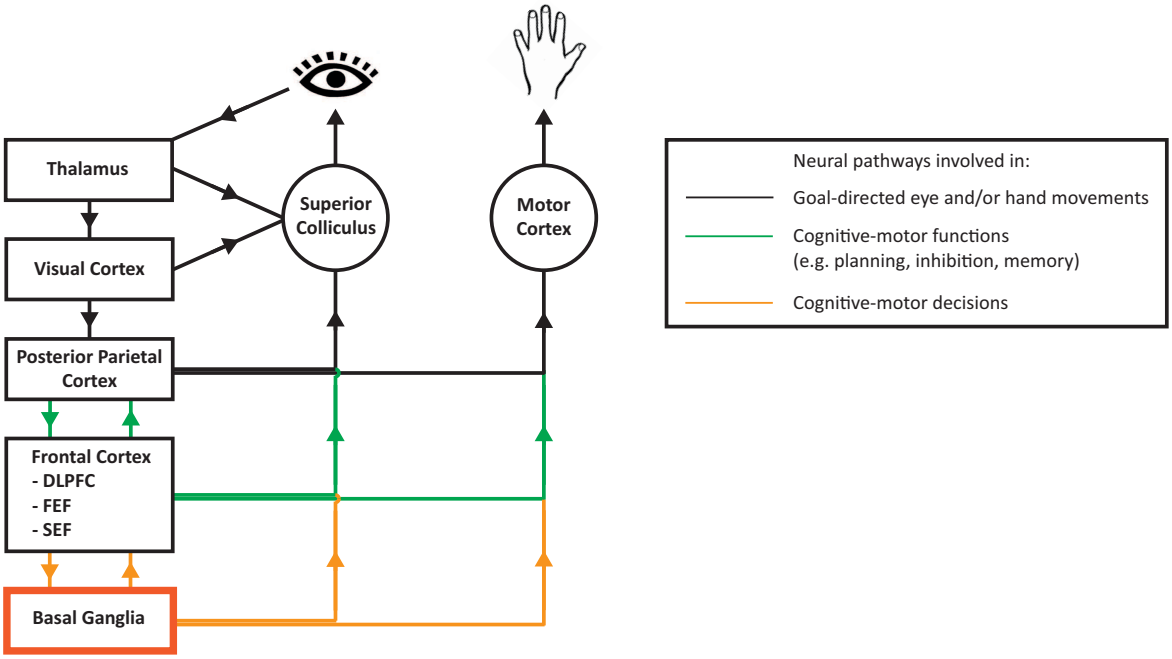

Figure 1-3: Simplified scheme of the neural pathways involved in generation of eye-and hand movements (de Boer, 2015)

The FAB score, published by Dubois et al. (2000), is a short test (approximately ten minutes) and covers six aspects of frontal lobe functions. For each aspect, a subject can score a total of three points. For example, one of the aspects is conceptualization. The subject is asked what the similarity is between two objects. The FAB can be used as an indication of frontal lobe dysfunction. A score below 13 is a reason to investigate the neuropsychological state of a subject in more detail.

The MSSE was devolved by Folstein et al. (1975). This questionnaire takes approximately ten minutes. It provides a measure of impaired overall cognition. The summed score of the individual items indicates the current severity of cognitive impairment. If a subject has a neurodegenerative disease, it is expected that the score will decrease over time as well. The test consist of two parts. In the first part, a subject only have to respond vocally. It covers orientation, memory and attention. The second part tests the ability to name, follow verbal and written commands, write a sentence spontaneously, and copy a complex polygon. On the first part subjects can score a maximum of 21 and on the second part 9.

The UPDRS is a method described by Goetz et al. (2007) and is an updated version of the original UPDRS method (Fahn & Elton, 1987). It is more extensive than the previous described tests and therefore lasts longer, approximately thirty minutes. It consists of four parts and has a total of fifty questions. The fist part is about *nonmotor aspects of experiences of daily living*. Aspects are varying from cognitive impairment to urinary problems. Part two covers *motor experiences of daily living*. This could be speech or handwriting. The third part focuses on *motor examination* like gait or rigidity. Finally, part four is about *motor complications* like dyskinesias. For PD patients only part three is assessed.

After subjects have conducted the UPDRS it is possible to indicate the modified Hoehn &

Yahr (Hoehn et al., 1998) gradation as recommended by Goetz et al. (2004). The gradations are:

Gradation 0.0 No indication of the disease
Gradation 1.0 Unilateral involvement only
Gradation 1.5 Unilateral and axial involvement
Gradation 2.0 Bilateral involvement without impairment of balance
Gradation 2.5 Mild bilateral disease with recovery on pull test
Gradation 3.0 Mild to moderate bilateral disease; some postural instability; physically independent
Gradation 4.0 Severe disability; still able to walk or stand unassisted
Gradation 5.0 Wheelchair bound or bedridden unless aided

Patients with a Hoehn & Yahr score above 3 are excluded from our study.

1-4 Eye-hand coordination tools at EMC

The questionnaires described in Section 1-3 are low resolution. A finer assessment of motor control is preferred and can be achieved by measuring the eye-hand coordination. To investigate the effect of a neurodegenerative disease on eye-hand coordination several tasks with different cognitive complexity are developed at the Erasmus MC (EMC), designed to test reflexes, decision making, memory and inhibition. To test these types of motor action several different experiments are conducted. In this section experiment conditions from Muilwijk et al. (2013) are described. The conditions were performed in early-stage PD patients as well as an age-matched control group.

During four eye-hand coordination tasks, movements of the hands and eyes were measured. The measurement setup consist of a touch screen, an eye-tracking device and a motion capturing system, see Figure 1-4.

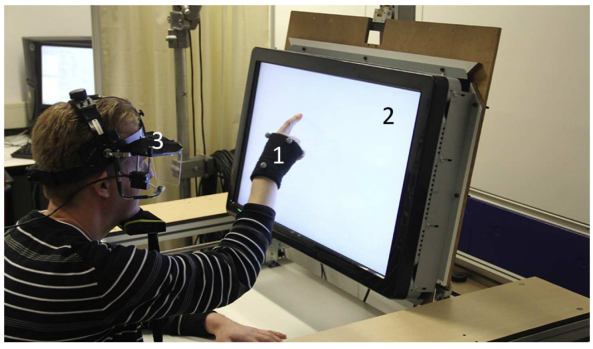

Figure 1-4: The setup at EMC with an infrared motion detection system (1), a touch screen (2), and an infrared eye-tracking system (3) (De Boer et al., 2013).

Four conditions, with different cognitive complexity, were tested, see Figure 1-5. At the start of every condition a start screen was shown (A in Figure 1-5). This screen consisted of a white dot and a purple bar. The subjects had to direct their gaze towards the white dot and

touch the purple bar. Condition one is the *pro-tapping task* (B in Figure 1-5). Subjects are instructed to touch the dot that appears on the screen as quickly and accurate as possible. This is designed to to test reflexes. The second condition is a *dual planning task* (C in Figure 1-5). A blue and a red dot appeared at the same time at a position horizontally and vertically mirrored from each other. The subjects were instructed to direct gaze towards the red dot while simultaneously touch the blue dot withing ten seconds as accurately as possible. The subjects were also instructed not to direct gaze towards the blue dot. This test is more complex as it involves reflexes, decision making and inhibition. The third condition is an *anti-tapping task* (D in Figure 1-5). In this test a red dot appeared in either the left or right side of the screen, the position along the x-axis varied. In this case the subjects were instructed to touch and direct their gaze towards the virtual position on the opposite of the screen. This task is mainly to test inhibition. Finally, the fourth condition is a *spatial memory task* (E in Figure 1-5). The start position remained a bit longer and a green dot flashed on a random position for 50 ms. Subjects were instructed to remember the position of the green dot and touch at the remembered position after four seconds as soon as the start position disappeared. During the start position subjects were not allowed to make any eye or hand movements.

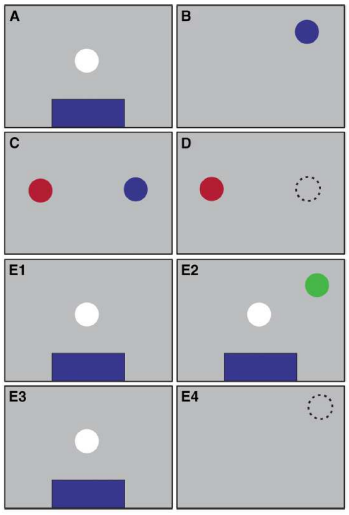

Figure 1-5: Overview of the touch screen representations of the starting position and each eye-hand coordination task. A: start screen, B: pro-tapping task, C: dual planning task, D: anti-tapping task and, E: spatial memory task (Muilwijk et al., 2013).

In the pro-tapping task, the kinematics of the eyes of PD patients were found to be similar to the controls. However, the inhibition and the execution of the hand movement were significantly slower in PD patients. The dual planning task turned out to be quite difficult for all subjects. The PD patients made an error in 56% of the trial and the controls in 44% of the trails. The initiation of eye movement towards the target was significantly faster for PD patients, but the initiation and execution of the hand movement slower. The results for the anti-tapping task were similar to the dual planning task. The initiation of the eye was faster in PD patients but hand movements were executed slower than the controls. The faster initiation of eye movement can be an indication that PD patients have difficulties to inhibit reflexive saccades. The percentage of failure was 36% for PD patients against 11% in

controls. Finally, in the spatial memory task the number of incorrect trails was higher for PD patients (31%) compared to the controls (17%). For this task only the execution of the hand movement was significantly slower in PD patients compared to controls.

Chapter 2

Tracking Tasks

An additional tool to objectively identify degraded motor control in PD could be the use of a tracking task. A tracking task is a manual control task that requires a human controller to steer a dynamic system along a certain target path while being perturbed by a disturbance. An example is riding a bicycle on a windy road. The road is the target path and the wind is the disturbance. To prevent falling down, the bicyclist uses several information inputs such as the visual, vestibular and somatosensory information about the current state of the bicycle and the road ahead. All the information needs to be integrated inside the brain of a human controller (HC). In general humans tend to perform similar on such kind of tasks. If a controller is not able to perform a certain manual task or shows different control behavior this might be an indication that motor control area's in the brain are effected by a neurodegenerative disease like PD.

2-1 Human controller in a manual control task

It would be ideal if a HC could be modeled by one single model for all different types of tasks. However, a HC is *a multimode, adaptive, learning controller, capable of exhibiting an enormous variety of behavior* (McRuer & Jex, 1967). This means that a human is able to adapt to a certain task. Modeling such diverse complex behavior is difficult. But it is possible to model the behavior for very specific tasks. A good example of such a task is a tracking task. A manual control task can be presented in a block diagram, see Figure 2-1. The block diagram differentiates between four kinds of variables that influence human control behavior in a closed-loop pilot-vehicle system.

The task variables are the most important ones. They define the task a HC has to complete. The *forcing functions* are the signals which are inserted in the system. These are mostly limited to a target signal and a disturbance signal. If there is only a target signal the task is called a target-following task. If there is only a disturbance signal the task is called a disturbance-rejecting task. A combination of these two tasks is also possible and thus is a target-following disturbance-rejecting task. There are many options in selecting a target

signal, it varies from a single sine wave to a multisine wave, but input signals like steps are also possible. The type of *display* is important since a HC control behavior depends on the information presented. The different types of displays will be discussed in more detail in Section 2-3. The *controlled element* represents the system that has to be controlled. To a large extend it defines the difficulty of the task and the required HC control strategy (McRuer et al., 1965).

Environmental variables define the environment in which the experiment performed, like the temperature and noise level. Their influence is not of interest en therefore they should be kept constant. For research involving PD patients the operator-centered variables are extra important. PD patients should be treated with additional care in terms of stress and fatigue. Finally, procedural variables should remain constant over all subjects to ensure consistent measurement data.

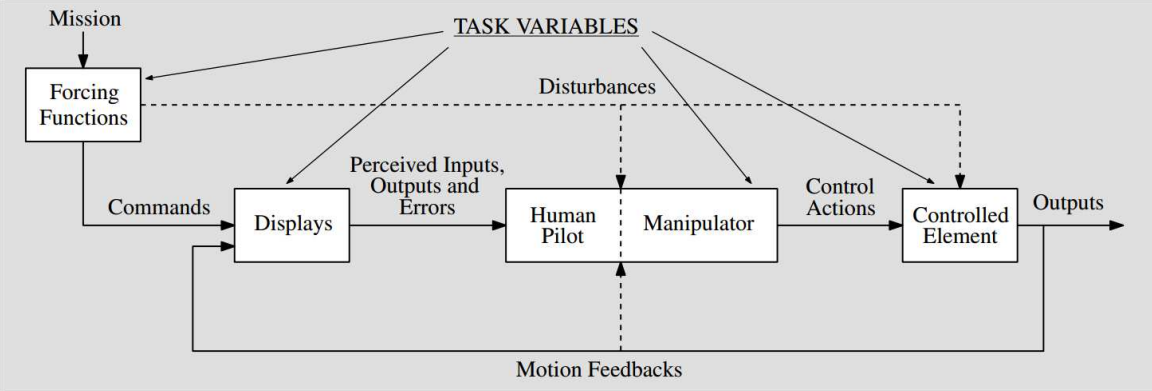

Figure 2-1: Variables affecting manual control behaviour (Pool, 2012) (first published in McRuer & Jex (1967)).

2-2 Successive Organization of Perception

Different control strategies are distinguished for tracking tasks. They were first described by Krendel & McRuer (1960) in the Successive Organization of Perception (SOP) scheme. The types of classifications are: compensatory, pursuit and precognitive control.

The *compensatory* control strategy is based on controlling a system purely on the error. The error is defined as the difference between the target signal and the system output, $e = f_t - \theta$. So if the controller is able to keep the error small, the θ will coincide with the f_t. Compensatory behavior can modeled with the crossover model (McRuer et al., 1965).

In *pursuit* a HC perceives the target signal and the system output and thus can derive the error. A HC will try to use all knowledge about the target signal to improve the performance. This could be by using predictable aspects of the signal or characteristics about the controlled element learned from previous experience to operate in an optimum manner.

Finally, for the highest level of the SOP, *precognitive* control, the operator operates in an open loop feedforward mode on the target signal. It is assumed there is complete information about the required input and no feedback control is necessary. After much practice, with both compensatory and pursuit displays, it is possible for a HC to approach the precognitive level when tracking single sine signals (Pew et al., 1967).

2-3 Displays

Three different types of displays typically used for tracking tasks can be distinguished. The compensatory, pursuit and preview displays.

A compensatory display shows only the error, see Figure 2-2a. For this type of display compensatory tracking behavior is expected. However, with a predictable target signal after enough runs pursuit behavior can be achieved (Wasicko et al., 1967). Compensatory tracking is difficult since the HC is not able to explicitly see what he is doing nor what he is supposed to be doing (Poulton, 1974). This might be a practical difficulty for experiments with PD patients.

In the pursuit display the system output and the target signal are presented, see Figure 2-2b. This makes it possible for the HC to derive the error. According to Poulton (1974) the pursuit display has three major advantages over the compensatory display. Firstly, the HC is able to predict the target signal more accurately and so reduce the time lag. Secondly, since the system output is visible the HC learns how to control the system more easily. Finally, the presented information helps the HC to detect and avoid mistakes earlier. Also, the tracking is at least as accurate as for compensatory displays. The provision of a pursuit display does not necessarily induce pursuit behavior (Wasicko et al., 1967). Flowers (1978) and Soliveri et al. (1997) used a pursuit display in combination with single-sine waves to investigate PD.

A preview display is a pursuit display in which a part of the path ahead is visible, see Figure 2-2c. This makes it possible for a HC to compensate for his own delay (Ito & Ito, 1975). The increase in duration of the preview time reduces the average time lag (Poulton, 1974). A human operator model for preview tracking task is derived by van der El et al. (2015). There was found that HC use a near-viewpoint to generate feedforward control for the high frequencies, while a far-viewpoint is used to generate feedback control at the lower frequencies van der El et al. (2015). The preview display in combination with random waves and single-sine waves was used by Jones & Donaldson (1989, 1996) to study the predictive motor planning in PD.

For the experiment involving PD patients a pursuit display can be used (Flowers, 1978; Soliveri et al., 1997). This is an intuitive task an therefore it is expected that patients will not have difficulties in understanding and performing the task. If a preview display (Jones & Donaldson, 1989, 1996) is used the task might become even more realistic, but identification of such a task is still an area to be explored (van der El et al., 2015).

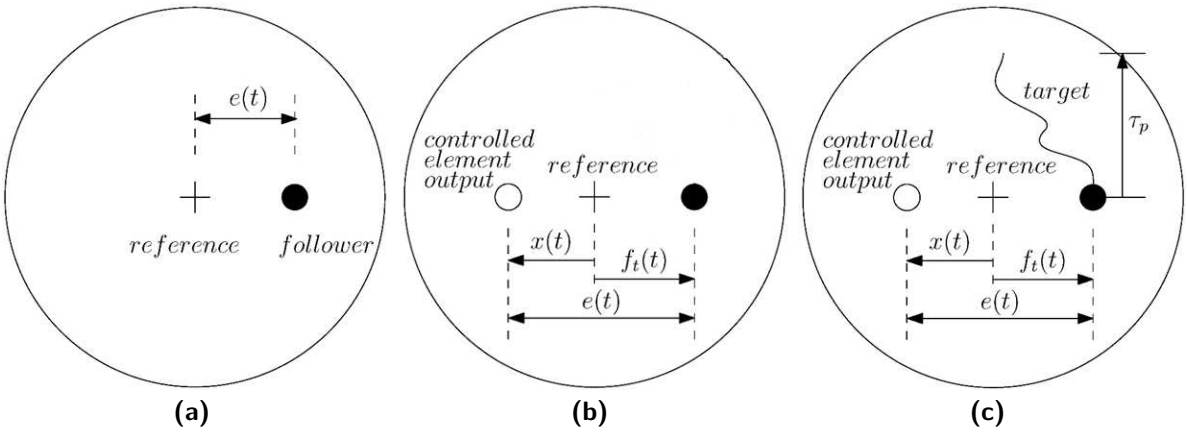

Figure 2-2: Compensatory, pursuit and preview displays (van der El et al., 2015).

Chapter 3

Identification Methods

In this thesis the objective is to quantify the degraded eye-hand coordination of PD patients. A tracking task in combination with system identification methods could be used to achieve this objective. A method to identify compensatory and (certain)pursuit tasks is the frequency-domain based Fourier Coefficient Method (FCM) (van Paassen & Mulder, 1998) which will be described in Section 3-1. The FCM has been successfully used to identify HC dynamics in similar tracking tasks (Zaal, Pool, De Bruin, et al., 2009). As an extra check the time-domain based Maximum Likelihood Estimation (MLE) (Zaal, Pool, Chu, Van Paassen, et al., 2009) is used and this method is described in Section 3-2.

3-1 Fourier Coefficient method

The FCM is a frequency-domain black-box identification method. This means that the dynamics of the to be identified system are unknown and no assumptions on these dynamics are made in advance. The systems that can be identified most straightforwardly are single-input-single-output systems. An example of such a system is an operator during a compensatory task, see Figure 3-1. In the diagram i is the input signal, e is the error, n is the remnant, u is the control input, m is the system output, Y_p are the operator dynamics and Y_c are the dynamics of the controlled element.

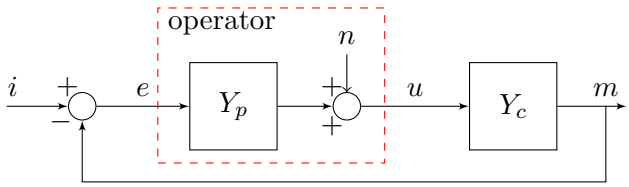

Figure 3-1: Block diagram of a target following task with a compensatory display.

In tracking tasks, the operator is modeled as a quasi-linear controller (McRuer & Jex, 1967). The human operator will give a linear response to the error summed with the remnant.

The remnant accounts for all the non-linearities in the operators control behavior (McRuer et al., 1965; Pool et al., 2010). For identification of the frequency response of the human operator applying compensatory behavior only the error, the control input and the remnant are important. It is possible to take the Fourier transform and assume the remnant to be zero, this can be seen in (3-1) and (3-2). The remnant can be dropped if a multisine input signal is used which will give power at certain discrete frequencies (van Paassen & Mulder, 1998). At these frequencies the signal to noise ratio is very high and the the remnant can thus be ignored. The frequency response should therefore only be estimated at the frequencies at which the input signal delivers power.

$$U(j\omega_t) = Y_p(j\omega_t)E(j\omega_t) + N(j\omega_t) \tag{3-1}$$

$$\hat{Y}_p(j\omega_t) = \frac{U(j\omega_t)}{E(j\omega_t)} \tag{3-2}$$

If a HC operates uses a pursuit control strategy the compensatory block diagram is no longer valid. The diagram can be extended, see Figure 3-2, where a HC is expected to react on the target signal as well as on the error.

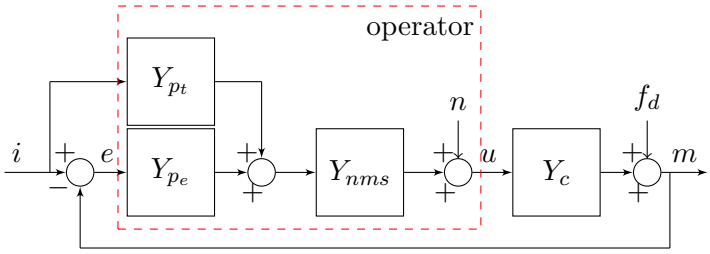

Figure 3-2: Two-channel operator block diagram.

For the identification of the two HC transfer functions, Y_{p_t} and Y_{p_e}, a disturbance signal is added (van Paassen & Mulder, 1998). The exciting frequencies of the disturbance signal should be different than the exciting frequencies of the target signal.

It is possible to determine the magnitude and phase of the estimated frequency response. The result is an indication of the model that can be used to describe the operator in an optimal way. A well known model for an operator follows from the original crossover model of McRuer & Jex (1967) and is called the *extended crossover model*, see (3-3). In the model K_p is the gain, τ the reaction time delay and in the fraction T_L is the lead time constant and T_I the lag time constant.

$$Y_p(j\omega) = \underbrace{K_e \frac{T_L j\omega + 1}{T_I j\omega + 1}}_{\text{pilot equalization}} e^{-j\omega\tau_e} \tag{3-3}$$

The model will adapt to the controlled element dynamics in such a way that the open-loop will show single integrator dynamics around the crossover frequency. This means that depending on the controlled element the equalization part of the extended crossover model can be reduced

to a pure gain, pure lead or pure lag (Pool et al., 2011). The model can be made valid over a wider frequency range by the addition of the neuromuscular system dynamics. It can be modeled as an second-order low-pass filter (3-4) (Damveld et al., 2009). The parameters are: natural frequency, ω_{nms}, and damping, ζ_{nms}.

$$Y_{nms} = \frac{\omega_{nms}^2}{(j\omega)^2 + 2\zeta_{nms}\omega_{nms}j\omega + \omega_{nms}^2} \tag{3-4}$$

After selecting a model, depending on the controlled element dynamics, a cost function is often used for fitting it to the estimated frequency response function from (3-2). Generally a model using more parameters will give a better fit to the data, but it is also more difficult to determine the influence of each individual parameter. A cost function that fits the data points from the frequency response at the input frequencies could be as in (3-5).

$$CF = \sum \|\hat{Y}_p(j\omega_t) - Y_p(j\omega_t)\|^2 \tag{3-5}$$

For the cost function the optimization will try and match the simulated Y_p as good as possible to the estimated $\hat{Y}_p$ by generating different sets of parameters using for example the *fmincon* function in MATLAB. After an optimum is reached the optimization will stop and a set of parameters to estimate the human controller is obtained. Using such very simple quasi-linear models it is possible to quantify human controller dynamics and typically explain between 70-95% of the measured signals (Pool, 2015).

A metric for the validation of an estimated model is the Variance Accounted For (VAF), (3-6). It shows how well the model can predict the measured output signal (Nieuwenhuizen et al., 2008). In the equation u_{exp} is the measured control signal and u_{sim} is the simulated control signal which is obtained by simulating an identified HC model with measured inputs. The VAF will be between the 0% and the 100%, where 100% means that the simulated control signal is identical to the measured control signal.

$$VAF = \left(1 - \frac{\sum |u_{exp} - u_{sim}|^2}{\sum u_{exp}^2}\right) \times 100\% \tag{3-6}$$

Extra information about the behavior of the controller can be derived using the effective open-loop describing function, Y_β. It has the property that the portions of the output, M, and the error, E, are linearly correlated with the input, I, as in Equation (3-7) and (3-8) (Wasicko et al., 1967).

$$\frac{M}{I} = \frac{Y_\beta}{1 + Y_\beta} \tag{3-7}$$

$$\frac{E}{I} = \frac{1}{1 + Y_\beta} \tag{3-8}$$

It has the same interpretation in the pursuit as in the compensatory situation. Therefore, a sufficient indication of pursuit behavior is that the effective open-loop function differs from

the compensatory effective open-loop function (Wasicko et al., 1967). For a single-loop model it is formulated as the estimated controller dynamics multiplied by the system dynamics (3-9).

$$Y_\beta = Y_p \cdot Y_c \tag{3-9}$$

3-2 Maximum Likelihood Estimation Method

A different method that is used for identification is the MLE method presented by Zaal, Pool, Chu, Van Paassen, et al. (2009). The main difference with the FCM is that the parameter estimation of the MLE is done directly in the time domain, see Figure 3-3. Instead of fitting on the frequency points, like the FCM, MLE directly fits a parametric model to the time-domain data. An advantage of this method is that time-domain data usually has more data points to make a fit. This can make the estimate more accurate, but will also require more computational power. Another disadvantage is that the model has to be chosen beforehand. In a frequency method it is easier to validate the choice for a selected HC model. For a time-domain method the input signal has less constraints, since the frequency components have less influence on the identifiably of the parameters. Also, for the MLE the initial values to start the optimization have a direct influence on the result and therefore should be be chosen carefully.

Using both a frequency-domain and a time-domain identification method is a good way to validate the results, since they should be similar.

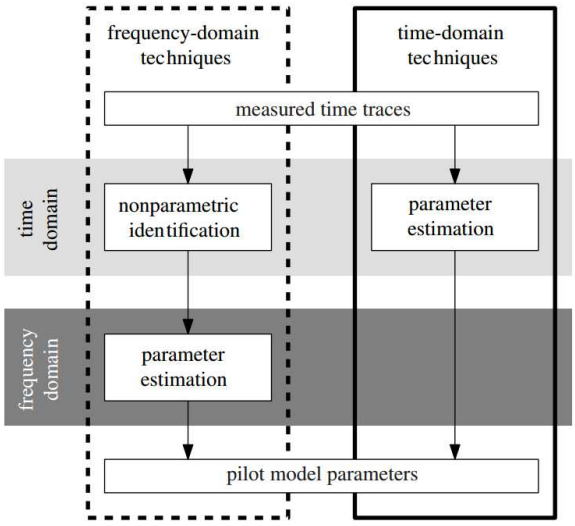

Figure 3-3: Comparison of pilot model parameter estimation methods (Zaal, Pool, Chu, Mulder, et al., 2009).

Chapter 4

Preliminary Experiments

In this chapter the preliminary experiments are described. Before conducting the final experiment several aspects have to be tested in an earlier stage. A task is designed and is described in Section 4-1. New forcing functions are needed and are described in Section 4-2. Two preliminary experiments were performed and are presented in Section 4-3.

4-1 Tracking task

For the preliminary experiments a pursuit display is used comparable to the display of Flowers (1978) and Soliveri et al. (1997). It is thought to provide a task that can be performed by PD patients. The task will be single-axis; the target will move on the horizontal axis only. The display will consist of a blue circle and a red filled circle, see Figure 4-1. The blue circle will move according to the forcing function while the red circle is controlled by the subject. This design is chosen since it is in line with the other tasks designed at the EMC (Muilwijk et al., 2013; De Boer et al., 2013). The controlled element will have single integrator dynamics, $Y_c = K_c/s$. This can be compared with automobile heading control by using a steering wheel (McRuer et al., 1965).

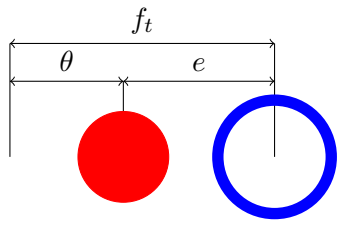

Figure 4-1: Pursuit display used in the preliminary experiment.

4-2 Design of the forcing functions

Typically a 81.92 second measurement time is used for tracking tasks (Zaal, Pool, De Bruin, et al., 2009; Pool et al., 2010). If an experiment has a sampling rate of 100 Hz this gives 8192 (2^{13}) data points which can be used for the Fourier transform used for the FCM (van Paassen & Mulder, 1998) described in Chapter 3. After consultation with the Neuroscience department at the EMC this measurement time was thought to be too long for PD patients. Consequence is that new forcing functions needed to be designed to guarantee excitation at the desired frequencies. The new measurement time is set to 40.96 seconds, during this period the data is collected. The sampling rate is 50Hz which is prescribed by the current Erasmus MC eye-hand test battery. This leads to 2048 (2^{11}) data points for the Fourier transform. With a run-in time of 9.04 seconds the length of one trial will be 50 seconds, which is thought to be acceptable for PD patients.

The task will be a combined target following, disturbance rejection task. Therefore there is need for a target signal and a disturbance signal (van Paassen & Mulder, 1998). Two input signals will give more data points to calculate the frequency response function, but it makes performing the task more demanding as well. The forcing functions should be designed in such a way that they excite the subjects at the desired frequencies (van Paassen & Mulder, 1998). The forcing functions used are composed as a sum of multiple sinusoids (4-1) (Damveld et al., 2010). Four parameters are involved. N_f is the number of sinusoid. Ten single sines waves added together is considered enough to create a random appearing signal. A_f are the amplitudes, ω_f the frequencies and ϕ_f the phase shifts.

$$f(t) = \sum_{k=1}^{N_f} A_f[k] sin(\omega_f[k]t + \phi_f[k]) \tag{4-1}$$

The frequencies, ω_f, of the signals are chosen in such a way that they cover a broad spectrum, between 0.1 and 20 rad/s. The frequencies are calculated using (4-2). n_f is a integer, commonly a prime number to avoid harmonic sine waves, and ω_m the base frequency: $\frac{2\pi}{T_m}$, where T_m is the measurement time. The frequency points are chosen to cover the spectrum as equally distributed as possible on a logarithmic scale. The values can be found in Table 4-1.

$$\omega_f = n_f \cdot \omega_m \tag{4-2}$$

The amplitudes, A_f, are determined by applying a filter (Zaal, Pool, De Bruin, et al., 2009), (4-3), with $T_{A_1} = 0.1$ and $T_{A_2} = 0.8$. After applying the filter the standard deviation of the signals is set to one to give the target and the disturbance signal the same power. The standard deviation of a multisine signal depends only on the amplitude of the single sine waves (Damveld et al., 2010) as can be seen in (4-4). The filter with the amplitudes at the chosen frequencies are shown in Figure 4-2. The numeric values for the amplitudes are presented in Table 4-1.

$$H_A(j\omega) = \frac{(1 + T_{A_1} j\omega)^2}{(1 + T_{A_2} j\omega)^2} \tag{4-3}$$

$$\sigma^2\{ft(t)\} = \sum_{j=1}^{N} \frac{A_j^2}{2} \tag{4-4}$$

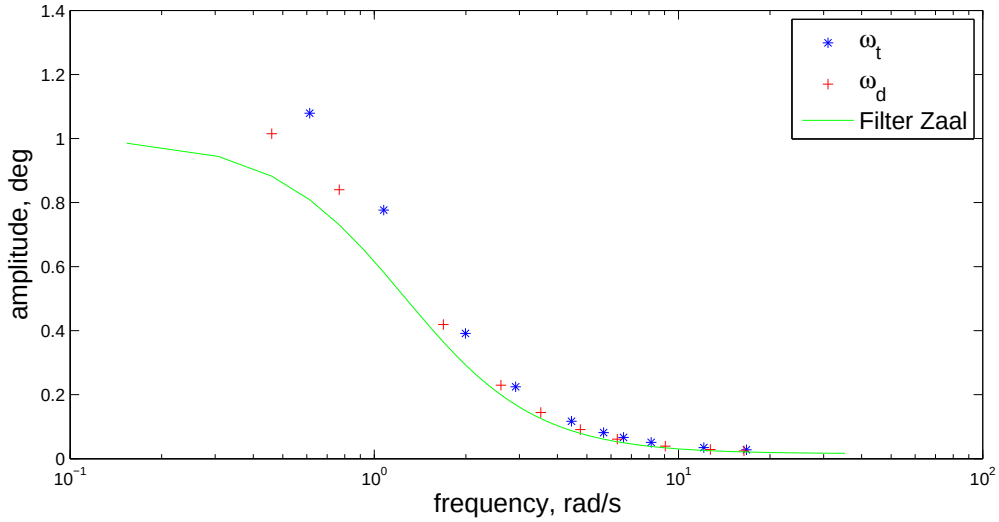

Figure 4-2: Target and disturbance forcing function spectra.

To determine the phases, ϕ_f, of the signals 10,000 random phase sets were generated. The phases define the appearance of the signal, an indication is the Crest Factor (CF), (4-5). Signals with a low CF create a flat signal while signals with a high CF have large peaks in the signal. Therefore the aim should lie on a average CF since it is not predictable and induces stationary behavior (Damveld et al., 2010) . The average obtained CF for the target signal was 2.33 and for the disturbance 2.20. A set of phases which generate forcing functions with these CF's is chosen and can be found in Table 4-1.

$$CF(f(t)) = \frac{max(f(t))}{rms(f(t))} \tag{4-5}$$

Now all the parameters of the multisine signals are determined it is possible to create the forcing functions. The time traces of the new forcing functions are presented in Figure 4-3. The first 9.04 seconds are used as run-in time. The first second the signals stays zero after which it comes to power in four seconds using a cosine function as given by (4-6) with $t = 4$.

$$f_{runin} = (cos(f \cdot t + 0.5 \cdot \pi))^2 \tag{4-6}$$

4-3 Preliminary experiments

The main experiment has to be performed at the EMC due to the involvement of PD patients. At the current measurement setup no joystick is available. A HOTAS Warthog

Table 4-1: Experiment forcing function properties

Target, f_t				Disturbance, f_d			
n_t	$\omega_t, rad/s$	A_t, deg	ϕ_t, rad	n_d	$\omega_d, rad/s$	A_d, deg	ϕ_d, rad
4	0.614	1.079	7.239	3	0.460	1.015	8.948
7	1.074	0.776	0.506	5	0.767	0.840	0.030
13	1.994	0.391	7.860	11	1.687	0.419	0.773
19	2.915	0.225	8.184	17	2.608	0.230	4.199
29	4.449	0.117	9.012	23	3.528	0.144	3.680
37	5.676	0.082	6.141	31	4.755	0.091	1.705
43	6.596	0.066	6.776	41	6.289	0.061	1.585
53	8.130	0.051	6.265	59	9.051	0.039	5.650
79	12.118	0.035	4.432	83	12.732	0.029	7.711
109	16.720	0.028	2.672	107	16.414	0.025	8.125

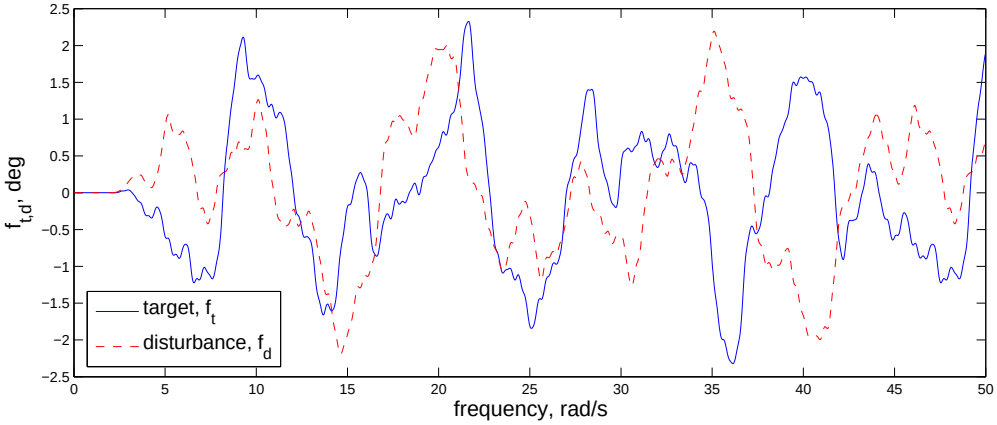

Figure 4-3: Time traces of the forcing functions

joystick (Thrustmaster, Hillsboro, Oregon, USA) was bought after a trade-off as presented in Appendix A. To test the new forcing functions and validate the newly acquired joystick two preliminary experiments were performed.

1. Validating the HOTAS Warthog stick
2. Verifying the designed forcing functions

The data for both preliminary test is collected in the Human-Machine Interaction Laboratory at the Faculty of Aerospace Engineering.

4-3-1 Validating the HOTAS Warthog stick

Goal

In this experiment the HOTAS Warthog stick will be compared with the elektro-hydrolic stick from the Human-Machine Laboratory at the TU Delft. Also the new forcing functions from Section 4-2 are used and thus can be checked if they are sufficient. Finally, the effective open-loop will be evaluated to determine if subjects show pursuit behavior. If pursuit behavior is lacking, single-loop identification can be used.

Setup

Three conditions are tested. The subjects will be three students with extensive tracking experience and three novice students. For Condition 1 the HMI joystick is used, with the settings of the van der El et al. (2015) experiment. Condition 2 is performed with the HMI joystick tuned in such a way to mimic the HOTAS Warthog characteristics. Condition 3 is performed with the HOTAS Warthog stick. Conditions were randomized over subjects using a Latin square design.

During the experiment the control signal, u, the error, e, and the system output, x, are recorded. Subjects had to perform ten runs of each condition from which the average of the last three were taken for measurements.

Results

In Figure 4-4a and Figure 4-4b an example time trace is presented for the averaged system output and averaged control signal from condition 2.

With the obtained time traces the FCM can be used to obtain the estimated frequency response as explained in Chapter 3. The estimated frequency response from subject 3 in condition 2 is plotted in Figure 4-5. It is expected to see a peak due to the neuromuscular system in the magnitude plot. However, it seems to be not captured completely. It could be that the spectrum of the input frequencies is not broad enough and should be extended to cover the full peak.

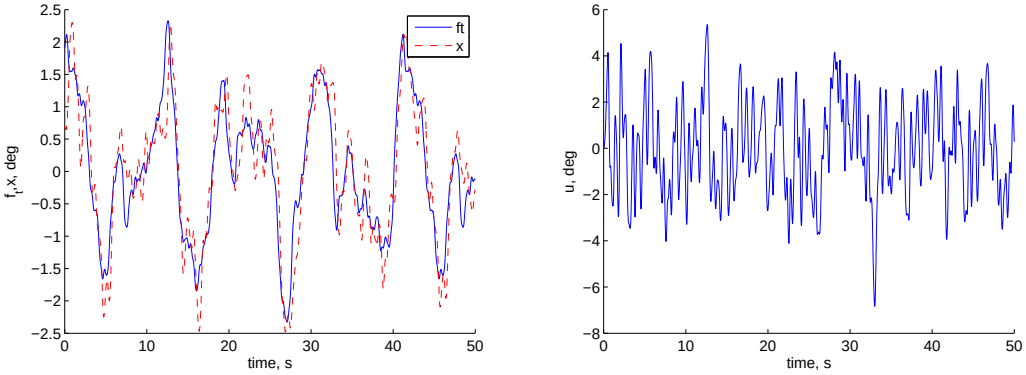

(a) Target signal and system output **(b)** Control signal

Figure 4-4: Averaged time traces for target signal, system output and input signal from subject 6.

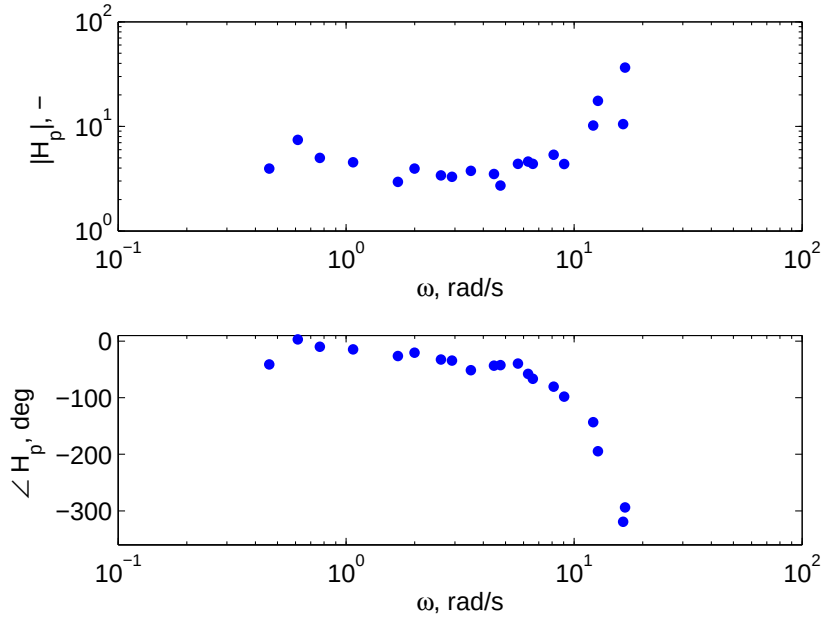

Figure 4-5: Fourier coefficients found for subject 3 in condition 2.

Using the estimated frequency response it is possible to fit a model. The model chosen is presented in (4-7) where Y_{nms} can be found in Section 3-1. A gain model is used since for an single integrator dynamics of the controlled system no lead or lag is expected (McRuer et al., 1965).

$$Y_p = K_p \cdot e^{-j\omega\tau} \cdot Y_{nms}(j\omega) \tag{4-7}$$

The results of the parameter estimation are in Figure 4-6. It shows that the parameters are not significantly different over conditions, which indicates that the control behavior for using the HOTAS Warthog stick is not different from the behavior induced by the HMI stick. For the score parameter, defined as (4-8), the control effort and the VAF the results are in Figure 4-7. The score parameter is below one for all conditions which means that the controller is reducing the error. If the score is above one the controller is increasing the error and a better strategy would be not controlling at all (which will give a score of one).

$$SC = \frac{\sigma_e^2}{\sigma_{ft}^2} \tag{4-8}$$

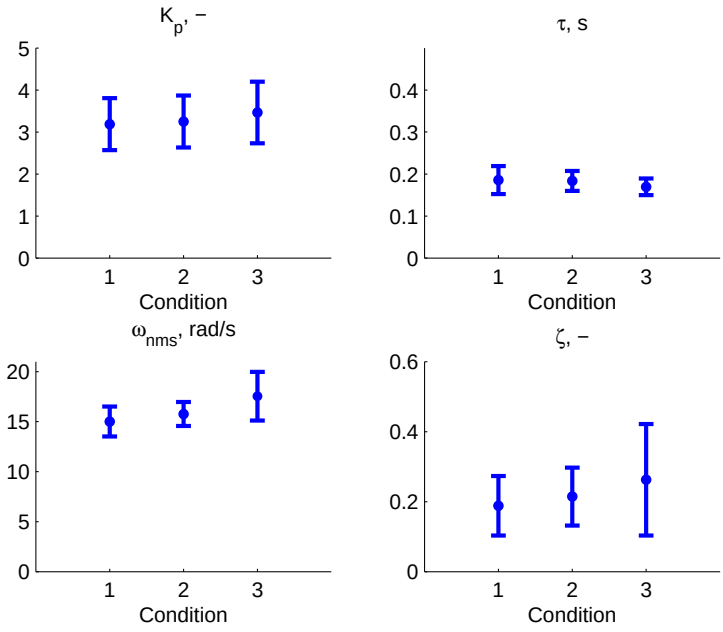

Figure 4-6: Parameters from the fitted model.

With the parameters from the estimation substituted into (4-7) the identification results can be plotted as in Figure 4-8. The model follows the estimated Fourier coefficients quite nicely.

In Figure 4-9 an example of a Y_β plot is given. Y_β is the effective open-loop describing function and can be used to check if pursuit behavior is used by the controller. As can be seen from

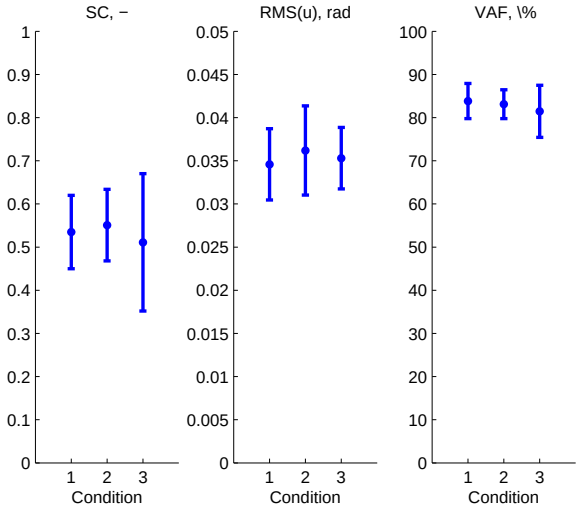

Figure 4-7: Performance measures.

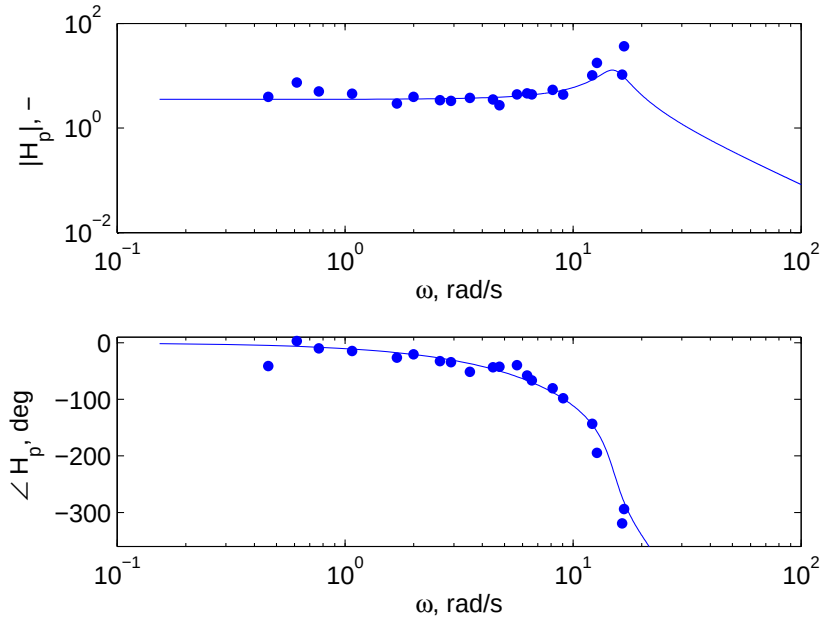

Figure 4-8: Estimated model from fitting model to the Fourier Coefficients.

the figure this is not the case, the disturbance data points are in line with the target data points. This is an indication that it is possible to discard the disturbance signal and single-loop identification can be used. An advantage is that the task will become considerably easier without disturbance. An easier task might be more suitable for PD patients. A disadvantage is that fewer data point are available for identification and the quality of the results could suffer from that.

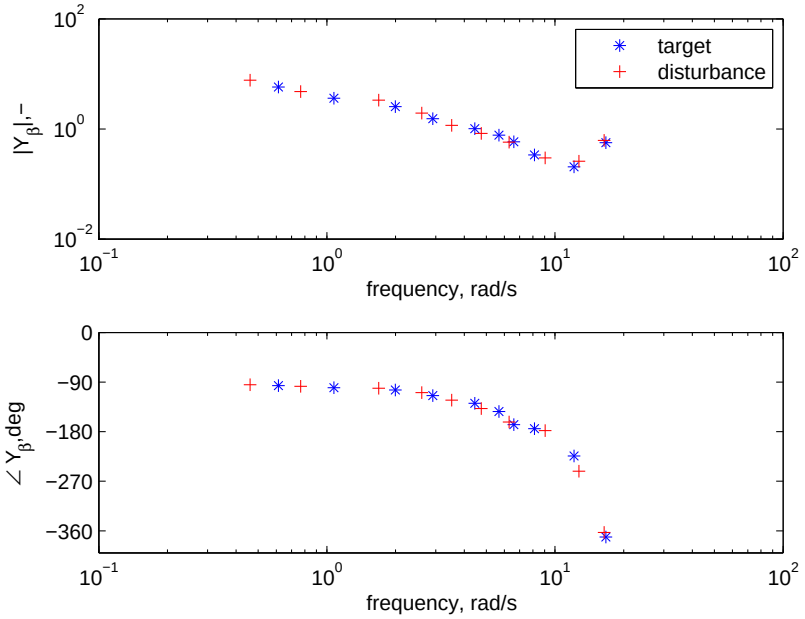

Figure 4-9: Open-loop describing function Y_β.

Conclusions

From the preliminary experiment there is concluded that the results from the HOTAS Warthog stick are not significantly different from the results from the HMI stick. This means similar results can be expected if the stick is used in the EMC setup. The second conclusion is that the input signal bandwidth was not broad enough. It needs an extra sine wave in the high frequency range to catch the complete neuromuscular peak of the subjects. From the effective open-loop response it could be seen that the subjects showed compensatory behavior. This means single-loop identification can be used. Therefore the disturbance signal can be discarded to simplify the tracking task for the PD patients.

4-3-2 Multisinus Experiment

Goal

From the validation experiment it was found that the disturbance signal could be discarded but the target signal might be extended to better cover the neuromuscular peak. In this

preliminary experiment it is checked if an extended target signal will indeed enable better neuromuscular system identification. The new target signal was constructed using the same methods as described in Section 4-2 and is presented in Table 4-2. The added sine wave is placed in the high frequency region, at 24 rad/s.

Setup

For this experiment three subjects are tested. All subjects have extensive tracking experience. Two conditions are performed. Condition 1, with the original target signal as presented in Table 4-1, but without disturbance. Secondly, Condition 2, is with the extended target signal constructed as in Table 4-2, also without disturbance.

Table 4-2: New experiment forcing function properties

Target, f_t			
$n_t, -$	$\omega_t, rad/s$	A_t, deg	ϕ, rad
4	0.614	1.079	7.239
7	1.074	0.776	0.506
11	1.994	0.391	7.860
17	2.915	0.225	8.184
23	4.449	0.117	9.012
29	5.676	0.082	6.141
37	6.596	0.066	6.776
53	8.130	0.051	6.265
79	12.118	0.035	4.432
109	16.720	0.028	2.672
157	24.084	0.024	8.009

Results

In this section the results of the multisine experiment will be presented in a similar manner as the validation experiment. For the multisine experiment the identification will be done using the MLE as well to verify the results from the FCM. Representative time-traces of the experiment are presented in Figure 4-10.

The estimated frequency responses for both conditions are presented in Figure 4-11 and show why the extra sinewave might be necessary. For Condition 1 there is a rising slope at the high frequencies, while for Condition 2 the peak due to the neuromuscular system can be seen. This result was found for all subjects.

The model used for the parameter estimation is extended compared to (4-7). A lead term is added to see if subjects develop lead during the task. The model is presented in (4-9). The results of the parameter estimation can be seen in Figure 4-13. .

The estimated model is able to make a good fit to the data, see Figure 4-12.

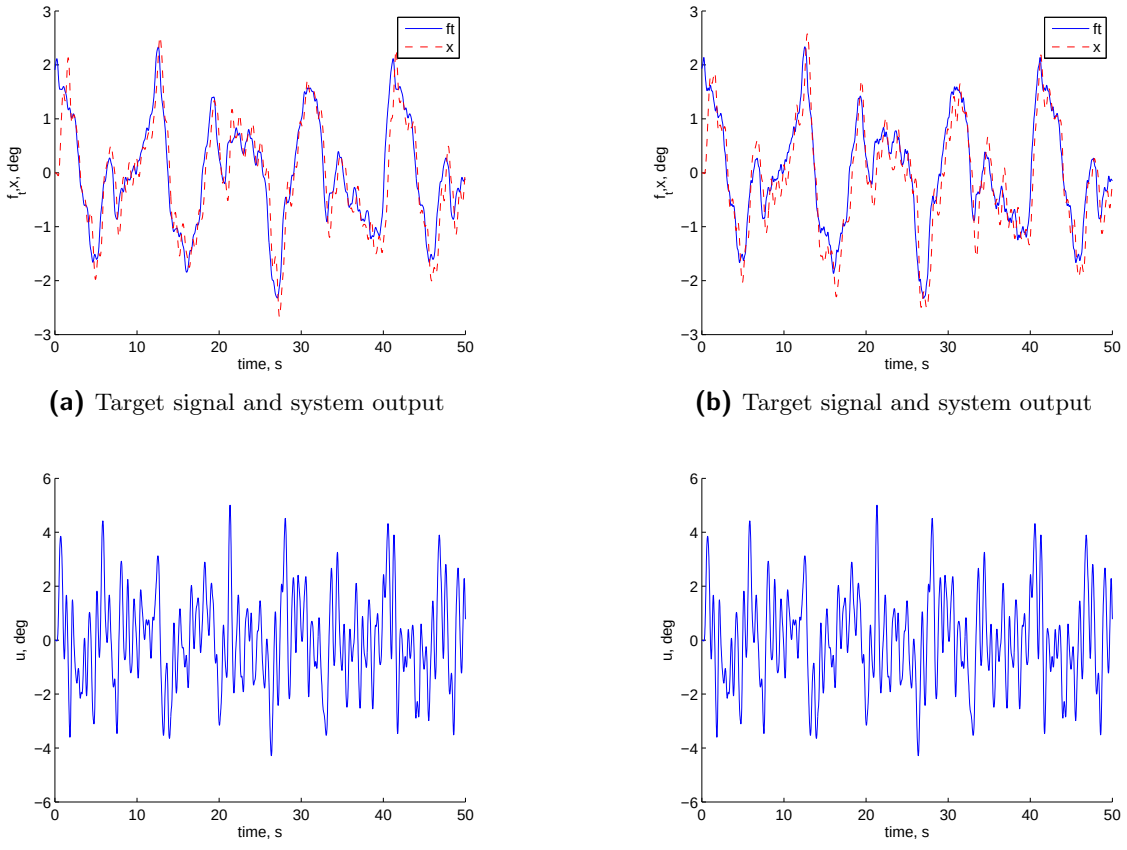

(a) Target signal and system output

(b) Target signal and system output

(c) Control input

(d) Control input

Figure 4-10: Time traces for the signals, on the left Condition 1 and on the right Condition 2.

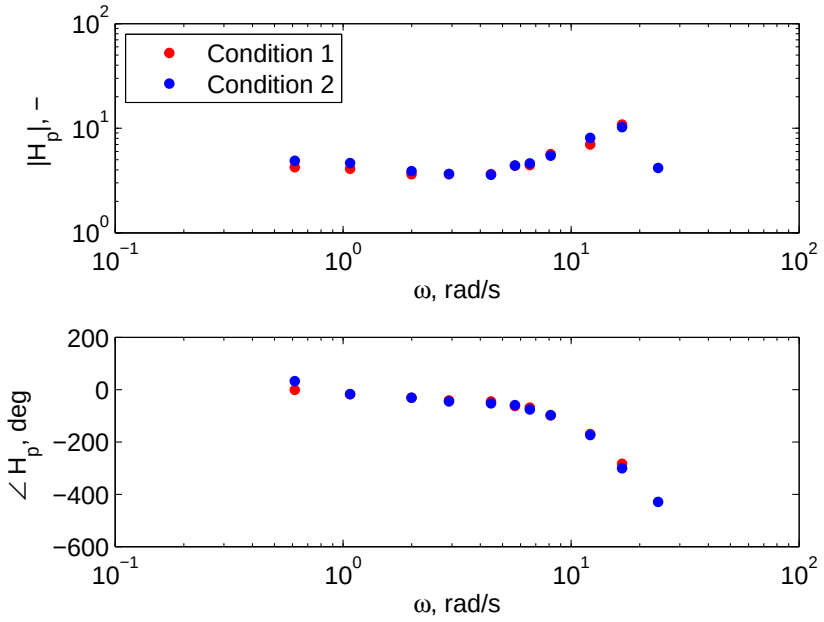

Figure 4-11: Fourier coefficients found using FCM for subject 1, both conditions.

$$Y_p = K_p(T_L j\omega + 1) \cdot e^{-j\omega\tau} \cdot Y_{nms} \tag{4-9}$$

The difficulty of the task is not increased by adding the extra frequency input. The score parameter does not significantly change, see Figure 4-14. For the control effect a similar trend is seen. In the figure the results of condition 1, only from data of the experienced subjects, from the validation experiment are also plotted for comparison. The score parameter is significantly larger when there is a disturbance signal and thus the task will be indeed less demanding for PD patients without it.

Another way to look a the data is to determine if PD patients have problems at a certain frequencies. This can be done by looking at the integral of the power spectrum of the error signal, see Figure 4-15. The steps in the figure appear at the input frequencies of the target function. The signals should end at the variance of the signals which is the case, indicated by the circles. From this data PD patients might show different results at certain frequencies compared to a control group, possibly due to resting and action tremor.

Conclusions

From the frequency response functions it can be concluded that the target signal with the extra input frequency is better able to capture the neuromuscular peak. The new task, without disturbance, is indeed easier to perform, and thus should be less demanding for PD

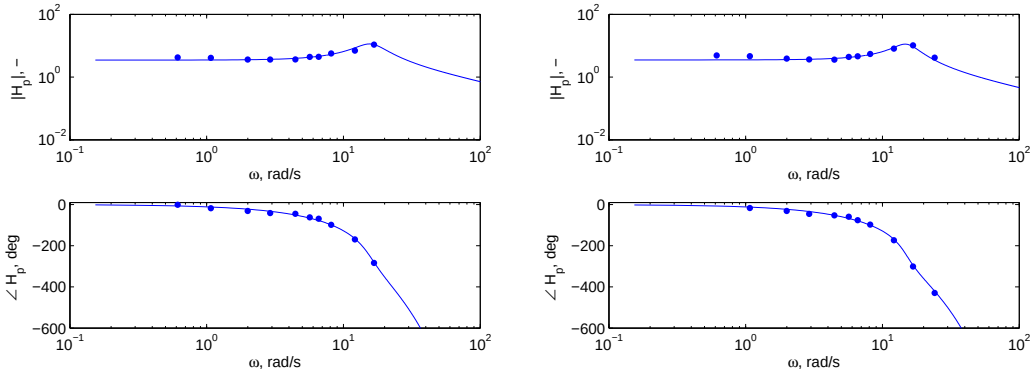

(a) Model fitted through data points, condition 1

(b) Model fitted through data points, condition 2

Figure 4-12: Describing functions as estimated with the FCM.

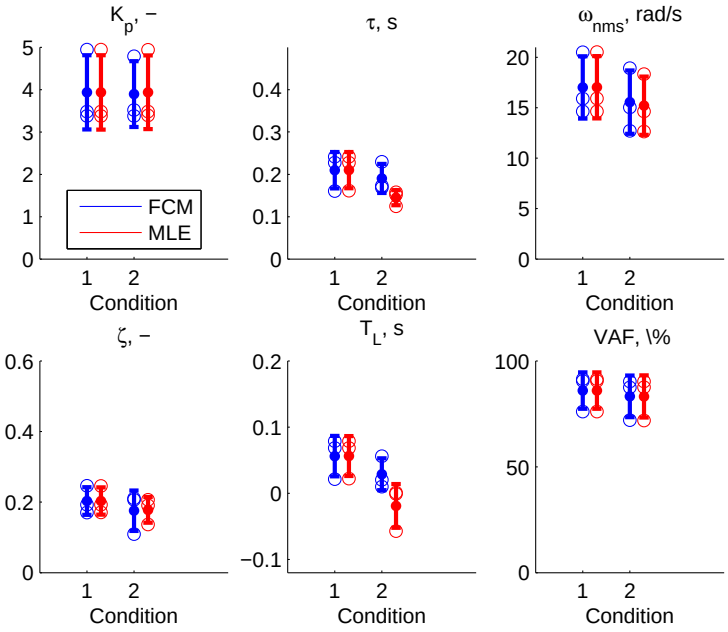

Figure 4-13: Parameters from the fitted model, in blue the parameters from the FCM and in red from the MLE.

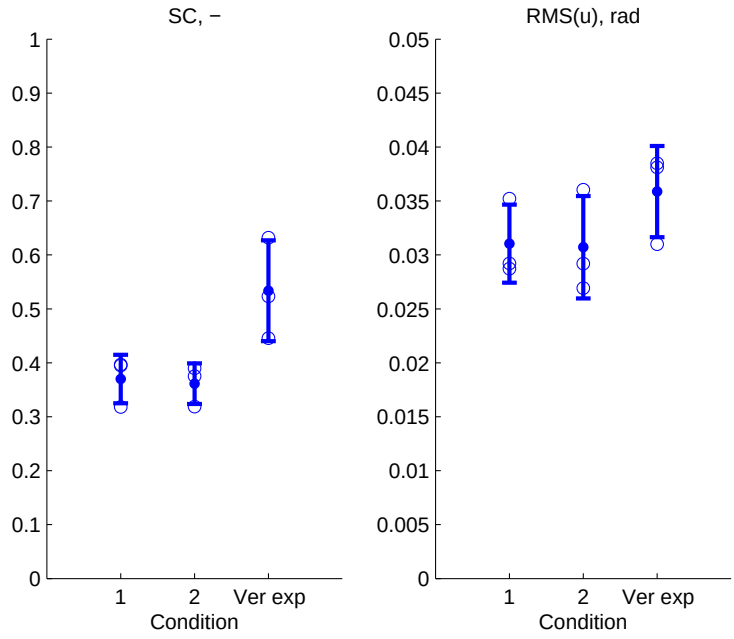

Figure 4-14: Score parameter and the root mean squared control input.

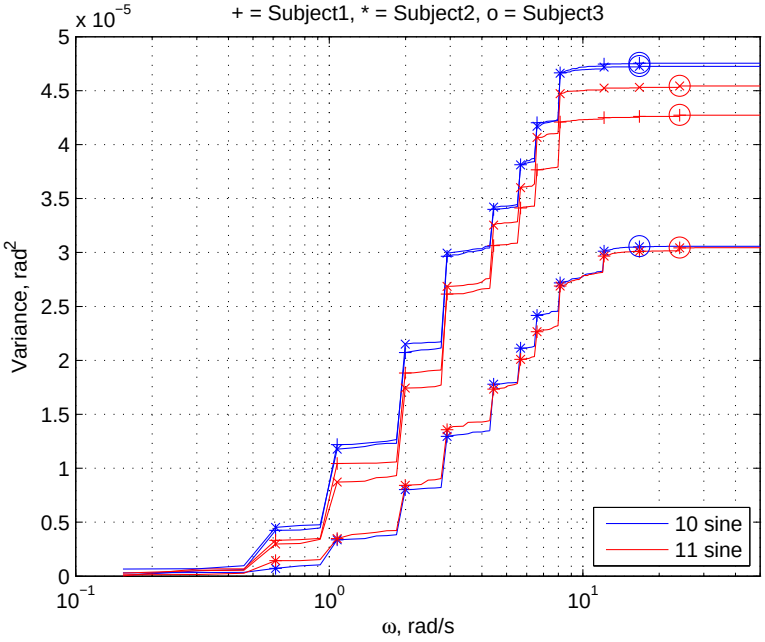

Figure 4-15: Integral of power spectrum of the error. The circles indicate the variance of the signals.

patients. A lead model was used but none of the subjects developed a lot of lead. The integral power spectrum could be used as an extra measure to find an indication of PD at certain frequencies.

Chapter 5

Experiment Proposal

From the literature and the results found in the preliminary experiments a final experiment is designed. It is thought that PD patients will be able to perform this experiment and the data collected is sufficient to enable a detailed analysis. The experiment is part of the PD research performed at the EMC.

5-1 Subjects

Subjects for this experiment will be diagnosed early-stage PD patients and an age and gender matched control group. This population is expected not to have earlier tracking experience. Before the experiment, subjects have to sign an informed consent form. The informed consent document can be found in Appendix B. This study aims for six PD patients and six controls. PD patients will be recruited from the department of Neurology of the EMC and for the control group commonly the spouse will participate. The study is approved by the ethical committees of the EMC and of the TU Delft.

5-2 Control task

The task that the subjects have to perform is a horizontal-axis target-following pursuit task. This is thought to be an intuitive task which can be accomplished by early stage PD patients. The methods used for identification (FCM and MLE) were tested in the preliminary experiments to be reliable for this tasks. The forcing function will be a multisine signal, consisting of eleven singe sine waves to cover a broad input spectrum. No disturbance is included. This reduces the workload and the preliminary experiments showed the disturbance is not necessary. Therefore, it is possible to use one-channel identification. The dynamics to control is a first order integrator. If a PD patient is not (or less) able to cope, this should emerge in the results. It is thought to be be a system that is relatively easy to control by healthy subjects.

5-3 Apparatus

The experiment is conducted at the EMC setup, see Figure 5-1. A HOTAS Warthog joystick (Thrustmaster, Hillsboro, Oregon, USA) will be used as input device. The gaze of the eyes will be registered using a infrared video eye tracking system (Chronos Vision, Berlin, Germany). This gives new insights into how (PD)subjects are performing the task. The subjects are seated in front of a 32-inch screen (ELO touch systems, Leuven, Belgium) where the pursuit task is shown. Their head needs to be on a chin rest to ensure minimal head movement and a fixed position due to the eye-tracking system.

Figure 5-1: A subject in the measurement setup at the EMC consisting of a screen (1), a modified HOTAS Warthog joystick (2), an infrared eye tracking system (3), and a chin rest (4).

5-4 Experiment setup

The intention is to let subjects perform each eight runs of the tracking task from which the last three will be used as measurement runs. An individual run lasts for 50 seconds of which the last 40.96 seconds is used as measurement data. Since the experiment is part of a set of experiment there is limited time available. With a run-time of 50 seconds and eight trails the total tracking task will last for around ten minutes, which is thought to be acceptable and within the time constraints. Still, during every experiment there need to be evaluated if the patient is able to continue with the task. Before the tracking task starts there is a test scenario. In this scenario there is no moving target but it can be used to familiarize with the setup and the dynamics of the controlled system. Subjects are instructed to keep the error as small as possible by minimizing the distance between a (blue)target circle symbol and a

(red) controlled filled circle symbol. For motivation the score parameter is shown after each run.

5-5 Additional verification experiment

Since the combination of a tracking task in combination with an eye-tracking system has not been done in the past an extra preliminary experiment is conducted for verification. Three novice and three subjects with extensive tracking experience will perform the designed task at the EMC setup. From the results the additional value of eye-traces in tracking experiments might be determined. This additional test will be reported on in the final thesis, together with the main experiment.

Bibliography

Andersen, O. T. (1986). A system for quantitative assessment of dyscoordination and tremor. *Acta Neurologica Scandinavica*, *73*(3), 291–294.

Cassell, K. J. (1973). The usefulness of a temporal correlation technique in the assessment of human motor performance on a tracking device. *Medical and biological engineering*, *11*(6), 755–761.

Chakravarthy, V. S., Joseph, D., & Bapi, R. S. (2010). What do the basal ganglia do? A modeling perspective. *Biological Cybernetics*, *103*(3), 237–253.

Damveld, H. J., Abbink, D. A., Mulder, M., Mulder, M., Paassen, M. M. van, Helm, F. C. T. van der, et al. (2009, August). Measuring the Contribution of the Neuromuscular System During a Pitch Control Task. In *Proceedings of the aiaa modeling and simulation technologies conference, chicago (il).*

Damveld, H. J., Beerens, G. C., Van Paassen, M. M., & Mulder, M. (2010, July). Design of Forcing Functions for the Identification of Human Control Behavior. *Journal of Guidance, Control, and Dynamics*, *33*(4), 1064-1081.

de Boer, C. (2015). Visuomotor integration in neurodegenerative brains.

De Boer, C., Van Der Steen, J., Schol, R. J., & Pel, J. J. M. (2013). Repeatability of the timing of eye-hand coordinated movements across different cognitive tasks. *Journal of Neuroscience Methods*, *218*(1), 131–138.

De Lau, L. M. L., & Breteler, M. M. B. (2006). Epidemiology of Parkinson's disease. *The Lancet. Neurology*, *5*(June), 525–535.

Dubois, B., Slachevsky, A., Litvan, I., & Pillon, B. (2000). The FAB: A Frontal Assessment Battery at Bedside. *Neurology*, *55*(11), 1621–1626.

Fahn, S., & Elton, R. (1987). Unified rating scale for parkinsons disease. *Recent developments in Parkinsons disease. Florham Park. New York: Macmillan*, 153–163.

Flowers, K. (1978). Some frequency response characteristics of parkinsonism on pursuit tracking. *Brain*, *101*(1), 19–34.

Folstein, M. F., Folstein, S. E., & McHugh, P. R. (1975). Mini-mental state: a practical method for grading the cognitive state of patients for the clinician. *Journal of psychiatric research*, *12*(3), 189–198.

Goetz, C. G., Fahn, S., Martinez-Martin, P., Poewe, W., Sampaio, C., Stebbins, G. T., et al. (2007). Movement disorder society-sponsored revision of the unified Parkinson's disease rating scale (MDS-UPDRS): Process, format, and clinimetric testing plan. *Movement Disorders*, *22*(1), 41–47.

Goetz, C. G., Poewe, W., Rascol, O., Sampaio, C., Stebbins, G. T., Counsell, C., et al. (2004). Movement disorder society task force report on the hoehn and yahr staging scale: status and recommendations the movement disorder society task force on rating scales for parkinson's disease. *Movement disorders*, *19*(9), 1020–1028.

Hikosaka, O., Takikawa, Y., & Kawagoe, R. (2000). Role of the basal ganglia in the control of purposive saccadic eye movements. *Physiological reviews*, *80*(3), 953–978.

Hoehn, M. M., Yahr, M. D., et al. (1998). Parkinsonism: onset, progression, and mortality. *Neurology*, *50*(2), 318–318.

Hufschmidt, A., & Lücking, C.-H. (1995). Abnormalities of tracking behavior in parkinson's disease. *Movement disorders*, *10*(3), 267–276.

Ito, K., & Ito, M. (1975). Tracking Behavior of Human Operators in Preview Control Systems. *Electrical Engineering in Japan (English translation of Denki Gakkai Ronbunshi)*, *95*(1), 120-127.

Jones, R. D., & Donaldson, I. M. (1989). Tracking tasks and the study of predictive motor planning in Parkinson's disease. *Images of the Twenty-First Century. Proceedings of the Annual International Engineering in Medicine and Biology Society,*, 1055–1056.

Jones, R. D., & Donaldson, I. M. (1996). Removal of the Visuospatial Component from Tracking Performance and its Application to Parkinson s Disease. *IEEE Transactions On Biomedical Engineering*, *43*(10), 1001–1010.

Kandel, E., Schwartz, J. H., Jessell, T. M., & Mack, S. (2013). *Principles of Neural Science*. New York, Chicago, San Francisco: McGraw-Hill Medical.

Krendel, E. S., & McRuer, D. T. (1960). A Servomechanics Approach to Skill Development. *Journal of the Franklin Institute*, *269*(1), 24-42.

Lees, A. J., Hardy, J., & Revesz, T. (2009). Parkinson's disease. *The Lancet*, *373*(9680), 2055–2066.

McRuer, D. T., Graham, D., Krendel, E. S., & Reisener, W. J. (1965). *Human Pilot Dynamics in Compensatory Systems, Theory Models and Experiments with Controlled Element and Forcing Function Variations* (Technical Report No. AFFDL-TR-65-15). Wright-Patterson AFB (OH): Air Force Flight Dynamics Laboratory, Wright-Patterson Air Force Base (OH).

McRuer, D. T., & Jex, H. R. (1967). A Review of Quasi-Linear Pilot Models. *IEEE Transactions on Human Factors in Electronics*, *HFE-8*(3).

Muilwijk, D., Verheij, S., Pel, J. J. M., Boon, A. J. W., & Van Der Steen, J. (2013). Changes in Timing and kinematics of goal directed eye-hand movements in early-stage Parkinson's disease. *Translational neurodegeneration*, *2*(1), 1.

Nieuwenhuizen, F. M., Zaal, P. M. T., Mulder, M., van Paassen, M. M., & Mulder, J. A. (2008, July-August). Modeling Human Multichannel Perception and Control Using Linear Time-Invariant Models. *Journal of Guidance, Control, and Dynamics*, *31*(4), 999–1013.

Pew, R. W., Duffendack, J. C., & Fensch, L. K. (1967, June). Sine-Wave Tracking Revisited. *IEEE Transactions on Human Factors in Electronics*, *HFE-8*(2), 130-134.

Pierrot-Deseilligny, C., Milea, D., & Müri, R. M. (2004). Eye movement control by the cerebral cortex. *Current Opinion in Neurology*, *17*(1), 17–25.

Pierrot-Deseilligny, C., Mri, R., Ploner, C., Gaymard, B., & Rivaud-Pchoux, S. (2003). Cortical control of ocular saccades in humans: a model for motricity. In *Neural control of space coding and action production* (Vol. 142, p. 3 - 17). Elsevier.

Pool, D. M. (2012). *Objective evaluation of flight simulator motion cueing fidelity through a cybernetic approach*. TU Delft, Delft University of Technology.

Pool, D. M. (2015). *System identification experiments*. University Lecture.

Pool, D. M., Van Paassen, M. M., & Mulder, M. (2010). Modeling Human Dynamics in Combined Ramp-Following and Disturbance-Rejection Tasks. *AIAA Modeling and Simulation Technologies Conference*(August).

Pool, D. M., Zaal, P. M. T., Damveld, H. J., Van Paassen, M. M., Van Der Vaart, J. C., & Mulder, M. (2011). Modeling Wide-Frequency-Range Pilot Equalization for Control of Aircraft Pitch Dynamics. *Journal of Guidance, Control, and Dynamics*, *34*(5), 1529–1542.

Poulton, E. C. (1974). *Tracking skill and manual control*. Academic Press.

Soliveri, P., Brown, R. G., Jahanshahi, M., Caraceni, T., & Marsden, C. D. (1997). Learning manual pursuit tracking skills in patients with Parkinson's disease. *Brain*, *120*(8), 1325–1337.

van der El, K., Pool, D. M., Damveld, H. J., Van Paassen, M. M., & Mulder, M. (2015). An Empirical Human Controller Model for Preview Tracking Tasks. *IEEE Transactions on Cybernetics*.

van Paassen, M. M., & Mulder, M. (1998). Identification of Human Operator Control Behaviour in Multiple-Loop Tracking Tasks. In *Proceedings of the seventh ifac/ifip/ifors/iea symposium on analysis, design and evaluation of man-machine systems, kyoto japan* (pp. 515–520). Pergamon.

Wasicko, R. J., McRuer, D. T., & Magdaleno, R. E. (1967). Human pilot dynamic response in single-loop systems with compensatory and pusuit displays. *Air Force Flight Dynamics Laboratory*, *Tech. Rep. No. AFFDL-TR-66-137*.

Zaal, P. M. T., Pool, D. M., Chu, Q. P., Mulder, M., Van Paassen, M. M., & Mulder, J. A. (2009). Modeling Human Multimodal Perception and Control Using Genetic Maximum Likelihood Estimation. *Journal of Guidance, Control, and Dynamics*, *32*, 1089–1099.

Zaal, P. M. T., Pool, D. M., Chu, Q. P., Van Paassen, M. M., Mulder, M., & Mulder, J. A. (2009). Modeling Human Multimodal Perception and Control Using Genetic Maximum Likelihood Estimation. *Journal of Guidance, Control, and Dynamics*, *32*(4), 1089-1099.

Zaal, P. M. T., Pool, D. M., De Bruin, J., Mulder, M., & Van Paassen, M. M. (2009). Use of Pitch and Heave Motion Cues in a Pitch Control Task. *Journal of Guidance, Control, and Dynamics*, *32*(2), 366-377.

Part IV

Preliminary Report Appendices

Appendix A

Selection of Control Device

For a tracking task a control device, usually a joystick, is necessary. The EMC setup did not contain a joystick so there was the need to purchase one. In this chapter the selection of the control device is described.

A-1 Requirements

For a the joystick of a tracking task there are certain requirements. The first requirement is the ease of use. Is the joystick plug and play, or in other words, does it have a USB connection. Secondly, the sensor is important, a Hall sensor was thought to be necessary. In such a sensor there is no contact so there is on wear which will make the joystick last longer. Furthermore, the better the accuracy, the better the results from a tracking task. For this the resolution is important. For good control of the stick a minimal break-out force is preferable. The break-out force is the force needed to get the stick moving. Finally, also the price is a requirement. Joysticks tend to become very expensive for a very high accuracy.

A-2 Comparison

Ten different joystick were found and compared. Different sticks in different sectors were found, e.g some are from the gaming industry, some from the aviation industry. The information found is presented in Table A-1. It was not possible to find all the information since some was not made available by the company.

A-3 Conclusion

After the research there was decided to purchase the Thrustmaster Hotas Wartog joystick. It has a good resolution due to the Hall sensor and the price is reasonable for initial research.

Table A-1: Joysticks

Manufacturer	Type/Series	USB	Hall	Resolution	Break out force	Price
Megatron	TRY52	yes	yes	12bit	5.6N	-
Altheris		no	-	-	-	-
P3America		no	-	-	-	-
Controldevices	CDJ900	no	yes	-	-	-
Apem	CJ	yes	yes	12bit	5.6N	€460
Thrustmaster	Hotas Wartog	yes	yes	16bit	-	€150
Apem	HG	yes	yes	-	7.7N	€690
BG Systems	JFx	yes	yes	-	2.7N	€2,800
Ottoexcellence	JH	yes	yes	-	-	-
Flightdecksolutions	A320 Pro-MX	yes	-	-	-	€1,200
Sensodrive	SENSO	no(CAN)	no(force feedback)	-	-	€25,000

url
http://www.megatron.de/en/products/hand-joysticks/hand-joystick-series-try52.html
http://www.altheris.com/products/joysticks-industrial.htm#90-100
http://www.p3america.com/industrial_joystick_full_size_selection_guide.htm
http://www.controldevices.net/Defence/CustomDesign/CDJ900.html
http://www.apem.com/Ergonomic-Hall-effect-hand-grip-joysticks-v9-d-805.html
http://www.thrustmaster.com/products/hotas-warthog
http://www.apem.com/Ruggedized-Hall-effect-hand-grip-joysticks-v9-d-179.html
http://www.bgsystems.com/products/JFx.html
http://www.ottoexcellence.com/shop-by-department/controls/joysticks/
http://www.flightdecksolutions.com/components/a320/a320-flight-controls/a320-pro-mx-series-sidestick/
http://www.sensodrive.de/EN/Produkte/Force-Feedback-Joystick.php

Downside is that the stick has a quite large dead-zone. The break-out force was also found to be larger than desired. To solve this problem the main spring inside the joystick was removed. The original A-10 replica handle could be distracting for PD patients. Therefore there was decided to replace the handle by a custom made handle, see Figure A-1.

Figure A-1: Modified HOTAS Warthog joystick in the EMC setup.

Appendix B

Informed Consent Document

Patiënteninformatie voor deelname aan het onderzoek:

Kan het meten van oogbewegingen en handbewegingen leiden tot betere diagnostiek bij Parkinsonsime?

Geachte heer/mevrouw,

Wij vragen u vriendelijk om mee te doen aan een medisch-wetenschappelijk onderzoek (zie titel). U beslist zelf of u wilt meedoen. Voordat u de beslissing neemt, is het belangrijk om meer te weten over het onderzoek. Lees deze informatiebrief rustig door. Bespreek het met partner, vrienden of familie. Ook is er een onafhankelijke persoon, die veel weet van het onderzoek. Lees ook de Algemene brochure. Daar staat veel algemene informatie over medisch-wetenschappelijk onderzoek in. Hebt u na het lezen van de informatie nog vragen? Dan kunt u terecht bij de onderzoeker. Op bladzijden 7 vindt u zijn contactgegevens.

1. Wat is het doel van het onderzoek?

U heeft waarschijnlijk een aantal onderzoeken achter de rug, waarna uw arts u heeft verteld dat u waarschijnlijk een vorm van Parkinsonisme heeft. Bij deze ziekte kan het voorkomen dat u al enkele problemen ervaart in het dagelijks leven, maar dat de huidige diagnostiek hier (nog) geen aandacht aan besteedt. Wij willen een methode ontwikkelen, waardoor het in de toekomst mogelijk is dat de verschillende vormen van Parkinsonisme met meer zekerheid en in een vroeg stadium herkend kan worden.

2. Hoe wordt het onderzoek uitgevoerd?

Het onderzoek vindt plaats op de afdeling neurowetenschappen van het Erasmus MC. Wij gaan uw beweeglijkheid, uw oogbewegingen en uw oog-hand coördinatie meten.

Uw beweeglijkheid zullen wij gaan meten met een standaard bewegingsonderzoek (UPDRS). Tijdens dit onderzoek zullen wij testen hoe soepel uw gewrichten zijn en hoe soepel u eenvoudige arm – en beenbewegingen kunt maken.
We meten oogbewegingen en oog-hand coördinatie juist omdat we weten dat de gebieden, die in de hersenen aangetast worden bij Parkinsonisme, deze bewegingen kunnen verstoren.
De oogbewegingen meten we met kleine camera's, welke u op uw hoofd draagt (zie afbeelding 1). Dit is niet zwaar en doet geen pijn. Tijdens het onderzoek plaatst u uw kin bovendien op een steun. Zo worden uw kin en hoofd ondersteund. De bewegingen van uw hand gaan we meten met markers die op een handschoen zijn aangebracht. Een camera kan dan precies registreren welke beweging uw hand maakt. U krijgt dan van ons opdrachten naar welke objecten u moet kijken en welke objecten u aan moet raken. Al met al zullen de testen samen een uur van uw tijd in beslag nemen.

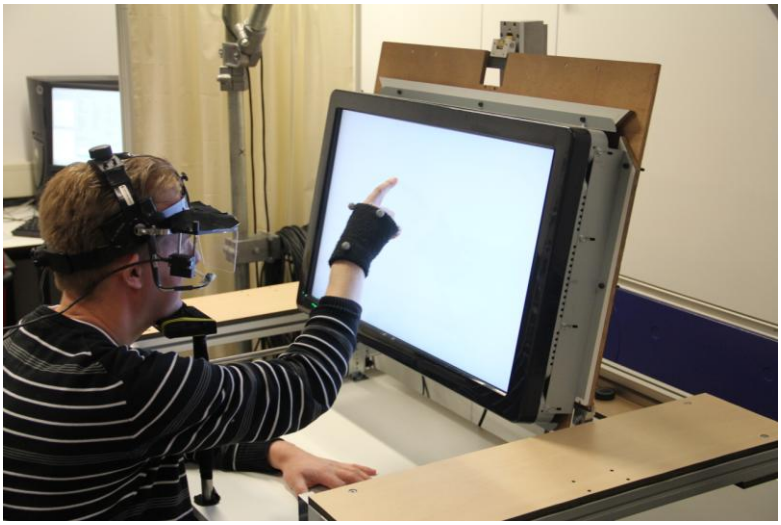

1. De camera op het hoofd en het hoofd steunt op een kinsteun. De handschoen met markers

3. Wat wordt er van u verwacht?

Van u wordt verwacht dat u zo goed mogelijk uw best doet tijdens de testen en zo goed mogelijk de aanwijzingen van de onderzoeker opvolgt. Daarnaast wordt er van u verwacht dat u naar het Erasmus MC komt, wij kunnen niet bij u thuis meten.

Ook willen wij u vragen om uw partner, broer, zus, een vriend of een kennis te vragen om ook deel te nemen aan dit onderzoek. Wij zoeken namelijk ook nog gezonde ouderen van 50 jaar en ouder om als controlepersoon aan het onderzoek mee te doen. Het meebrengen van een controlepersoon voor het onderzoek is geheel vrijwillig.

4. Wat zijn mogelijke voor - en nadelen van deelname aan dit onderzoek?

Er zijn voor u geen directe voordelen van dit onderzoek te verwachten. U helpt wel mee om in de toekomst een betere diagnose te kunnen stellen. Meedoen aan het onderzoek brengt géén risico voor uw gezondheid met zich mee.

Een nadeel van het onderzoek is dat er van u een kleine tijdsinvestering wordt verwacht. Het onderzoek duurt ongeveer een uur per persoon. Om de belasting voor u zo minimaal mogelijk te houden streven wij ernaar om het onderzoek te combineren met een (poli)klinische afspraak die u al heeft bij het Erasmus MC.

5. Wat gebeurt er als u niet wenst deel te nemen aan dit onderzoek?

U beslist zelf of u meedoet aan het onderzoek. Deelname is vrijwillig. Als u besluit niet mee te doen, hoeft u verder niets te doen. U hoeft niets te tekenen. U hoeft ook niet te zeggen waarom u niet wilt meedoen. Als u patiënt bent, krijgt u gewoon de behandeling die u anders ook zou krijgen. Als u wel meedoet, kunt u zich altijd bedenken en toch stoppen. Ook tijdens het onderzoek.
Binnen 2 weken na het ontvangen van deze brief zullen wij telefonisch contact met u opnemen om te vragen of u mee wilt doen of dat u dit niet wilt, waarna wij uw gegevens uit ons bestand zullen halen.

6. Wat gebeurt er als het onderzoek is afgelopen?

Uw gegevens worden gecodeerd verwerkt en na het onderzoek zullen uw adresgegevens uit ons bestand gehaald worden.

7. Bent u verzekerd wanneer u aan het onderzoek meedoet?

De toetsende commissie heeft ontheffing verleend van de verplichting een verzekering af te sluiten voor de deelnemers aan dit onderzoek, omdat zij van mening is dat dit onderzoek weinig of geen risico met zich meebrengt.

8. Wat gebeurt er met uw gegevens?

In de algemene brochure is uitgelegd dat de onderzoeker gegevens over u verzamelt en deze vertrouwelijk behandelt. Dit betekent dat een aantal personen uw medische status en de gegevens van het onderzoek mogen inzien. Deze personen mogen de gegevens gebruiken voor dit onderzoek, maar zij mogen deze gegevens alleen bekend maken zonder daarbij uw naam of andere persoonlijke gegevens te vermelden. Uw identiteit blijft dus altijd geheim. De onderzoeker bewaart de gegevens met een code. Dit betekent dat op de studie- documenten in plaats van uw naam enkel een letter-cijfercode staat. Alleen de onderzoeker houdt een lijst bij waarop staat welke letter- cijfercode bij welke naam hoort.

Normaal gesproken heeft alleen uw behandelend arts en zijn/ haar team inzage in uw gegevens. Als u meedoet aan deze studie krijgen meer mensen inzage in uw medische gegevens en studiegegevens. De personen die inzage kunnen krijgen in uw gegevens zijn:

- de medewerkers van het onderzoeksteam,
- de leden van de toetsingscommissie die de studie heeft goedgekeurd,
- de bevoegde medewerkers van de Inspectie voor de Gezondheidszorg.

Na de studie worden de gecodeerde gegevens gedurende 15 jaar bewaard. Dit is nodig om alles goed te kunnen controleren. Bovendien willen wij graag uw gegevens gebruiken voor andere onderzoeken die worden uitgevoerd naar verschillende vormen van Parkinsonisme. Deze onderzoeken hebben dus eenzelfde doel als het onderzoek waarvoor u nu wordt gevraagd. Het is dus niet zo dat uw gegevens ook zullen worden gebruikt voor onderzoek naar een geheel andere aandoening of een heel ander probleem. Vanzelfsprekend blijft de vertrouwelijkheid die we hierboven hebben beschreven altijd gelden. Vindt u het goed als wij uw

gegevens bewaren en gebruiken? Als u dat niet wilt, respecteren wij dat natuurlijk. U kunt uw keuze op het toestemmingsformulier aangeven.

Mogelijk willen we u in de toekomst opnieuw benaderen voor vervolgonderzoek. Op het toestemmingsformulier kunt u aangeven of u dit goed vindt.

9. Zijn er extra kosten / is er een vergoeding wanneer u besluit aan dit onderzoek mee te doen?

Wanneer u besluit mee te doen aan dit onderzoek en wij slagen erin om het onderzoek te combineren met een (poli)klinische afspraak die u al heeft op het Erasmus MC heeft u geen recht op vergoeding. Wanneer u apart naar het Erasmus MC komt voor dit onderzoek heeft u recht op vergoeding van uw parkeerkosten.

10. Welke medisch-ethische toetsingscommissie heeft dit onderzoek goedgekeurd?

De Medisch Ethische Toetsings Commissie Erasmus MC heeft dit onderzoek goedgekeurd. Meer informatie over de goedkeuring vindt u in de algemene brochure.

11. Wilt u nog iets weten?

Indien u tijdens de studie vragen of klachten heeft, vragen wij u contact op te nemen met een van de onderstaande onderzoekers of uw behandelend arts. U kunt voor vragen of klachten tijdens kantooruren contact opnemen met de volgende personen:

Dr. Hans van der Steen
Hoofdonderzoeker
Vestibulaire en oculomotorische onderzoeksgroep
Afdeling Neurowetenschappen, Erasmus MC
(tel) 010-7043572

Dr. Ir. Johan Pel
Onderzoeker
Afdeling Neurowetenschappen, Erasmus MC
(tel) 010-7043385

Drs. Casper de Boer
Onderzoeker
Afdeling Neurowetenschappen, Erasmus MC
(tel) 010-7043383

Buiten kantooruren of bij noodgevallen (24 uur bereikbaar wanneer nodig) kunt u contact opnemen met de volgende personen:

Dr. Ir. Johan Pel
Onderzoeker
Afdeling Neurowetenschappen, Erasmus MC
(tel) 06-28674609

Drs. Casper de Boer
Onderzoeker
Afdeling Neurowetenschappen, Erasmus MC
(tel) 06-51144762

Indien u twijfelt over deelname kunt u een onafhankelijke arts raadplegen, die zelf niet bij het onderzoek betrokken is, maar die wel deskundig is op het gebied van dit onderzoek en uw ziekte. Ook als u voor of tijdens de studie vragen heeft die u liever niet aan de onderzoekers stelt, kunt u contact opnemen met de onafhankelijke arts.

De onafhankelijke arts is:
Dr. J.W.M. Krulder, geriater in het Vlietland ziekenhuis te Schiedam. Telefonisch bereikbaar op 010-8935316.

Als u niet tevreden bent over het onderzoek of de behandeling kunt u terecht bij de onafhankelijke klachtencommissie van het Erasmus MC. De klachtencommissie is te bereiken op telefoonnummer 010-7033198.

Met vriendelijke groeten,

Het onderzoeksteam

12. Bijlagen:

- Algemene brochure medisch – wetenschappelijk onderzoek met mensen (ontvangt u apart bij deze informatiebrief).
- Toestemmingsformulier.
- Toestemmingsformulier video.

Toestemmingsformulier voor deelname aan het onderzoek:

Kan het meten van oogbewegingen en handbewegingen leiden tot betere diagnostiek bij Parkinsonisme?

Ik heb de informatiebrief voor de proefpersoon gelezen. Ik kon aanvullende vragen stellen. Mijn vragen zijn genoeg beantwoord. Ik had genoeg tijd om te beslissen of ik meedoe.

Ik weet dat meedoen helemaal vrijwillig is. Ik weet dat ik op ieder moment kan beslissen om toch niet mee te doen. Daarvoor hoef ik geen reden te geven.

Ik weet dat sommige mensen mijn gegevens kunnen zien. Die mensen staan vermeld in de Algemene brochure.

Ik geef toestemming om mijn gegevens te gebruiken, voor de doelen die in de informatiebrief staan.

Ik geef toestemming om mijn gegevens 15 jaar na afloop van dit onderzoek te bewaren.

Ik geef wel/geen* toestemming om mijn gegevens 15 jaar na afloop van dit onderzoek te bewaren, zodat deze in de toekomst misschien gebruikt kunnen worden voor onderzoek met eenzelfde onderzoeksdoel.

Ik geef wel/geen* toestemming om mij in de toekomst opnieuw te benaderen voor vervolgonderzoek.

Ik vind het goed om aan dit onderzoek mee te doen.

Naam proefpersoon:
Handtekening: Datum: __ / __ / __

Ik verklaar hierbij dat ik deze proefpersoon volledig heb geïnformeerd over het genoemde onderzoek.

Als er tijdens het onderzoek informatie bekend wordt die de toestemming van de proefpersoon zou kunnen beïnvloeden, dan breng ik hem/haar daarvan tijdig op de hoogte.

Naam onderzoeker (of diens vertegenwoordiger):
Handtekening: Datum: __ / __ / __

---

* Doorhalen wat niet van toepassing is.

Toestemmingsformulier videopname tijdens bewegingsonderzoek:

Kan het meten van oogbewegingen en handbewegingen leiden tot betere diagnostiek bij Parkinsonisme?

Ik geef wel/geen* toestemming om videobeelden te maken van het bewegingsonderzoek (UPDRS) zoals dit staat beschreven in de informatiefolder.

Ik geef wel/geen* toestemming om de gegevens van deze videobeelden te verwerken voor de doeleinden van het onderzoek.

Ik geef wel/geen* toestemming om mijn gegevens van de videobeelden gedurende maximaal 15 jaar na afloop van het onderzoek te bewaren.

Naam proefpersoon:
Handtekening: Datum: __ / __ / __

Naam onderzoeker (of diens vertegenwoordiger):
Handtekening: Datum: __ / __ / __

---

* Doorhalen wat niet van toepassing is.